UDK 66:54(05) CODEN HMIDA 8 ISSN 0367–598X

1 Hemijska industrija

Vol. 76

Časopis Saveza hemijskih inženjera Srbije

Chemical Industry

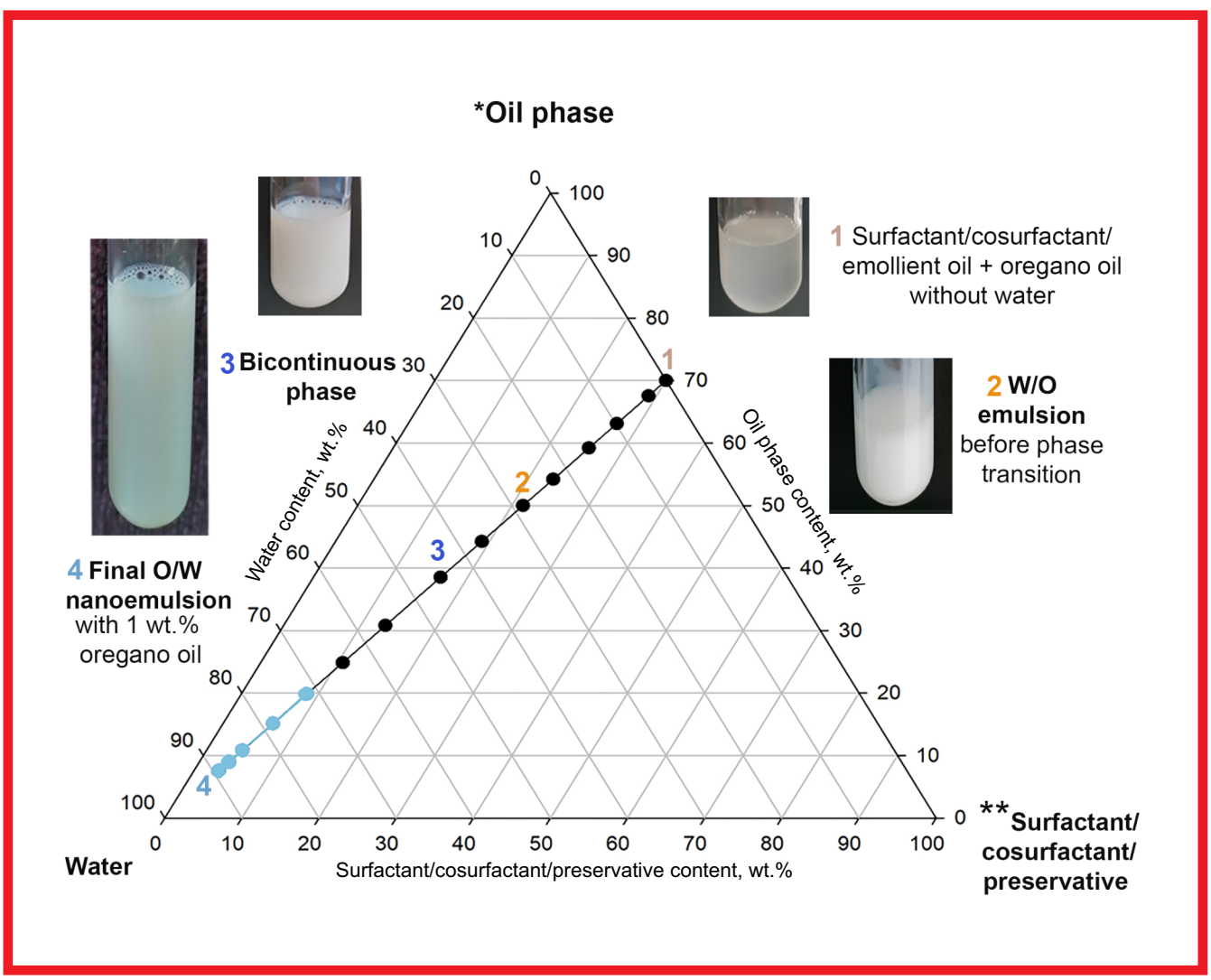

Aktivnosti Saveza hemijskih inženjera Srbije pomažu:

**MINISTARSTVO PROSVETE,
NAUKE I TEHNOLOŠKOG RAZVOJA
REPUBLIKE SRBIJE**

Tehnološko-metalurški fakultet
Univerziteta u Beogradu, Beograd

Institut za tehnologiju nuklearnih i
drugih mineralnih sirovina, Beograd

Hemijski fakutet Univerziteta u
Beogradu, Beograd

Prirodno-matematički fakultet
Univerziteta u Novom Sadu, Novi Sad

Institut za opštu i fizičku hemiju,
Beograd

Tehnološki fakultet
Univerziteta u Novom Sadu, Novi Sad

NU Institut za hemiju, tehnologiju i metalurgiju
Univerziteta u Beogradu, Beograd

Institut IMS, Beograd

Tehnološki fakultet
Univerziteta u Nišu, Leskovac

Fakultet tehničkih nauka,
Kosovska Mitrovica

Chemical Industry
Химическая промышленность

Hemijska industrija

Časopis Saveza hemijskih inženjera Srbije
Journal of the Association of Chemical Engineers of Serbia
Журнал Союза химических инженеров Сербии

VOL. 76 **Beograd, januar-februar 2022.** **Broj 1**

Izdavač
Savez hemijskih inženjera Srbije
Beograd, Kneza Miloša 9/I

Glavni urednik
Bojana Obradović

Zamenica glavnog i odgovornog urednika
Emila Živković

Pomoćnik glavnog i odgovornog urednika
Ivana Drvenica

Urednici
Enis Džunuzović, Ivana Banković-Ilić, Maja Obradović, Dušan Mijin, Marija Nikolić, Tatjana Volkov-Husović, Đorđe Veljović,

Članovi uredništva
Nikolaj Ostrovski, Milorad Cakić, Željko Čupić, Miodrag Lazić, Slobodan Petrović, Milovan Purenović, Aleksandar Spasić, Dragoslav Stoiljković, Radmila Šećerov-Sokolović, Slobodan Šerbanović, Nikola Nikačević, Svetomir Milojević

Članovi uredništva iz inostranstva
Dragomir Bukur (SAD), Jiri Hanika (Češka Republika), Valerij Meshalkin (Rusija), Ljubiša Radović (SAD), Constantinos Vayenas (Grčka)

Likovno-grafičko rešenje naslovne strane
Milan Jovanović

Redakcija
11000 Beograd, Kneza Miloša 9/I
Tel/fax: 011/3240-018
E-pošta: shi@ache.org.rs
www.ache.org.rs

Izlazi dvomesečno, rukopisi se ne vraćaju

Za izdavača: Ivana T. Drvenica

Sekretar redakcije: Slavica Desnica

Izdavanje časopisa pomaže
Republika Srbija, Ministarstvo prosvete, nauke i tehnološkog razvoja

Uplata pretplate i oglasnog prostora vrši se na tekući račun Saveza hemijskih inženjera Srbije, Beograd, broj 205-2172-71, Komercijalna banka a.d., Beograd

Menadžer časopisa i Kompjuterska priprema
Aleksandar Dekanski

Štampa
Razvojno-istraživački centar grafičkog inženjerstva, Tehnološko-metalurški fakultet, Univerzitet u Beogradu, Karnegijeva 4, 11000 Beograd

Indeksiranje
Radovi koji se publikuju u časopisu *Hemijska Industrija* ideksiraju se preko *Thompson Reuters Scietific®* servisa *Science Citation Index - Expanded™* i *Journal Citation Report (JCR)*

SADRŽAJ/CONTENTS

Hemijska industrija and the Association of Chemical Engineers of Serbia join the centenary celebration of the Institution of Chemical Engineers

Bojana Obradovic

[1]*University of Belgrade, Faculty of Technology and Metallurgy, Karnegijeva 4, P.O. Box 3503, 11120 Belgrade, Serbia*

EDITORIAL

Hem. Ind. **76 (1)** 1-3 (2022)

Available on-line at the Journal web address: http://www.ache.org.rs/HI/

The year 2022 is marking 100 years from inauguration of the Institute of Chemical Engineers (IChemE). After the first attempts to form a Society of Chemical Engineers in 1880, which resulted in foundation of the Society of Chemical Industry in 1881, IChemE was founded on May 2, 1922 in London gathering chemical engineering professionals from industry and academia. At the first Annual General Meeting in 1923 IChemE counted over 200 members, while today, it is a multi-national institution with primary offices in the UK and Australia with over 30,000 members worldwide and it is recognized as one of the leading professional organizations of chemical engineers.

In the cause of this important anniversary, IChemE is organizing a series of events aimed at promotion of chemical engineering as a profession and chemical engineers who contributed to the Institution. The program is titled "ChemEng Evolution" and includes different activities such as webinar panel discussions, a blog series, and a series of feature articles in The Chemical Engineer magazine. A dedicated website is established (https://www.chemengevolution.org/) offering articles and programs in different theme sections such as Sustainability & Environment, Education & Technology, Social Experience, Energy, Processes & Safety, Food & Water, Built Environment & Transport, Health, and Materials. The webinar series started in February, while announced panel discussions include "Shaping the future of Chemical Engineering Education" (March 9, 2022, 08:30 GMT), "The potential future trajectories of society and how the work of the chemical engineering profession may be tasked to add value" (April 13, 2022, 08:30 BST), "Redefining the Energy Mix: What does the future of energy look in the transition to Net Zero?" (May 11, 2022, 08:30 BST), "New SAFE Processes for a sustainable world" (June 8, 2022, 08:30 BST) and "Chemical Engineering for Sustainable Food and Water-Feast or Famine?" (July 13, 2022, 08:30 BST). The program is free and open to all upon registration at the ChemEng Evolution website.

The website also presents the especially interesting section "Inspirational chemical engineers", which tells stories of IChemE Past Presidents about chemical engineers that inspired them the most. Similarly, the section "Our members tell their own personal stories" presents the stories of chemical engineers, members of IChemE, about their work and life experiences. These sections are also open for contributions and IChemE invites participation of chemical engineers with their inspirational stories.

In partnership with ITN Productions Industry News, IChemE has produced a documentary "Serving Society" that looked at the role of the chemical engineer and how the profession is addressing some of the biggest challenges in our society today. The showcase premiered on the IChemE YouTube channel on January 25, 2022, while the full program and the individual films that were used in its production, can be watched at the IChemE website (https://www.icheme.org/).

The journal ***Hemijska industrija*** and the Association of Chemical Engineers of Serbia (AChE) join the centenary celebration of IChemE and invite all our contributors and members to take part in the very interesting and attractive program "ChemEng Evolution". As this year is the 75th anniversary of the journal ***Hemijska industrija*** and the next year marks the 70th anniversary of AChE, we take this opportunity to promote chemical engineering as a profession and a

Corresponding author: Bojana Obradovic, University of Belgrade, Faculty of Technology and Metallurgy, Karnegijeva 4, P.O. Box 3503, Belgrade, Serbia
E-mail: hi_ed@ache.org.rs

scientific discipline and invite scientific contributions in all various chemical engineering subdisciplines as well as inputs with news and stories from the industrial practice.

Hemijska industrija i Savez hemijskih inženjera Srbije se pridružuju proslavi stogodišnjice Instituta hemijskih inženjera (IChemE)

Bojana Obradovic

[1]*Univerzitet u Beogradu, Tehnološko-metalurški fakultet, Karnegijeva 4, P.O. Box 3503, 11120 Beograd, Srbija*

REČ UREDNIKA

Institut hemiskih inženjera (*Institution of Chemical Engineers*, *IChemE*) ove godine obeležava stogodišnjicu svoga postojanja. Posle prvih pokušaja osnivanja Društva hemijskih inženjera (*Society of Chemical Engineers*) 1880. godine, iz kojih je proizašlo osnivanje Društva za hemijsku industriju (*Society of Chemical Industry*) 1881. godine, organizacija *IChemE* je osnovana 2. maja 1922. godine u Londonu kao društvo koje okuplja hemijske inženjere iz industrije i akademije. Na prvoj godišnjoj skupštini održanoj 1923. g. društvo je brojalo oko 200 članova dok je danas to multinacionalna organizacija sa glavnim kancelarijama u Velikoj Britaniji i Australiji i sa preko 30.000 članova širom sveta što je čini jednom of vodećih profesionalnih organizacija hemijskih inženjera.

Povodom ove značajne godišnjice, *IChemE* organizuje seriju događaja koji imaju za cilj promovisanje hemijsko inženjerske profesije i hemijskih inženjera koji su doprineli razvoju ove organizacije. Program je nazvan "HI evolucija" (*ChemEng Evolution*) i sadrži različite aktivnosti kao što su panel diskusije putem vebinara, serije blogova i kolekcije tematskih članaka u časopisu *The Chemical Engineer*. Otvorena je posebna internet strana (https://www.chemengevolution.org/) na kojoj se mogu naći članci i programi u različitim tematskim oblastima kao što su: održivost i životna sredina, prosveta i tehnologija, društveno iskustvo, energija, procesi i sigurnost, hrana i voda, građevinski objekti i transport, zdravstvo, i materijali. Serija vebinara je počela u februaru ove godine, a najavljene su sledeće panel doskusije u narednom periodu: "Shaping the future of Chemical Engineering Education" (9. mart 2022, 08:30 po griničkom srednjem vremenu, GMT), "The potential future trajectories of society and how the work of the chemical engineering profession may be tasked to add value" (13. april, 2022, 08:30 h po britanskom letnjem vremenu, BST), "Redefining the Energy Mix: What does the future of energy look in the transition to Net Zero?" (11. maj 2022, 08:30 h po britanskom letnjem vremenu, BST), "New SAFE Processes for a sustainable world" (8. jun 2022, 08:30 h po britanskom letnjem vremenu, BST) and "Chemical Engineering for Sustainable Food and Water- Feast or Famine?" (13. jul 2022, 08:30 h po britanskom letnjem vremenu, BST). Program je besplatan i otvoren za sve uz registraciju na internet strani "HI evolucije".

Internet strana obuhvata i posebno zanimljiv odeljak "Inspirativni hemijski inženjeri" u kome su prikazane priče bivših predsednika *IChemE* o hemijskim inženjerima koji su za njih predstavljali najveću inspiraciju. Ne manje zanimljiv je i odeljak "Naši članovi pričaju svoje lične priče" u kome hemijski inženjeri, članovi *IChemE*, pričaju o svojim životnim i radnim iskustvima. Ovi odeljci su takođe otvoreni i *IChemE* poziva hemijske inženjere da pošalju svoje inspirativne priče.

Organizacija *IChemE* je u partnerstvu sa producentskom kućom "*ITN Productions Industry News*" snimila dokumentarnu emisiju "U službi društva" (*Serving Society*) u kojoj je sagledana uloga hemijskih inženjera i kako se ta profesija suočava sa nekim od najvećih izazova u našem društvu danas. Emisija je premijerno emitovana na *YouTube* kanalu 25. januara 2022. godine, dok se ceo program i pojedinačni filmovi koji su korišćeni u sastavljanju emisije mogu naći na internet stranici *IChemE* (https://www.icheme.org/).

Časopis ***Hemijska industrija*** i Savez hemijskih inženjera Srbije se priključuju proslavi stogodišnjice *IChemE* i pozivaju svoje saradnike i članove da uzmu učešće u veoma interesantnom i atraktivnom programu "HI evolucija". Ove godine je i 75 godina od prvog izlaska suplementa Industrijskog biltena koji je kasnije prerastao u nezavisan časopis ***Hemijska industrija***, a 2023. godine se navršava 70 godina od osnivanja Saveza, tako da koristimo tu priliku da promovišemo hemijsko inženjerstvo kao struku i naučnu disciplinu. Istovremeno upućujemo i poziv za dostavljanje naučnih priloga iz ove oblasti i srodnih disciplina, kao i vesti i reportaža iz industrijske prakse.

Differential scanning calorimetry-based investigations of erythritol – sodium chloride phase change composites for thermal energy storage

Paul Gregory Felix, Velavan Rajagopal and Kannan Kumaresan

PSG College of Technology, Coimbatore, India

Abstract

Low thermal conductivity of organic phase change materials (PCMs) for thermal energy storage systems induces the necessity to apply suitable heat transfer enhancement techniques for these materials. The purpose of this study was to improve thermal conductivity of a PCM erythritol by using sodium chloride as an additive, such that the material can be applied for steam cooking systems when integrated with solar parabolic trough collectors. In this study, erythritol-NaCl composites were synthesized by using the melting method, and the key physicochemical properties of the composites were estimated by using differential scanning calorimetry (DSC) coupled with thermo-gravimetric analysis (TGA). The observations indicate that there has been a significant improvement in the thermal conductivity of erythritol supplemented with NaCl. Further, thermal behaviour of the material indicates that it is suitable for steam cooking applications. Furthermore, mathematical models based on the experimental observations can be potentially utilized for further studies of erythritol-NaCl composites.

Keywords: composites; latent heat storage; mathematical modelling; steam cooking; thermal conductivity.

Available on-line at the Journal web address: http://www.ache.org.rs/HI/

ORIGINAL SCIENTIFIC PAPER

UDC: 616-073.66:(547.427.1+ 661.833`032.1)

Hem. Ind. **76 (1)** 5-18 (2022)

1. INTRODUCTION

Parabolic trough collectors (PTCs) find applications in cooking using solar energy and have potential benefits in elimination of green house gases (GHGs) [1-4]. Thermal energy storage (TES) systems when integrated with such PTCs [5-8] can be a potential technology for steam cooking over 24 h. Phase change materials (PCMs) can serve as potential TES media for this application owing to their latent heat storage [9]. PCMs store and release energy by virtue of their latent heat of phase transition without any significant temperature change, so that PCMs can store higher heat amounts than the sensible TES systems [10]. To be specific, organic PCMs exhibit stable melting and solidification cycles [11] at a broad spectrum of phase transition temperatures [12], possess significant latent heat of phase transition [13], are non-toxic [14], do not exhibit supercooling [13-15] and resistant to corrosion [16]. It has been identified that such organic PCMs when integrated with steam cooking systems can convert the complete steam cooking process to rely on renewable energy sources and, further, the higher latent heat of fusion of such materials will reduce the system size, since the higher latent heat of phase transition, the lower will be the quantity of PCM required. Among the various organic PCMs, erythritol ((2*R*,3*S*)-butane-1,2,3,4-tetrol [17]), as a PCM, gains importance. Erythritol ($C_4H_{10}O_4$) is a sugar alcohol [18] that can be suitable for medium temperature applications [19] as well as for solar TES applications owing to its high volume latent heat of 502.9 J cm^{-3} [20]. Next, from a steam cooking perspective, a PCM will be suitable for steam generation only if its melting temperature lies between 110-130 °C, so that the output steam can be maintained at a minimum of 100 °C. When erythritol is considered, it has a satisfactory latent heat of fusion values [21] and a melting point [22] suitable for the application. Furthermore, since erythritol is a food additive [23], it is conveniently safe to use in operation for steam cooking.

Still, it has been noted that a drawback of organic PCMs is in lower thermal conductivities, which can result in higher thermal resistances [24-26]. High thermal resistances would hinder the heat transfer through the material, resulting in

Corresponding authors: Paul Gregory Felix, PSG College of Technology, Coimbatore, India; Tel. +91-9629431403
E-mail: 1807rm01@psgtech.ac.in
Paper received: 26 May 2021; Paper accepted: 11 February 2022; Paper published: 25 February 2022.
https://doi.org/10.2298/HEMIND210526003F

longer charging times. Charging time is the time required for the material to heat from its ambient temperature to the desired temperature (post-melting). Erythritol, being an organic PCM, does not present an exception exhibiting low thermal conductivity [27,28]. For example, in an experimental study on erythritol as a PCM filling annular space of a shell-and-tube unit (between the cylinders of 45 mm OD and 100 mm ID and height of 900 mm), it was observed that approximately 12 h was needed for erythritol to completely charge [29]. Hence thermal conductivity improvement is required as the PCM should be charged within daytime, as the charging process is dependent on solar PTCs. In this direction, addition of high thermal conductivity additives to the base PCM has been reported as one of the promising methods [30]. In such a way phase change composites (PCCs) are obtained. For improvement the erythritol thermal conductivity different additives were investigated such as expanded graphite [27], percolated aluminium filler [31], modified carbon nanotubes [28], vermiculate with graphite [32], spherical graphite [33], and nickel nanoparticles [33]. Researchers have also synthesized PCCs based on erythritol by addition of copper, aluminium, SiO_2, and TiO_2 nanoparticles individually, which led to significant improvements in the thermal conductivity [34]. However, all of the aforementioned additives require at least to some extent specialized chemical preparation and processing techniques, and hence a readily available additive will be less complex in the PCC synthesis as well as more economical.

Preliminary literature search shows that physicochemical properties of sodium chloride (NaCl) are convincingly appropriate to be used as an additive to erythritol, which has hardly been investigated so far. The key physicochemical properties of NaCl are presented in Table 1.

Table 1. Physico-chemical properties of NaCl

Property	Magnitude	Reference
Specific heat, kJ kg^{-1} K^{-1}	0.88	[35]
Density, kg m^{-3}	2176	[36]
Thermal conductivity, W m^{-1} K^{-1}	6.1 at 30 °C; 3.5 at 140 °C	[37]
Melting temperature, °C	803.4	[38]

Hence, this study commenced with a hypothesis that, addition of NaCl as a higher thermal conductivity material than erythritol, will improve the overall thermal conductivity of the resulting PCC. Furthermore, NaCl being non-toxic can be conveniently used for steam cooking applications as it will not be harmful if any leaks or accidents occur in the system. Therefore, in this study, erythritol-NaCl PCCs were synthesized and experimentally investigated regarding intended thermal conductivity improvements. Also, parametric mathematical models were built using the estimated parameters to aid researchers to perform numerical studies on erythritol-NaCl PCCs.

2. MATERIALS AND METHODS

2. 1. Study design

This study was conducted in three phases comprising: the synthesis of the erythritol-based PCCs, estimation of key physicochemical properties of the synthesized PCCs, and, ultimately, mathematical modelling to map variations in the key physicochemical properties as shown in Figure 1. Firstly, a certain quantity of pure erythritol was subjected to controlled heating (until complete melting) by using an electric heater followed by cooling such that the melting and solidification behavior could be observed. Further, as it was previously reported [39] that pure erythritol undergoes a mass loss when heated beyond approximately 220 °C, we have also verified such behavior of the material. Following preliminary investigations, erythritol-based PCCs were then synthesized, and the key physicochemical properties were estimated experimentally by using differential scanning calorimetry (DSC) and thermo-gravimetric analysis (TGA). The obtained results were used to derive mathematical models for deeper interpretation.

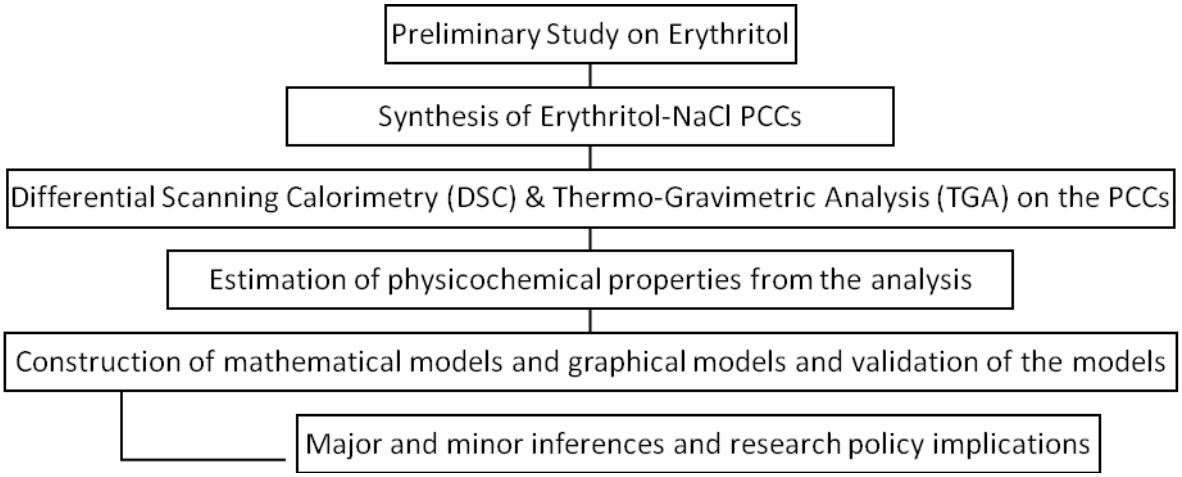

Figure 1. A schematic representation of the study design adopted in the present work

2. 2. Synthesis of the PCCs

Erythritol-NaCl PCCs were synthesized at four different NaCl mass contents: 10, 20, 30 and 40 %. The composition was designed so that the obtained composite would exhibit both the latent heat of fusion of pure erythritol as well as the high thermal conductivity of NaCl. Analytical grade erythritol with 99 % purity was procured from Shandong Sanyuan Biotechnology, China for the synthesis and used without any further chemical and physical processing. Also, industry-grade NaCl (Baba Chemicals, India) was utilized for the synthesis as commercial and edible grade NaCl are not recommended due to possible iodized form. All PCCs were synthesized by adopting the melting method from literature [40,41] so that NaCl was added to erythritol in molten state. A detailed schematic presentation of the procedure that was adopted for the synthesis of all PCCs is presented in Figure 2.

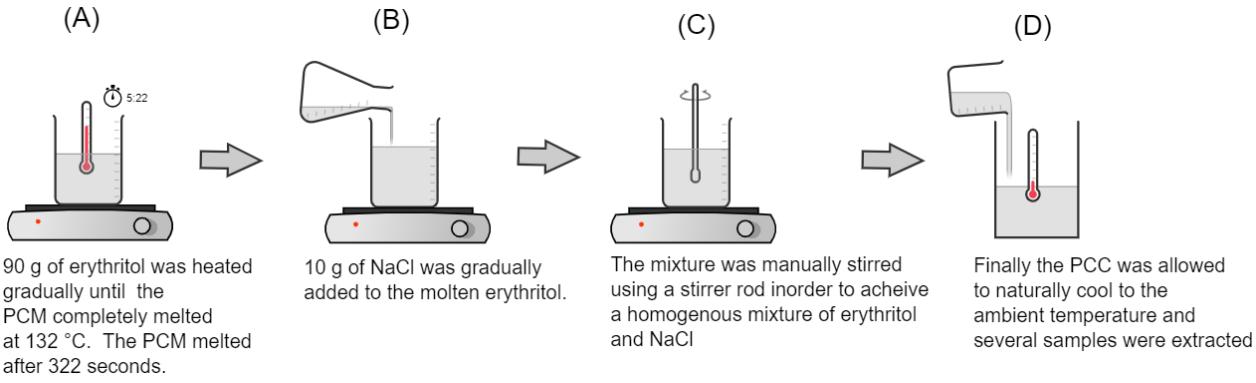

Figure 2. This illustration depicts the synthesis methodology adopted in this current study. In this procedure a 1000 W hot-plate apparatus (Sigma, India) was utilized for heating. All of the synthesis procedures were carried out at PSG College of Technology and for each PCC synthesized, five sets of replicate experimentations were carried out.

2. 3 Estimation of physicochemical properties of the obtained PCCs

All of the synthesized PCCs were subjected to DSC-TGA experimental analysis. During the DSC-TGA procedure, the sample PCC was placed in an aluminium crucible and both materials were subjected to uniform heating, temperature development was monitored, and the resulting heat flux magnitudes were recorded. All DSC-TGA experimental analyses were performed by using a NETZSCH STA 449F3 STA449F3A-1100-M apparatus (NETZCH, Germany). Uniform heating rate of 10 K min^{-1} was applied in all investigations and all experiments were carried out in an N_2 environment. All samples were subjected to the analysis up to 300 °C. High-temperature studies were not necessary in the present case since the synthesized PCCs are intended for TES applications for steam cooking purposes, and thus will not be subjected to very high temperatures. DSC-TGA analyses served to plot the heat flux (ϕ) and the sample mass in respect to the initial mass

(m_{pcc}) as functions of the PCC temperature (T). A sample curve for the heat flux profile recorded for the erythritol sample is presented in Figure 3 for illustration.

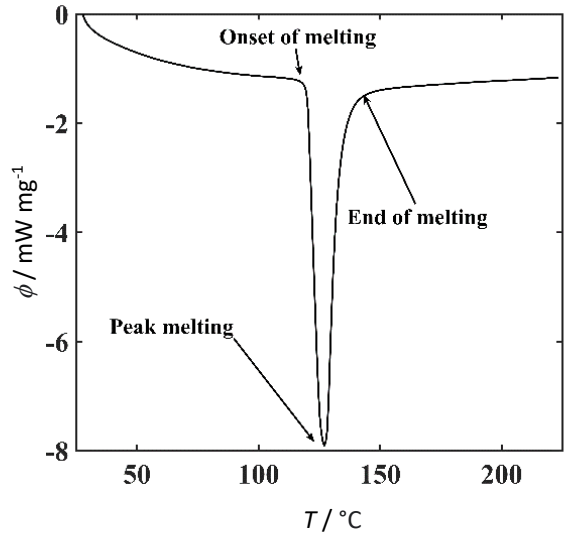

Figure 3. An illustration of the DSC heat flux profile (obtained for erythritol sample) for interpretation

From the heat flux profile, the peaking zone was identified as the phase transition zone [42] and the corresponding melting temperatures were recorded. Further, the area under the melting curve (A_m) was utilized to estimate the latent heat of fusion (λ) of the sample. The mathematical formulation utilized to estimate the latent heat magnitude from the DSC observation is presented by the equation (1):

$$\lambda = \frac{A_m}{\frac{\delta T}{\delta t}} \tag{1}$$

The activation energy (E_a) was estimated by adopting the Coats-Redfurn method by utilizing the TGA thermogram [43]. This method has been adapted from the Arrhenius equation [44-46]. In this method, the first order reaction is represented as in equation (2):

$$\log\left(\frac{-\log(1-\alpha)}{T^2}\right) = \log\frac{AR_m}{\beta' E_a}\left(1-\frac{2RT}{E_a}\right) - \frac{E_a}{2.303RT} \tag{2}$$

In the equation, α denotes the instantaneous fraction of the sample decomposed, A denotes the frequency factor, R is the universal gas constant and β' is the employed heating rate (in the TGA process). In the Eq. (2), the term E_a / 2.3030R was estimated by estimating the slope of the plot of log [-log (1-α)/T^2] *vs.* 1000/T. Then, the activation energy (E_a) was estimated by applying the equation (3):

$-E_a/2.303R$ = Slope (3)

Thermal conductivities for all compositions were estimated by adopting the thermal resistance methodology. This method is based on the fundamental thermal conductivity equation as shown in the equation (4):

$Q = k\,(\delta T/L)\,A_{CS}$ (4)

This methodology has previously been adopted by several researchers to estimate the thermal conductivity magnitudes from the DSC-TGA thermograms [47-49]. In this approach a plot of the differential power in DSC-TGA (ΔP) and the programmed temperature (T_{pr}) was determined, and the slope was equated to the thermal resistance (R_c) by adopting the equation (5):

$$\frac{d\Delta P}{dT_p} = \frac{2}{R_c} \tag{5}$$

Further, the thermal conductivity was estimated for each composition by utilising the equation (6):

$$R_c = \frac{l^h}{k_{s/l} A_{CS}} \tag{6}$$

The procedure was performed individually for solid temperature and liquid temperature ranges and ultimately the solid phase and liquid phase thermal conductivities were obtained. In the equations, k represents the thermal conductivity, A_{cs} represents the cross-sectional area of the material, l^h represents the height of the sample when placed in the DSC-TGA apparatus. Dimensions of the aluminium crucible equipped was utilised to estimate the dimensional parameters required to estimate the thermal resistance R_c.

Further, the liquid fraction (β) was estimated by utilizing the model proposed by Beata *et al.* [50], as presented by the equation:

$$\beta = \begin{cases} \dfrac{T - T_{ms}}{T_{me} - T_{ms}} & T_{ms} < T < T_{me} \\ 0 & T < T_{ms} \\ 1 & T_{me} < T \end{cases} \tag{7}$$

were T_{ms} denotes the onset temperature of melting, T_{me} denotes the completion temperature of melting. Also, the apparent heat capacity (C) was estimated independent of the mass by correlating the heat flux (ϕ), temperature (T), and time (t), by using the equation (8):

$$C = \phi\, t \,/\, T \tag{8}$$

For the above correlation, the instantaneous heat flux magnitudes recorded by the DSC-TGA apparatus were utilised together with the corresponding instantaneous temperature. Further, the time needed for the sample to reach that particular temperature was also recorded and was utilised in the estimation.

The charging time (t_c) expressed per unit mass of the composites was observed in order to estimate the improvement of the material functionality by addition of NaCl. In this study, the charging time was discretized into three parts for the analysis. The time taken by the PCM/PCC to rise from the ambient temperature to the onset of melting (solidus temperature) was termed as solid sensible charging time (t_{ss}) and the time taken by the material to change phase completely was termed as melting time (t_m). In other words, melting time can be considered as the time taken by the material to change from the onset melting temperature (T_{ms}) to the end melting temperature (liquidus temperature). Further, the time taken by the material to rise from the end melting temperature (T_{me}) to the desired temperature is termed as liquid sensible charging time (t_{ls}). The total charging time was estimated by the summation of the afore mentioned charging times. Since this study is intended for a TES application in a steam cooking system, in the charging time estimation the final temperature was considered to be 140 °C. It is desired for PTCs for steam cooking applications to provide steam at a temperature in the range 140-160 °C to charge the PCCs, and hence the temperature was chosen.

2. 4. Mathematical modelling of the estimated parameters

Mathematical modelling of the estimated parameters for the PCMs and PCCs was performed in order to get an insight into the material behaviour at a holistic level. The Stefan's condition for PCM mathematical modelling provides scope for individual parametric modelling of latent heat of fusion (λ), solid-phase thermal conductivity (k_s) and liquid phase thermal conductivity (k_l). The Stefan's condition is presented by the equation (9) [24]:

$$\lambda\rho\left(\frac{\mathrm{d}S(t)}{\mathrm{d}t}\right) = k_s\left(\frac{\delta T_s}{\delta t}\right) - \left(\frac{\delta T_l}{\delta t}\right) \tag{9}$$

In the present study, parametric mathematical modelling of λ, k_s and k_l was performed by using the Gauss-Newton iterative algorithm and asymptomatic regression models were applied for modelling. The general form for asymptomatic regression models (concave and convex) is presented as:

$$f(x) = \theta_1 - \theta_2\, e^{-\theta_3 m} \tag{10}$$

where θ_1, θ_2 and θ_3 represent asymptotic regression constants and m represents the content of NaCl in the composition.

3. RESULTS AND DISCUSSION

3. 1. Preliminary investigations of erythritol

Erythritol, when subjected to controlled heating was observed to thermally behave similarly to smart materials. When erythritol was heated, physical changes were absent up to 120 °C during which time the heat transfer was carried out completely by conduction. Beyond this temperature, there was a slight phase change near the bottom of the beaker, followed by considerable development in the melting front thereon. Further, during the phase change, motion of the solid and the liquid phases was observed due to the density difference, which indicates the convective heat transfer during the melting process. Change of color was not observed during the study. Upon completion of melting, erythritol appeared to be a viscous, clearly transparent liquid. Next, the liquid was allowed to naturally cool and after solidification, clear crystallite formation was observed. During solidification, the layer of the fluid facing the mouth of the beaker (in contact with air) and that in contact with the glass beaker were the first to solidify after which the solidification pattern spread out to the other parts of the material. Even though this preliminary investigation has provided an insight into the behaviour of the material; this investigation could not provide an accurate measurement of the melting temperature as the study was performed by using a conventional thermometer. The photographs of the melting and crystallization phenomena have been provided in the Supplementary material (Fig. S-1). But despite the shortcomings, heat absorption and heat releasing phenomena of the material have been well observed and this has paved the way for further intricate analysis.

3. 2. Variation in the physicochemical parameters of the PCCs

By the TGA analysis, mass losses of erythritol and all synthesized PCCs upon heating were determined. The plot of the sample mass in respect to the initial mass (m_{pcc}) *vs*. temperature is presented in Figure 4(a). It can be observed that all investigated materials behave similarly. Initiation of the significant the mass loss was only near 220 °C. If the TGA plot is intricately observed, it can be noticed that erythritol shows lower mass stability than its derivative PCCs. At 300 °C, it can be observed that there is only 20% of the residual mass of erythritol, whereas nearly 60 % residual mass for the 40 % NaCl material. For the materials with 10 and 20 % NaCl, the mass residual was 40 % , while for the 30 % NaCl material, it was nearly 25 %. The PCC with 20 % NaCl showed a profile with a sharp, though statistically insignificant drop (2.7 %) in the mass during the initial stages of heating.

The thermal degradation temperature (T_d) of the PCCs is presented in Figure 4(b) while the heat flux in Figure 4(c). A steady decrease in the heat flux during the initial stages of heating can be observed for all materials, followed by a steep descent and minimum and then another steady region. The largest minimum heat flux value was determined for erythritol while the lowest for the PCC with 40 % NaCl. In all cases, the melting zone lies between 110 and 140 °C. The area of the peak flux was evaluated and the latent heats of fusion were estimated according to the Eq. (1). The differential $(\delta T/\delta t)$ was experimentally recorded. The results are presented in Figure 4(d) showing that the latent heat of fusion decreases with the increase in the NaCl content in the PCC. From the heat flux graph, the onset of melting temperature (T_{ms}), peak melting temperature (T_{mp}), and the end melting temperature (T_{me}) were estimated (Fig. 4(e)). It can be observed that the addition of NaCl has not imposed any significant change in the melting range. Nevertheless, the fact that the magnitudes of T_{ms} for compositions of 20-40 % NaCl are lower than those for 0 and 10 % NaCl, the decrease has been considered insignificant as the difference between the highest and the lowest T_{ms} magnitude is only 5.2 %. The highest T_{ms} magnitude has been reported for 10 % NaCl (120.3 °C) case and the lowest magnitude has been reported for 40 % NaCl case (114 °C).

Activation energies were estimated by adopting Eqs. (2)-(3). The estimated activation energies are presented in the Supplementary material (Fig. S-2). All investigated PCCs have shown statistically equivalent activation energies. It should be noted that the PCCs with 20 and 30 % NaCl have shown similar magnitudes of both the latent heat of fusion and the activation energy. Solid and liquid phase thermal conductivities were calculated by using the Eq. (6). Estimated solid and liquid thermal conductivities are presented in Figure 5(a) showing significant increases in magnitudes up to nearly 3 and 2.5 times, respectively.

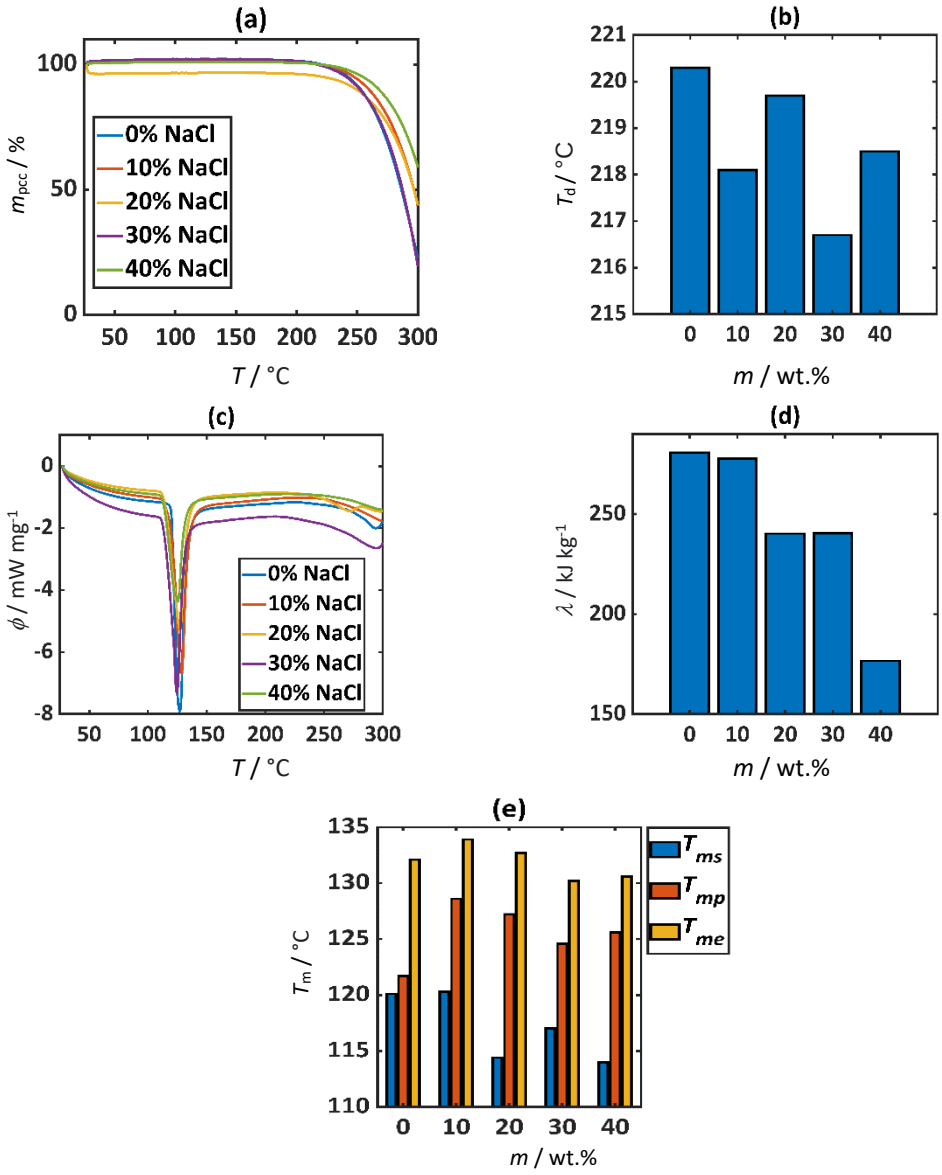

Figure 4. a - variation in the sample mass in respect to the initial mass (m_{pcc}) vs. T during the TGA analysis; b - variation in the thermal degradation temperature (T_d) with respect to the mass content of NaCl; c - variation of the instantaneous heat flux (ϕ) with temperature; d - the variation in the latent heat of fusion (λ) with respect to the mass content of NaCl; e - variation in the various melting temperatures (T_{ms}, T_{mp} and T_{me}) with respect to the mass content of NaCl. Data presents average values of 3 experimental repetitions. In the figures, m indicates the content of NaCl in erythritol

Liquid fraction profiles calculated based on experimentally determined temperature values and Eq. (7) are presented in Figure 5(b). Apparent heat capacity profiles calculated by using Eq. (8) and experimental values are presented in Figure 5(c). The heat capacities showed a sharp increase during the onset of melting and a sharp decrease during the end of melting. The T-history was generated by utilizing the equipment logger. As a uniform heating rate was provided to the material, the corresponding material temperature was also recorded. Temperature history (T-history) of the investigated materials is determined and presented in Figure 5(d). It can be observed that the PCCs exhibited faster melting than erythritol. To intricately analyse the T-history phenomenon, a specific temperature zone between 100 to 130 °C is enlarged (Fig. 5(e)) showing that the increase in NaCl content enhances the temperature increase rate of the PCCs. The T-history profile presents the duration of temperature development for one milligram of the sample. Hence it can be stated that the addition of NaCl to erythritol reduces the charging time of the obtained PCCs.

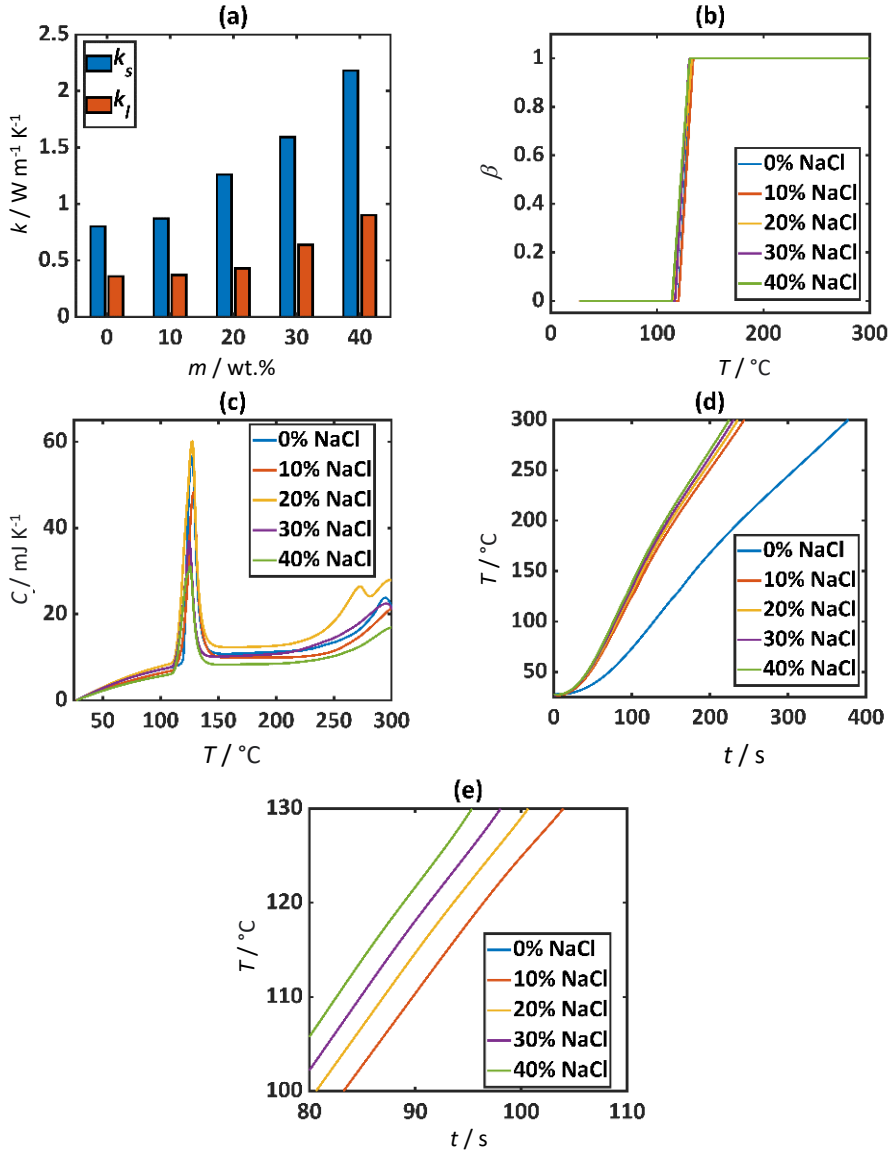

Figure 5. a - variation of solid thermal conductivity k_s and liquid thermal conductivity k_l with respect to the quantity of NaCl in erythritol; b - variation in liquid fraction (β) contour with respect to temperature; c - variation of apparent heat capacity (C) with temperature; d,e - T-history of the PCC samples. In the figures, m indicates the content of NaCl in erythritol

The total charging time per unit mass of the PCC along with times of separate charging phases is presented in Figure 6.

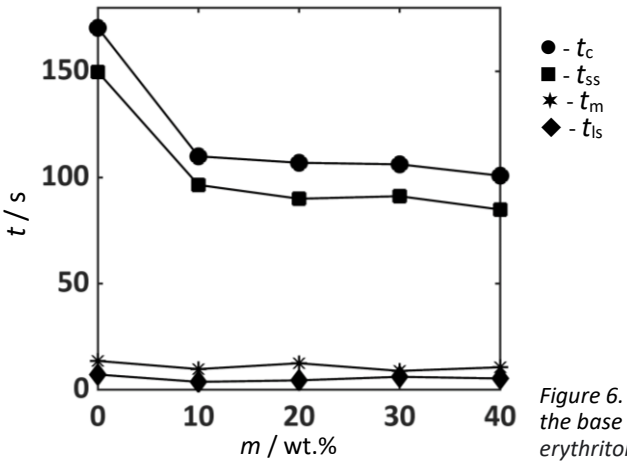

Figure 6. Variation of charging time with respect to the quantity of NaCl in the base PCM erythritol. In the figure, m indicates the content of NaCl in erythritol

From the figure, it is apparent that the charging time decreases with an increase in the NaCl fraction, and it is interesting to further note that the solid sensible time contributes the most to the overall charging time. In the Figure 6, t_{ss} denotes the solid sensible time, t_{ls} denotes the liquid sensible time, t_m denotes the melting time and t_c denotes the charging time. All time components indicate the time for one milligram of the samples. A detailed description on the various time components is provided in the Materials and Methods section

3. 3. Discussion on the thermal behaviour of the PCCs

The obtained experimental results have been compared to the observed charging times. It can be inferred that the solid thermal conductivity plays a major role in the sensible heat transfer in the PCCs. By comparing Figures 5(a) and 6, it can be noted that there is a decrease in the solid sensible charging time with a proportional increase in the solid thermal conductivity magnitude. Also, it can be observed that although there is a significant increase in the liquid thermal conductivity magnitudes, the liquid sensible time has not shown any significant change. This phenomenon is due to the basic phase change mechanism that liquid heat transfer is convection-dominated. However, the DSC-TGA analysis cannot give information on the convection magnitude. This study was commenced with a hypothesis that the addition of a higher thermal conductivity material will decrease the charging time of the resulting PCCs and the hypothesis has been validated by using the experimental observations. Table 2 presents the variation in the key physicochemical parameters of the PCCs in a more comprehensive way.

Table 2. Variations in parameters (in comparison to those of pure erythritol)

m_{NaCl} / wt.%	Increase of k_s, %	Increase of k_l, %	Decrease of λ, %	Decrease of t_c, %
10	9	6	1	36
20	58	23	14	37
30	100	82	14	37
40	173	156	37	41

The current experimental observations indicate a decrease in the latent heat with the increase in the thermal conductivity, which conforms to several literature reports. For instance, a study on nanoparticle dispersed in a PCM has shown the latent heat variation for the PCCs before and after addition of nanoparticles [51]. Also, it has been observed that the latent heat of phase transition decreases with the addition of a high thermal conductivity material in many systems studied in literature such as: eicosane - silver nanoparticle PCC, octadecane-CuO nanoparticles PCC, 1-do-decanol-graphite nanoparticles PCC, RT22-graphene nanoparticle PCC, *etc.* Similarly, in another research it was reported that addition of graphene nanoparticles to pure erythritol, there was a decrease in the latent heat with the increase in the thermal conductivity [41].

The observed heat flux profiles can be utilized as an indication of the trend of the latent heat of fusion. It can be observed from Figure 5(c), that the highest heat flux peak was achieved for erythritol (having the highest latent heat) while the lowest peak was observed for the PCC with 40 % NaCl (having the lowest latent heat). Hence, the heat flux curve can be presented as a comparative model to infer whether there is a decreasing or an increasing trend in the latent heat. However, computations have to be made to estimate the exact magnitude of the latent heat of fusion. Also, it was observed that the thermal degradation temperature (t_d) for all the composites is nearly 220 °C. From the TES application perspective, the maximal application temperature will be 140 °C and hence all the investigated PCCs are suitable for this use. Further, the estimated activation energy for all of the cases conforms to the limits of activation energy for sugar alcohols [52]. It has been observed that the magnitudes of the key physicochemical parameters estimated for erythritol conform to several literature sources, as shown in Table 3.

Table 3. Comparison of parameters for erythritol determined experimentally in the present study with literature reports.

Parameter	Current Study	Literature reports	Reference
k_s / W m^{-1} K^{-1}	0.798	0.733	[53]
k_l / W m^{-1} K^{-1}	0.357	0.326	[53]
λ / k J kg^{-1}	280.7	284 - 370	[54]
T_{mp} / °C	121.7	120.39, 120	[29],[41]

3. 4. Mathematical modelling of the parameters and discussion

To aid the solution for a typical Stefan problem, mathematical models were formulated for predictions of latent heat of fusion, solid thermal conductivity and liquid thermal conductivity. The mathematical models are presented by Eqs. (10) - (13) and the graphical form of the models is presented in Figure 7. In the equations, m represents wt.% of NaCl in the material.

$$\lambda = 289.798 - 10.0862\ e^{0.0598649m} \quad (11)$$

$$k_s = 0.387994 + 0.375957\ e^{0.03905574m} \quad (12)$$

$$k_l = 0.294262 + 0.0435885\ e^{0.0659759m} \quad (13)$$

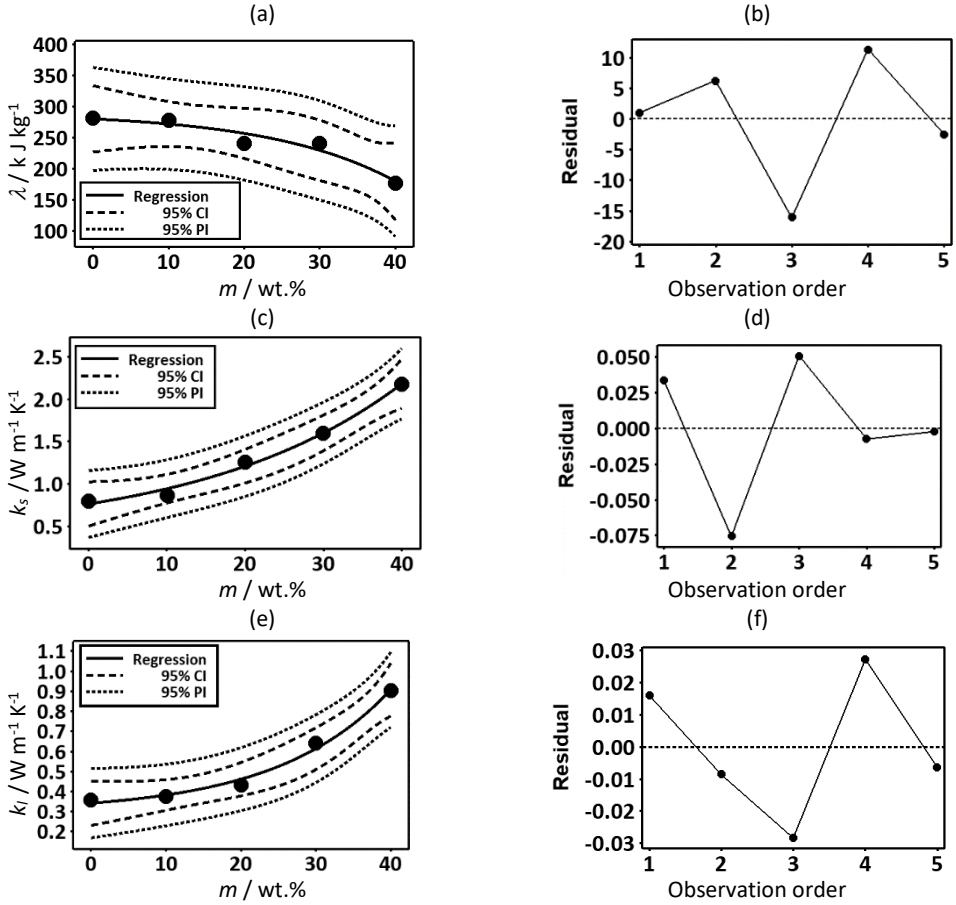

Figure 7. a - graphical form of the latent heat of fusion model; b - residuals for the latent heat of fusion model; c - graphical form of the solid thermal conductivity model. ; d - residuals for the solid thermal conductivity model; e - graphical form of the liquid thermal conductivity model; f - residuals for the liquid thermal conductivity model. In the figures, residuals indicate the difference between the observed value and the fitted value. Further, observation order indicates the index of the input wt.% magnitude of NaCl. Since there are 5 compositions, five observation orders were reported. Furthermore, CI represents the Confidence Interval and PI represents the Prediction Interval for the regressions. m indicates the content of NaCl in erythritol

As it is shown, all of the model predictions are within a 95 % confidence level and can be used as a tool to predict the behaviour of key physicochemical properties of the PCCs. From an applicability perspective, the models can be utilized for an effective system design. While selecting a specific composition of the PCC for the desired application, these mathematical models can be utilized to estimate the mass of the PCM/PCC required and thereby aid the system sizing. To facilitate optimization and to completely study the holistic behavior of the PCCs, four graphical contour models were built using the DSC-TGA observations and the constructed mathematical models (Fig. 8). The models were constructed by utilizing the distance method of interpolation and by utilizing a regular mesh for estimation [55]. Since a regular mesh and a uniform interpolation method was adopted, 5 observatory data values were sufficient for the construction of the models. The contour models plot solid thermal conductivity and liquid thermal conductivity in two

dimensions and consider the latent heat of fusion, melting time, the quantity of NaCl and peak melting temperature in the third dimension individually.

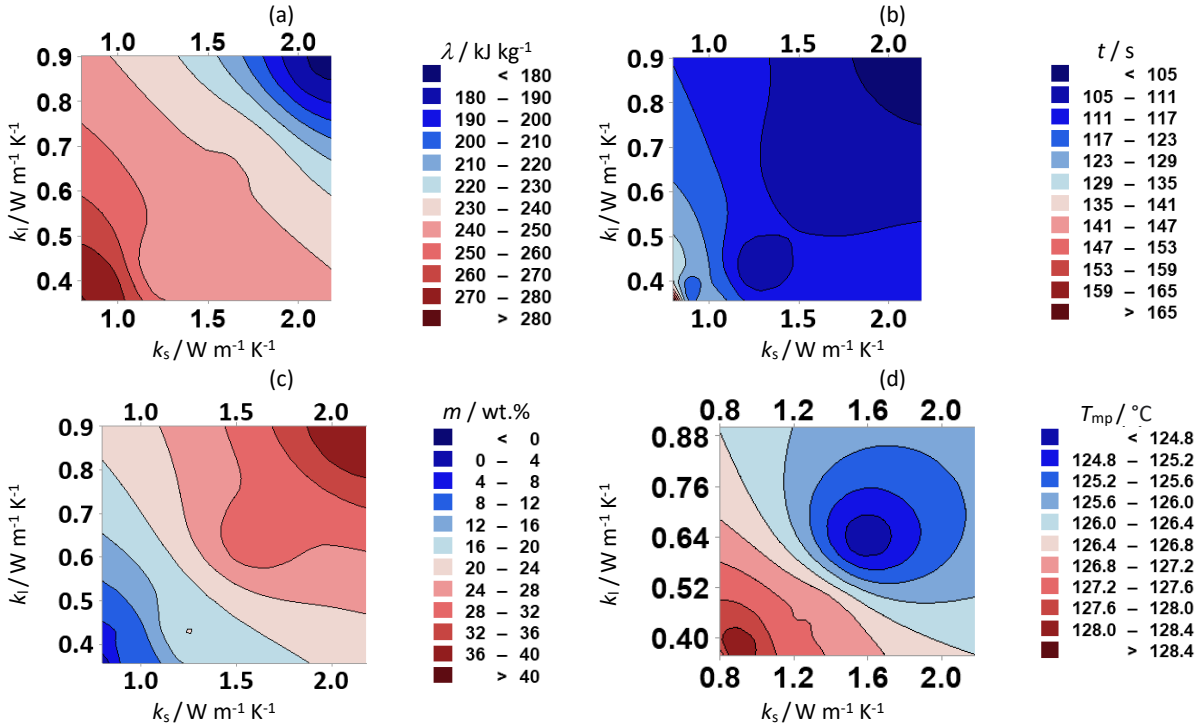

Figure 8. Contour plots of the solid (k_s) and liquid (k_l) thermal conductivities with respect to different parameters: a - latent heat of fusion (λ); b - melting time (t); c - mass content of NaCl; and d - peak melting temperature (T_{mp}). In the figures, m indicates the content of NaCl in erythritol.

From Figure 8(a), it can be inferred that lower solid thermal conductivity and lower liquid thermal conductivity are connected with a higher latent heat of fusion. Also, Figure 8(b) presents the apparent notion that the higher the thermal conductivities, the lower will be the charging time. When correlated with the contour from Figure 8(c), it can be inferred that the higher quantities of NaCl result in higher magnitudes of thermal conductivity. Figure 8(d) gains attention as it presents a unique understanding of the peak melting temperature of the NaCl containing PCCs. Since the peak melting temperature (T_{mp}) was estimated in relation to the solid and thermal conductivities, this visualisation presents an understanding from a thermal conductivity perspective. If it is compared with Figure 8(c), it can be noted that this behaviour of T_{mp} is inverse to that of the NaCl mass content behaviour. From a broader perspective, it was discussed earlier that the melting temperature was not significantly changed with the addition of NaCl. Despite insignificant magnitude changes, this contoured model has provided an insight that the higher the thermal conductivities, the lower will be the peak melting temperatures. The built contour plots are valid and reliable as they reflect the DSC-TGA observations.

4. CONCLUSION

In summary, this study has experimentally investigated the thermal behaviour of the erythritol-NaCl PCCs. NaCl has been identified as a potential additive to erythritol as it significantly improved the thermal conductivity of the composites, thereby reducing the charging time. Also, it has been observed that there is an insignificant change in the melting temperature and the activation energy of the PCCs with the addition of NaCl. Further, the DSC-TGA based approach has been inferred to be effective for thermal investigations of PCMs and PCCs as it is systematic providing explicit and implicit estimation of multiple parameters, and hence the methodology is highly recommended for similar investigations. The experimental results were shown as reliable by the comparison with literature reports for erythritol PCMs. Further, the formulated mathematical models and graphical interpretations find applicability in optimizing the

composition and also in the TES system design. From a steam cooking perspective, the synthesized erythritol-PCCs can be envisaged as a potential thermal storage medium that does not degrade at the application temperature.

Acknowledgements: These authors would like to thank the Department of Science and Technology (DST), Government of India and the management of the PSG College of Technology, Coimbatore for their financial support to undertake this project.

REFERENCES

[1] Indora S, Kandpal TC. Institutional cooking with solar energy: A review. *Renew Sustain Energ Rev* 2018;84:131–54. https://doi.org/https://doi.org/10.1016/j.rser.2017.12.001

[2] Motwani K, Patel J. Cost analysis of solar parabolic trough collector for cooking in Indian hostel–a case study. *Int J Ambient Energy* 2019;0(0):1–17. https://doi.org/10.1080/01430750.2019.1653968

[3] Kalogirou SA. Solar thermal collectors and applications. *Prog Energ Combust* 2004;30(3):231-295. https://doi.org/10.1016/j.pecs.2004.02.001

[4] Ravi Kumar K, Krishna Chaitanya NVV, Sendhil Kumar N. Solar thermal energy technologies and its applications for process heating and power generation. *J Clean Prod* 2021;282:125296. https://doi.org/10.1016/j.jclepro.2020.125296

[5] Koçak B, Fernandez AI, Paksoy H. Review on sensible thermal energy storage for industrial solar applications and sustainability aspects. *Sol Energy* 2020;209:135–69. https://doi.org/10.1016/j.solener.2020.08.081

[6] Akba T, Baker D, Yazıcıoğlu AG. Modeling, transient simulations and parametric studies of parabolic trough collectors with thermal energy storage. *Sol Energy* 2020;199:497–509. https://doi.org/10.1016/j.solener.2020.01.079

[7] Ghazouani M, Bouya M, Benaissa M, Anoune K, Ghazi M. Thermal energy management optimization of solar thermal energy system based on small parabolic trough collectors for bitumen maintaining on heat process. *Sol Energy* 2020;211:1403–21. https://doi.org/10.1016/j.solener.2020.10.074

[8] Biencinto M, Bayón R, González L, Christodoulaki R, Rojas E. Integration of a parabolic-trough solar field with solid-solid latent storage in an industrial process with different temperature levels. *Appl Therm Eng* 2021;184:116263. https://doi.org/10.1016/j.applthermaleng.2020.116263

[9] Shchukina EM, Graham M, Zheng Z, Shchukin DG. Nanoencapsulation of phase change materials for advanced thermal energy storage systems. *Chem Soc Rev* 2018;47(11):4156–75. https://doi.org/10.1039/c8cs00099a

[10] Sutjahja IM, Rahman A, Putri RA, *et al.* Electrofreezing of the phase-change material $CaCl_2{\cdot}6H_2O$ and its impact on supercooling and the nucleation time. *Hem Ind* 2019;73(6):363–74. https://doi.org/10.2298/HEMIND190803034S

[11] Jahanpanah M, Sadatinejad SJ, Kasaeian A, Jahangir MH, Sarrafha H. Experimental investigation of the effects of low-temperature phase change material on single-slope solar still. *Desalination* 2021;499:114799. https://doi.org/10.1016/j.desal.2020.114799

[12] Atinafu DG, Ok YS, Kua HW, Kim S. Thermal properties of composite organic phase change materials (PCMs): A critical review on their engineering chemistry. *Appl Therm Eng* 2020;181:115960. https://doi.org/10.1016/j.applthermaleng.2020.115960

[13] Magendran SS, Khan FSA, Mubarak NM, *et al.* Synthesis of organic phase change materials (PCM) for energy storage applications: A review. *Nano-Structures and Nano-Objects* 2019;20:100399. https://doi.org/10.1016/j.nanoso.2019.100399

[14] Singh P, Sharma RK, Ansu AK, Goyal R. Study on thermal properties of organic phase change materials for energy storage. *Mater Today Proc* 2020;28(4):2353–7. https://doi.org/10.1016/j.matpr.2020.04.640

[15] Sharma RK, Ganesan P, Tyagi V V., Metselaar HSC, Sandaran SC. Developments in organic solid-liquid phase change materials and their applications in thermal energy storage. *Energy Convers Manag* 2015;95:193–228. https://doi.org/10.1016/j.enconman.2015.01.084

[16] Atinafu DG, Dong W, Huang X, Gao H, Wang G. Introduction of organic-organic eutectic PCM in mesoporous N-doped carbons for enhanced thermal conductivity and energy storage capacity. *Appl Energy* 2018;211:1203–15. https://doi.org/10.1016/j.apenergy.2017.12.025

[17] Carly F, Vandermies M, Telek S, *et al.* Enhancing erythritol productivity in Yarrowia lipolytica using metabolic engineering. *Metab Eng* 2017;42:19–24. https://doi.org/10.1016/j.ymben.2017.05.002

[18] Coccia G, Aquilanti A, Tomassetti S, Comodi G, Di Nicola G. Design, realization, and tests of a portable solar box cooker coupled with an erythritol-based PCM thermal energy storage. *Sol Energy* 2020;201:530–40. https://doi.org/10.1016/j.solener.2020.03.031

[19] Anish R, Mariappan V, Joybari MM, Abdulateef AM. Performance comparison of the thermal behavior of xylitol and erythritol in a double spiral coil latent heat storage system. *Therm Sci Eng Prog* 2020;15:100441. https://doi.org/10.1016/j.tsep.2019.100441

[20] Yuan M, Ye F, Xu C. Supercooling study of erythritol/EG composite phase change materials. *Energy Procedia* 2019;158:4629–34. https://doi.org/10.1016/j.egypro.2019.01.744

[21] Junior JFR, Oliveski RDC, Rocha LAO, Biserni C. Numerical investigation on phase change materials (PCM): The melting process of erythritol in spheres under different thermal conditions. *Int J Mech Sci* 2018;148:20–30. https://doi.org/10.1016/j.ijmecsci.2018.08.006
[22] Nazzi Ehms JH, De César Oliveski R, Oliveira Rocha LA, Biserni C. Theoretical and numerical analysis on phase change materials (PCM): A case study of the solidification process of erythritol in spheres. *Int J Heat Mass Transf* 2018;119:523–32. https://doi.org/10.1016/j.ijheatmasstransfer.2017.11.124
[23] Rakicka-Pustułka M, Mirończuk AM, Celińska E, Białas W, Rymowicz W. Scale-up of the erythritol production technology – Process simulation and techno-economic analysis. *J Clean Prod* 2020;257:120533. https://doi.org/10.1016/j.jclepro.2020.120533
[24] Fleischer AS. Thermal energy storage using phase change materials: Fundamentals and applications. Springer, Cham, 2015. https://doi.org/10.1007/978-3-319-20922-7
[25] Casini M. Phase-change materials. *Smart Build.* 2016;179–218. https://doi.org/10.1016/B978-0-08-100635-1.00005-8
[26] Kuznik F, Johannes K, David D. Integrating phase change materials (PCMs) in thermal energy storage systems for buildings. Adv. Therm. Energy Storage Syst. Methods Appl. Woodhead Publishing Limited; 2014;325–56. https://doi.org/10.1533/9781782420965.2.325
[27] Yuan M, Ren Y, Xu C, Ye F, Du X. Characterization and stability study of a form-stable erythritol/expanded graphite composite phase change material for thermal energy storage. *Renew Energy* 2019;136:211–22. https://doi.org/10.1016/j.renene.2018.12.107
[28] Shen S, Tan S, Wu S, *et al.* The effects of modified carbon nanotubes on the thermal properties of erythritol as phase change materials. *Energy Convers Manag* 2018;157:41–8. https://doi.org/10.1016/j.enconman.2017.11.072
[29] Wang Y, Wang L, Xie N, Lin X, Chen H. Experimental study on the melting and solidification behavior of erythritol in a vertical shell-and-tube latent heat thermal storage unit. *Int J Heat Mass Transf* 2016;99:770–81. https://doi.org/10.1016/j.ijheatmasstransfer.2016.03.125
[30] Singh R, Sadeghi S, Shabani B. Thermal conductivity enhancement of phase change materials for low-temperature thermal energy storage applications. *Energies* 2019;12(1). https://doi.org/10.3390/en12010075
[31] Sheng N, Dong K, Zhu C, Akiyama T, Nomura T. Thermal conductivity enhancement of erythritol phase change material with percolated aluminum filler. *Mater Chem Phys* 2019;229:87–91. https://doi.org/10.1016/j.matchemphys.2019.02.033
[32] Leng G, Qiao G, Xu G, Vidal T, Ding Y. Erythritol-Vermiculite form-stable phase change materials for thermal energy storage. *Energy Procedia* 2017;142:3363–8. https://doi.org/10.1016/j.egypro.2017.12.471
[33] Oya T, Nomura T, Tsubota M, Okinaka N, Akiyama T. Thermal conductivity enhancement of erythritol as PCM by using graphite and nickel particles. *Appl Therm Eng* 2013;61(2):825–8. https://doi.org/10.1016/j.applthermaleng.2012.05.033
[34] Soni V, Kumar A, Jain VK. Performance evaluation of nano-enhanced phase change materials during discharge stage in waste heat recovery. *Renew Energy* 2018;127:587–601. https://doi.org/10.1016/j.renene.2018.05.009
[35] Qu L. Investigating the Relationship between Salinity and Specific Heat Capacity. *Queensl Acad* n.d. http://nexusstem.co.uk/wp-content/uploads/2017/01/Queensland-Academies-1.pdf
[36] Knowino. Density (chemistry), https://www.tau.ac.il/~tsirel/dump/Static/knowino.org/wiki/Density_(chemistry).html
[37] Brown HM. The thermal conductivity of sodium chloride at elevated temperatures. PhD Thesis, University of Missouri, 1955. https://scholarsmine.mst.edu/cgi/viewcontent.cgi?article=3590&context=masters_theses
[38] Ferguson JB. The melting and freezing point of Sodium Chloride. *J Phys Chem* 1921;26(7):626–30
[39] Zeng JL, Chen YH, Shu L, *et al.* Preparation and thermal properties of exfoliated graphite/erythritol/mannitol eutectic composite as form-stable phase change material for thermal energy storage. *Sol Energy Mater Sol Cells* 2018;178:84–90. https://doi.org/10.1016/j.solmat.2018.01.012
[40] Shin HK, Rhee KY, Park SJ. Effects of exfoliated graphite on the thermal properties of erythritol-based composites used as phase-change materials. *Compos Part B Eng* 2016;96:350–3. https://doi.org/10.1016/j.compositesb.2016.04.033
[41] Vivekananthan M, Amirtham VA. Characterisation and thermophysical properties of graphene nanoparticles dispersed erythritol PCM for medium temperature thermal energy storage applications. *Thermochim Acta* 2019;676:94–103. https://doi.org/10.1016/j.tca.2019.03.037
[42] Shawe J, Riesen R, Widmann J, Schubnell M. Interpreting DSC curves Part 1: Dynamic measurements. 2000. https://www.eng.uc.edu/~beaucag/Classes/Characterization/DSCParts/Artifacts%20in%20DSC%20Usercom_11.pdf
[43] Calculate Activation Energy from TGA data using Origin Software. *Nanoencryption* https://youtu.be/eLqShUApVXM?t=403
[44] Moon B, Jun N, Park S, Seok CS, Hong US. A study on the modified Arrhenius equation using the oxygen permeation block model of crosslink structure. *Polymers (Basel)* 2019;11(1). https://doi.org/10.3390/polym11010136
[45] Peleg M, Normand MD, Corradini MG. The Arrhenius equation revisited. *Crit Rev Food Sci Nutr* 2012;52(9):830–51. https://doi.org/10.1080/10408398.2012.667460
[46] Laidler KJ. The development of the arrhenius equation. *J Chem Educ* 1984;61(6):494–8. https://doi.org/10.1021/ed061p494
[47] Camirand CP. Measurement of thermal conductivity by differential scanning calorimetry. *Thermochim Acta* 2004;417(1):1–4. https://doi.org/10.1016/j.tca.2003.12.023

[48] Camirand C. Étude de la chaleur spécifique et de la conductivité thermique des hydrures métalliques par calorimétrie différentielle. Thèse et mémoire, Université du Québec à Trois-Rivières, 2000. https://depot-e.uqtr.ca/id/eprint/3139 in French
[49] Flynn JH, Levin DM. A method for the determination of thermal conductivity of sheet materials by differential scanning calorimetry (DSC). *Thermochim Acta* 1988;126:93–100. https://doi.org/10.1016/0040-6031(88)87254-X
[50] Niezgoda-Zelasko B. The Enthalpy-porosity Method Applied to the Modelling of the Ice Slurry Melting Process during Tube Flow. *Procedia Eng* 2016;157:114–21. https://doi.org/10.1016/j.proeng.2016.08.346
[51] Eanest Jebasingh B, Valan Arasu A. A comprehensive review on latent heat and thermal conductivity of nanoparticle dispersed phase change material for low-temperature applications. *Energy Storage Mater* 2020;24:52–74. https://doi.org/10.1016/j.ensm.2019.07.031
[52] Okoro HK, Odebunmi EO. Kinetics and mechanism of oxidation of sugar and sugar alcohols by KMnO4. *Int J Phys Sci* 2009;4(9): 673ED0819348. https://doi.org/10.5897/IJPS.9000340
[53] Mayilvelnathan V, Valan Arasu A. Experimental investigation on thermal behavior of graphene dispersed erythritol PCM in a shell and helical tube latent energy storage system. *Int J Therm Sci* 2020;155:106446. https://doi.org/10.1016/j.ijthermalsci.2020.106446
[54] Gunasekara SN, Stalin J, Marçal M, *et al.* Erythritol, glycerol, their blends, and olive oil, as sustainable phase change materials. *Energy Procedia* 2017;135:249–62. https://doi.org/10.1016/j.egypro.2017.09.517
[55] MINITAB. Interpolation method for mesh. *MINITAB*. https://support.minitab.com/en-us/minitab/18/help-and-how-to/graphs/how-to/general-graph-options/display-options/interpolation-method-for-mesh/

Diferencijalna skenirajuća kalorimetrijska ispitivanja faznopromenljivog kompozita eritritol – natrijum hlorid za primenu u skladištenju toplotne energije

Paul Gregory Felix, Velavan Rajagopal i Kannan Kumaresan

Univerzitet PSG College of Technology, Coimbatore, India

(Naučni rad)

Izvod

Zbog niske toplotne provodljivosti organskih faznopromenljivih materijala (phase change materials-PCM), njihova primena u sistemima za skladištenje toplotne energije zahteva korišćenje odgovarajućih tehnika radi poboljšanje prenosa toplote. Cilj ove studije je bio poboljšanje toplotne provodljivosti eritritola kao faznopromenljivog materijala, korišćenjem natrijum-hlorida (NaCl) kao aditiva, tako da se materijal može primeniti za sisteme za kuvanje na pari kada je integrisan sa solarnim paraboličnim kolektorima. Eritritol-NaCl smeše su sintetisane metodom topljenja, a ključne fizičko-hemijske osobine smeše su određene primenom diferencijalne skenirajuće kalorimetrije (DSC) u kombinaciji sa termo-gravimetrijskom analizom (TGA). Resultati pokazuju da je došlo do značajnog poboljšanja toplotne provodljivosti eritritola sa dodatkom NaCl u odnosu na čist eritritol. Takođe, termičko ponašanje materijala ukazuje na to da je pogodan za kuvanje na pari. Razvijeni matematički modeli zasnovani na eksperimentalnim rezultatima u ovoj studiji, mogu se potencijalno koristiti za dalja istraživanja kompozita eritritol-NaCl.

Ključne reči: kompoziti (smeša); skladištenje latentne toplote; matematičko modelovanje; kuvanje na pari; toplotna provodljivost

Effects of Poly(diallyldimethylammonium chloride) addition on the curing kinetics of urea-formaldehyde adhesives for particleboards

Mlađan M. Popović[1], Nevena Vukić[2], Milanka R. Điporović-Momčilović[1], Jaroslava Budinski-Simendić[3], Ivana Gavrilović-Grmuša[1], Jasmina J. Popović[1] and Ivan Ristić[3]

[1]*University of Belgrade - Faculty of Forestry, Kneza Visalia 1, 11030 Belgrade, Serbia*
[2]*University of Kragujevac - Faculty of Technical Sciences Čačak, Svetog Save 65, 32102 Čačak, Serbia*
[3]*University of Novi Sad - Faculty of Technology Novi Sad, Boulevard cara Lazara 1, 21102 Novi Sad, Serbia*

Abstract

Addition of poly(diallyldimethylammonium chloride) (PDDA) on the performances of urea-formaldehyde (UF) adhesives was evaluated in this work. Three types of UF adhesives were prepared, one without PDDA addition, and two types with PDDA addition of 1 and 3 wt.% per dry UF adhesive mass. These UF adhesive systems were used for producing experimental particleboard panels. The addition of PDDA decreased the thickness swelling of the panel samples, while the internal bond of the particleboards increased significantly only at the highest PDDA content (3 wt.%). Differential scanning calorimetry (DSC) was applied to address the influence of PDDA on UF adhesive curing kinetics. DSC scans were performed in non-isothermal regimes using different heating rates (5, 10, and 20 °C·min^{-1}). The activation energy (E_a) of the curing reaction showed slightly lower values for the UF adhesive systems containing PDDA. However, the peak temperatures and enthalpy of reaction did not change significantly. The Kissinger-Akahira-Sunose and Friedman iso-conversional methods were applied to investigate the effects of PDDA addition on the UF adhesive curing process.

Keywords: polyelectrolyte; thermoset adhesive; differential scanning calorimetry; iso-conversion method; properties of wood-based panels.

Available on-line at the Journal web address: http://www.ache.org.rs/HI/

ORIGINAL SCIENTIFIC PAPER

UDC: 665-026.772:678.028

Hem. Ind. **76 (1)** 19-28 (2022)

1. INTRODUCTION

Poly(diallyldimethylammonium chloride) (PDDA) is a positively charged linear polyelectrolyte (Fig. 1), which can be regarded as both the conducting and ion exchange polymer. It is often used in water purification and wastewater treatment, as a coagulation and flocculation agent, as well as in a papermaking process as a pitch control and sizing agent.

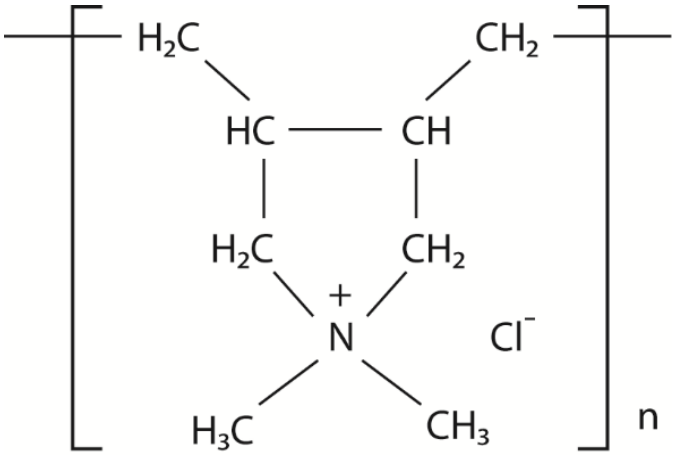

Figure 1. The chemical structure of poly(diallyldimethylammonium chloride) (PDDA)

Corresponding authors: Mlađan M. Popović, University of Belgrade ,Faculty of Forestry, Kneza Višeslava 1, 11030 Belgrade, Serbia; Tel. +381(0)11 3053
E-mail: mladjan.popovic@sfb.bg.ac.rs
Paper received: 14 September 2021; Paper accepted: 7 February 2022; Paper published: 28 February 2022.
https://doi.org/10.2298/HEMIND210914001P

However, a growing number of studies have shown successful applications of PDDA in other areas. It can be a functional, reducing and stabilizing agent in the preparation of graphene based composites for use in highly selective electrochemical sensors for various substances, such as esculetin [1], 4-chlorophenol [2], paracetamol, and diclofenac [3], β-nicotinamide adenine dinucleotide [4] and levofloxacin [5]. PDDA is used as a dispersive agent to obtain supermagnetic Fe_3O_4/PDDA nanocomposites [6]. Furthermore, its application for enhancing anion exchange membranes has shown promising results in redox flow batteries [7] and microbial fuel cells [8,9].

Addition of PDDA is an efficient and simple method for improving adhesion between a coating and a substrate because it creates a nano-structural functional surface. Hence, it is used as a linking agent to prepare nanocomposite films based on lignocellulosic materials [10,11], PDDA/sodium-silicate films with superhydrophobic surfaces [12], and silver/PDDA nanocomposites [13].

Since the PDDA polymer consists of positively charged ammonium groups across its chain, it can adsorb onto negatively charged surfaces [14]. Conveniently, the main chemical constituents of wood consist of anionic groups, such as carboxyl acid groups and ionisable hydroxyl groups [15]. In papermaking industry, PDDA acts as a bridging agent, attaching the wood resin particles onto cellulose fibres [16]. Hence, it was interesting to investigate the ability of PDDA polymer to enhance the adhesion of wood particles in the process of particleboard production. Another goal of this work is to evaluate the effects of the PDDA addition on the curing reaction of urea-formaldehyde (UF) adhesives. The UF adhesive, itself, is still highly used as an adhesive in the wood-based panels industry, specifically for the production of interior classes of particleboards and fibreboards.

2. EXPERIMENTAL

2. 1. Materials

PDDA (Poly(diallyldimethylammonium chloride) solution, 409014, Sigma-Aldrich, St. Louis, USA) used in the present study had the molar mass of 8,000 g mol^{-1} and the pH value of the solution of 5.0 to 7.0. The basic characteristics of the commercial UF adhesive used in the present study were as follows: dry matter content was 66.92% [17]; viscosity was 432 mPa·s, determined by the rotational viscometer method [18]; pH was 7.98 [19] and density was about 1270 kg m^{-3} (determined in the present study by an areometer).

The UF adhesive was prepared with the addition of $(NH_4)_2SO_4$ (Superlab, Beograd), as a hardener, in the amount of 0.5 % dry weight per dry weight of the adhesive. Similarly, two UF adhesive mixtures with the PDDA polyelectrolyte were prepared with the same hardener addition. In this case, the polyelectrolyte solution was mixed directly with the UF adhesive first. The additions of PDDA to UF adhesive were 1.0 and 3.0 %, based on the dry weight of both components. The concentration of the UF adhesive and the UF adhesive systems with PDDA were lowered to 50 % by adding the distilled water during the adhesive preparation prior to the $(NH_4)_2SO_4$ addition.

Wood particles were obtained from the Kronospan factory in Lapovo (Serbia), presenting the fraction used for surface layers of industrially produced particleboard panels.

2. 2. Preparation of particleboard panels

Three types of experimental particleboard panels were made, distinguished only by the applied adhesive system: one type was made with the UF adhesive without PDDA addition (control), and two types were made with modified UF adhesives having 1 and 3 % of PDDA (per dry adhesive weight), designated here as UF-PE1 and UF-PE3, respectively.

The application of UF adhesive systems onto wood particles was performed in the laboratory blender equipped with the Multispray 940 nozzle (SCHLICK, Germany). The adhesive was added at the concentration of 10 % of dry adhesive per dry wood particles, for all panel types.

The experimental particleboards were produced in a laboratory hot press, under the maximum specific pressure of 2 N·mm^{-2}, and at the temperature of hot plates of 200 °C. All particleboard types had the nominal thickness of 9 mm, format of 450 × 450 mm, and the targeted density was 700 kg·m^{-3}.

Standard test methods were used to determine the following properties of experimental panels: moisture content [20], density [21], thickness swelling [22] and internal bond strength [23]. Dimensions of all test pieces were 50 × 50 mm × thickness. Total of 8 test pieces from a single panel were used for determination of the moisture content, while each of the other properties was evaluated by using 10 test pieces. Before each measurement, test pieces were conditioned to constant mass in the standard atmosphere (65 % and 21 °C) inside a desiccator with saturated solution of ammonium nitrate (NH_4NO_3). The analysis of variance (ANOVA) was used to compare the test results between the panel types. Statistical comparison was performed at the confidence level of 95 %.

2. 3. DSC measurements

Differential scanning calorimetry (DSC) was used to evaluate the time dependant thermal response of the adhesive systems. The tests were performed with a DSC Q20 instrument (TA Instruments, New Castle, DE, USA). All DSC scans were run in non-isothermal regimes, in the temperature range of 30 - 200 °C, and at the constant heating rates of 5, 10 and 20 °C·min^{-1}, thus providing the values of heat flow (W·g^{-1}) plotted against the temperature (°C). The instrument software (TA Universal Analysis, New Castle, DE, USA) was used for determination of the peak temperature and enthalpy. The methodology of DSC measurements is the same as described in the previous work [24].

2. 4. Iso-conversional methods

Model-free kinetic methods of Kissinger-Akahira-Sunose (KAS) and Friedman were applied to further analyse the data obtained from DSC measurements. Both methods follow the basic iso-conversional principle that the reaction rate ($\mathrm{d}\alpha/\mathrm{d}t$) at a certain conversion (α) depends on the temperature, and thus allowing the determination of the activation energy (E_a) as a function of conversion [25,26]. The KAS method uses the Coats-Redfern approximation and it is classified as the integral method [27,28], presented by the following equations:

$$\ln\left(\frac{\beta}{T^2}\right) = A' - \frac{E_a(\alpha)}{RT} \tag{1}$$

$$A' = \ln\left(\frac{AR}{E_a(\alpha)}\right) - \ln g(\alpha) \tag{2}$$

where β is the heating rate (K·min^{-1}), E_a is the activation energy (kJ·mol^{-1}), A is the preexponential factor and R is the gas constant. By using the multiple heating rates, the activation energy can be found from the slope of the straight line obtained by plotting $\ln(\beta/T^2)$ *vs.* $1/T$.

The Friedman method presents a differential iso-conversional method and does not use any mathematical approximation [27,29]. The relevant equations are given as follows:

$$\ln\left(\beta\frac{\mathrm{d}\alpha}{\mathrm{d}T}\right) = A' - \frac{E_a(\alpha)}{RT} \tag{3}$$

$$A' = \ln A + \ln f(\alpha) \tag{4}$$

The activation energy at a certain conversion $E_a(\alpha)$ can be obtained by linear regression after plotting the $\ln(\beta\,\mathrm{d}\alpha/\mathrm{d}T)$ *vs.* $1/T$ for different values of α [26].

Using data from non-isothermal DSC scans, the Friedman model was also applied for isothermal predictions, *i.e.* to predict the conversion rate of UF adhesive curing with time at the given temperature. Hence, the reaction time t_α at a certain degree of conversion α can be calculated according to Eq. 5 [28].

$$t_\alpha = \int_0^\alpha \frac{e^{\frac{E_a(\alpha)}{RT}}}{e^{A'(\alpha)}}\mathrm{d}\alpha \tag{5}$$

3. RESULTS AND DISCUSSION

Basic properties of the experimental particleboards, such as the panel thickness, density and moisture content are given in the Table 1. The statistical evaluation of these results showed insignificant differences between the panel types, thus suggesting that the PDDA addition did not influence these properties.

Table 1. Thickness, density, and moisture content of experimental panels

Property	Control panel (UF adhesive)	UF-PE1 panel (UF + 1 % PDDA)	UF-PE3 panel (UF + 3 % PDDA)
Thickness, mm	8.80 ± 0.13	8.73 ± 0.12	8.77 ± 0.18
Density, kg·m^{-3}	723.6 ± 49.22	728.8 ± 29.13	731.8 ± 37.77
Moisture content, %	8.78 ± 0.24	8.83 ± 0.45	9.00 ± 0.24

ANOVA test did not find significant differences at the confidence level of 95 %

Results of the thickness swelling and internal bond strength are graphically presented in Figure 2 and are statistically compared in Table 2. Since paraffin (wax) was not used in the production phase, all of the panel types were characterised by remarkably high values of thickness swelling, clearly exceeding the upper limit of 17 %, as stated by the standard EN 312 for the P3 class of particleboards [30]. The statistical comparison between the panel types has shown a significant difference only between the control type and the panel type with the addition of 3 % of PDDA (UF-PE3). However, the general trend suggests that the thickness swelling decreases with the addition of PDDA.

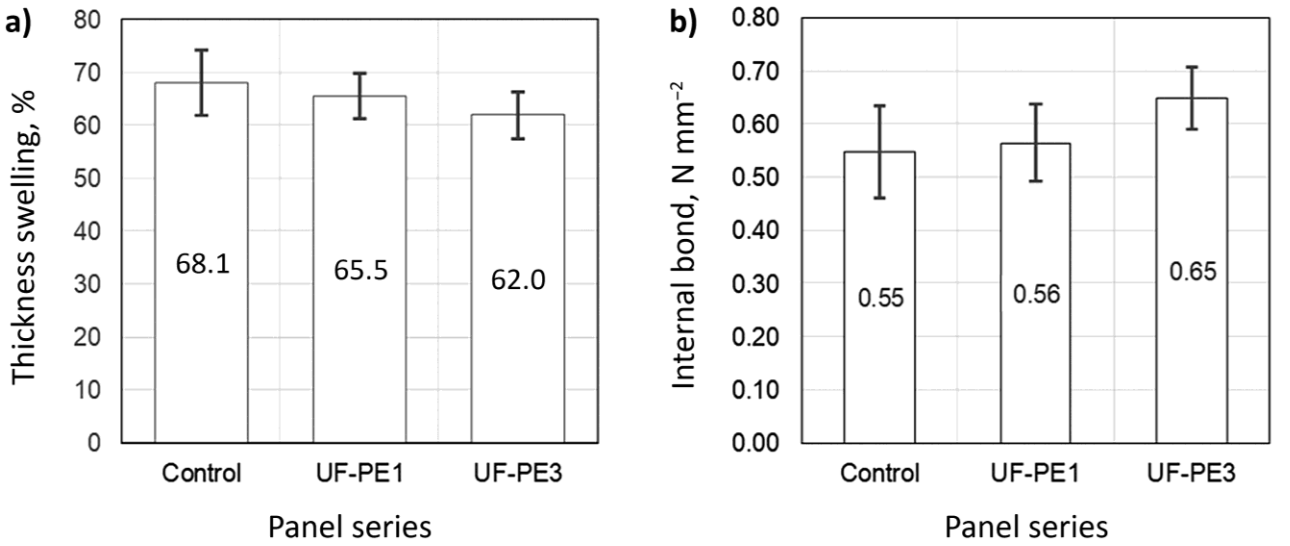

Figure 2. Thickness swelling (a) and internal bond (b) of the control panel and the panels made with UF adhesives containing 1% and 3% of PDDA (vertical error bars show standard deviations)

In contrast to thickness swelling, the internal bond test showed satisfactory results for all panel types. The internal bond strength values were well above 0,40 N·mm^{-2}, a minimum requirement for P2 class of particleboards according to standard EN 312 [30], for all specimens. Although significant differences were not found between the control type and the UF-PE1 panels, the statistically highest value was recorded for the UF-PE3 panel type (Table 2), which again suggests that the addition of PDDA had a beneficial effect in terms of the internal bond strength.

Table 2. Statistical comparison of the thickness swelling and internal bond values for the particleboards obtained with the control UF adhesive and the UF adhesive containing 1 % (UF-PE1) and 3 % (UF-PE3) of PDDA polyelectrolyte (per dry adhesive weight)

Property	Thickness swelling			Internal bond		
Between groups	*F*	*p*-value	*F* crit	*F*	*p*-value	*F* crit
Control / UF-PE1	0.9440	0.3477	4.6001	0.2002	0.6609	4.5431
Control / UF-PE3	5.2067*	0.0387	4.6001	8.3564*	0.0112	4.5431
UF-PE1 / UF-PE3	2.6001	0.1292	4.6001	7.5263*	0.0144	4.4940

*denotes a statistically significant difference at the confidence level of 95 %

3. 1. Curing kinetics of UF adhesive systems

Figure 3 shows the characteristic thermographs of DSC tests, performed in this research. The curing reaction of each UF adhesive system (the control UF adhesive, and the UF-PE1 and UF-PE3 adhesives, having PDDA contents of 1 and 3 wt.%, respectively) are presented by three distinct curves in regard to the heating rate (5, 10, and 20 °C·min^{-1}). The exothermal region of the curve, representing the curing reaction, shifts towards the higher temperature zone as the heating rate increases. In addition, the DCS curves also feature an endothermic region, occurring above the temperature of around 135 °C. This could be attributed to the melting and decomposition of urea which starts to occur at 133 °C [31].

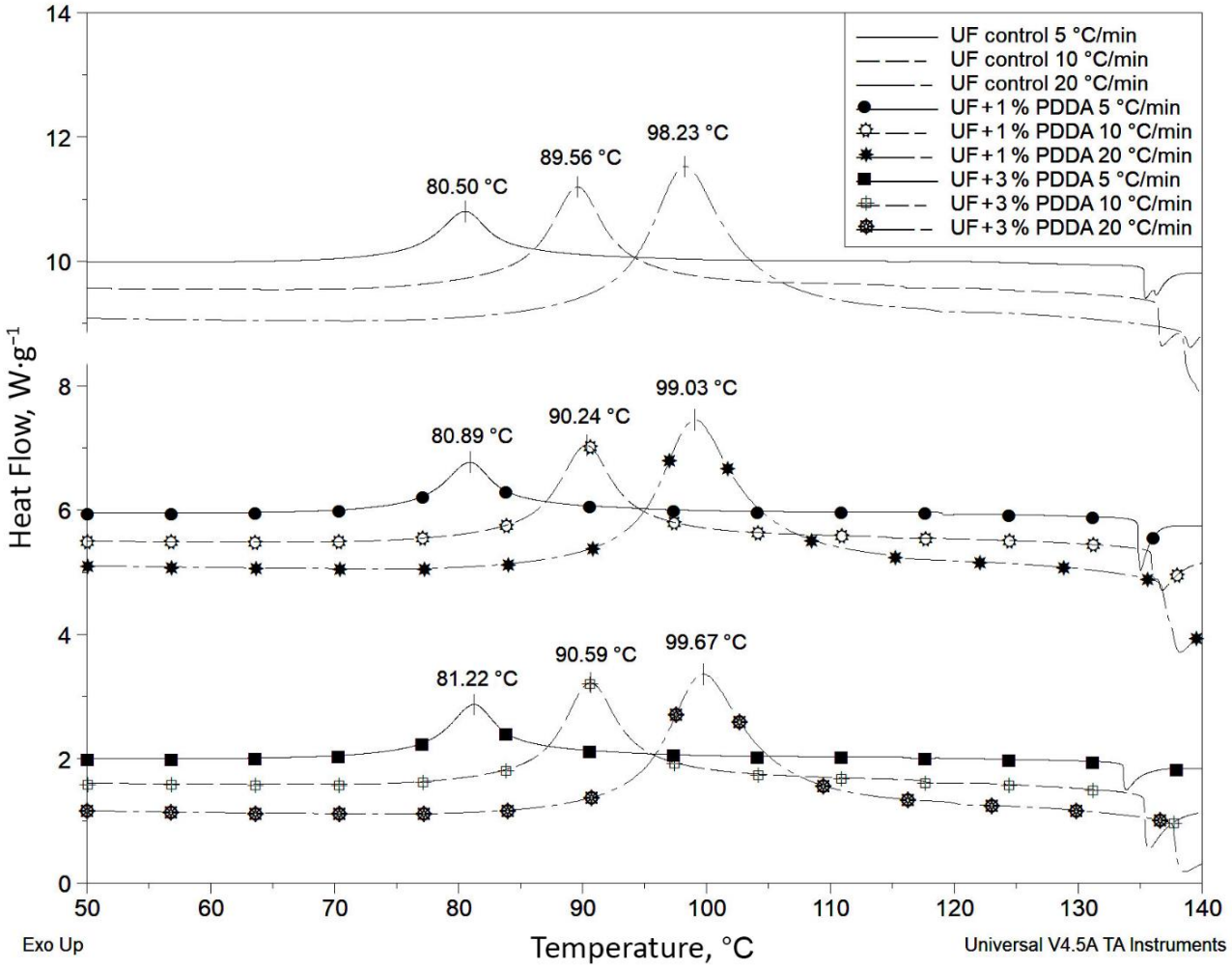

Figure 3. DSC thermographs of the curing reaction of pure (control) UF adhesive and the UF adhesives with PDDA contents of 1 and 3 wt.%, obtained at the heating rates of 5, 10 and 20 °C/min

Tables 3 and 4 present basic parameters of curing reactions of the control UF adhesive and its systems with PDDA. Peak temperatures of the curing reactions do not significantly differ between the UF adhesive types, as shown in Table 3. However, the apparent activation energy, calculated by the general Kissinger model, slightly decreases with the addition of PDDA.

Values for the enthalpy integrals in regard to the heating rate are given in Table 4. It is interesting to notice that the enthalpy of curing reaction decreases as the heating rate increases, which is observed for all of the UF adhesive types. This phenomenon might be attributed to the shorter reaction time available for the complete crosslinking of the adhesive at higher heating rates [28]. However, no apparent influence of the PDDA addition on the enthalpy integrals could be observed.

Table 3. Peak temperatures at different heating rates (β) and activation energy (E_a) of the curing reaction of the control UF adhesive and UF adhesives with PDDA contents of 1 wt.% and 3 wt.%

Sample	Peak temperature, °C			E_a / kJ·mol^{-1}	r^2
	β = 5 °C·min^{-1}	β = 10 °C·min^{-1}	β = 20 °C·min^{-1}		
UF (control)	80.5	89.56	98.23	79.29	0.9992
UF / 1 wt.% PDDA	80.89	90.24	99.03	77.60	0.9988
UF / 3 wt.% PDDA	81.22	90.59	99.67	76.44	0.9994

Table 4. Enthalpy (ΔH) of the curing reaction at different heating rates (β) of the control UF adhesive and UF adhesives with PDDA contents of 1 and 3 wt.%

Sample	ΔH / J·g^{-1}			ΔH / J·g^{-1}
	β = 5 °C·min^{-1}	β = 10 °C·min^{-1}	β = 20 °C·min^{-1}	
UF (control)	76.62	75.92	72.02	74.85 ±2.48
UF / 1 wt.% PDDA	75.31	71.34	67.47	71.37 ±3.92
UF / 3 wt.% PDDA	77.2	75.4	65.19	72.60 ±6.48

The selected iso-conversional methods were applied to determine the activation energy dependence on the conversion for the investigated UF adhesive systems. The results are given in Tables 5 and 6 as well as in Figure 4.

Table 5. Kinetic parameters of the curing reaction of UF adhesives obtained by the KAS iso-conversional model

α / %	UF control			UF-P1 (1 % PDDA content)			UF-P3 (3 % PDDA content)		
	E_a / kJ·mol^{-1}	r^2	A'	E_a / kJ·mol^{-1}	r^2	A'	E_a / kJ·mol^{-1}	r^2	A'
5	84.55	0.9999	-19.25	79.04	0.9991	-17.30	76.52	0.9995	-16.37
10	81.86	0.9999	-18.12	77.89	0.9992	-16.72	76.05	0.9995	-16.03
20	79.68	0.9999	-17.18	77.15	0.9994	-16.28	75.77	0.9996	-15.77
30	78.59	0.9999	-16.71	76.68	0.9994	-16.02	75.37	0.9997	-15.54
40	77.96	0.9999	-16.42	76.28	0.9995	-15.81	74.95	0.9998	-15.33
50	77.39	1.0000	-16.17	75.79	0.9997	-15.59	74.42	0.9999	-15.10
60	76.80	1.0000	-15.91	75.24	0.9999	-15.35	73.83	1.0000	-14.84
70	76.28	0.9999	-15.66	74.88	1.0000	-15.15	73.45	1.0000	-14.64
80	76.35	0.9994	-15.56	75.41	0.9999	-15.21	74.1	0.9999	-14.74
90	76.88	0.9976	-15.51	77.23	0.9989	-15.59	76.4	0.9997	-15.28
95	76.42	0.9954	-15.16	78.77	0.9979	-15.89	78.21	0.9997	-15.68

Table 6. Kinetic parameters of the curing reaction of UF adhesives obtained by the Friedman iso-conversional model

α / %	UF control			UF 1 % PE (1 % addition of PDDA)			UF 3 % PE (3 % addition of PDDA)		
	E_a / kJ·mol^{-1}	r^2	A'	E_a / kJ·mol^{-1}	r^2	A'	E_a / kJ·mol^{-1}	r^2	A'
10	69.78	0.9998	-26.49	72.36	0.9997	-27.32	73.65	0.9995	-27.78
20	69.61	0.9992	-26.95	73.49	0.9998	-28.24	74.35	1	-28.56
30	69.16	0.9998	-27.3	72.36	0.9999	-28.37	71.33	0.9998	-28.05
40	70.09	0.9998	-27.9	70.9	0.9998	-28.16	69.2	0.9985	-27.61
50	68.99	0.9975	-27.65	68.12	0.9975	-27.35	65.81	0.9975	-26.58
60	68.25	0.9914	-27.34	66.83	0.9912	-26.85	64.35	0.9956	-26.01
70	70.35	0.9817	-27.74	70.51	0.9857	-27.78	68.82	0.994	-27.19
80	77.23	0.9756	-29.47	79.89	0.9829	-30.33	79.84	0.9945	-30.27
90	79.71	0.9766	-29.47	85.87	0.986	-31.48	87.64	0.9976	-32.01
95	75.12	0.9734	-27.15	86.94	0.9892	-31.01	87.85	0.9994	-31.26

Application of the KAS method shows slight and uniform decrease of E_a as the curing reaction progresses until 80 % of the conversion. This pattern is similar for all UF adhesive systems, with the control UF adhesive achieving the highest E_a levels and the UF adhesive with 3 % of PDDA having the lowest E_a levels. After the conversion degree (α) of 80 %,

both UF adhesive systems with PDDA exhibited a slight increase in the activation energy. In comparison to the KAS method, application of the Friedman method has shown quite different E_a dependences on the conversion for the investigated UF adhesive systems. All UF adhesive systems featured a steep increase of E_a after reaching 60 to 70 % of the conversion. The increase in E_a at the later stage of conversion is probably caused by the diffusion controlled reaction [32]. This increase was most noticeable for the UF adhesive systems with PDDA, and it was also depicted by the KAS method at the very end of conversion.

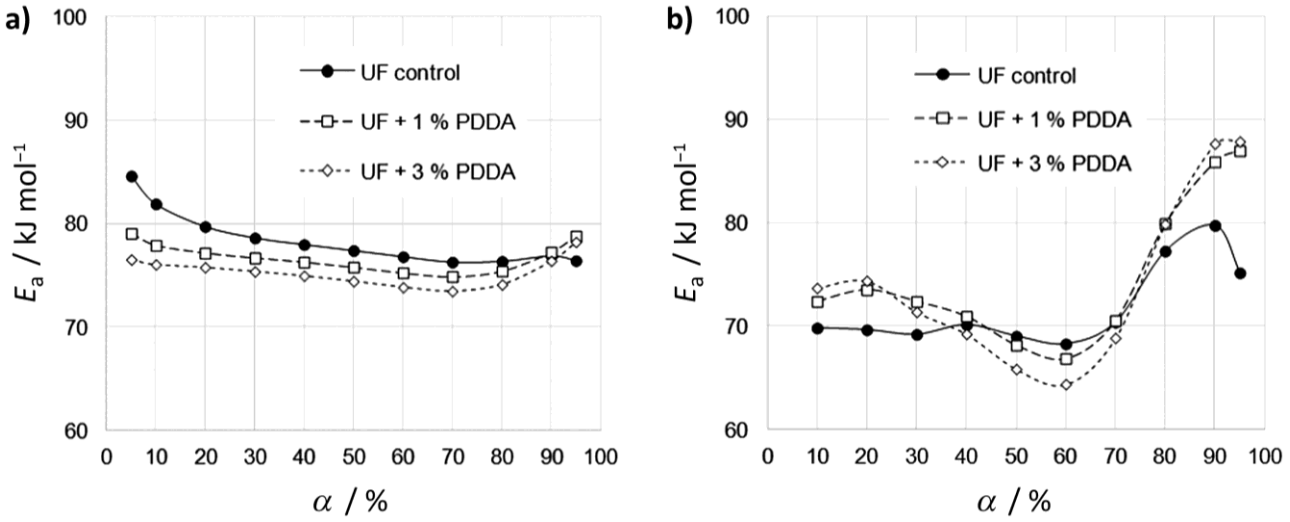

Figure 4. Energy of activation (E_a) dependence on the conversion (α) for different UF adhesives, according to KAS (a) and Friedman (b) iso-conversional models

The Friedman iso-conversional method was used to predict the curing mechanism at isothermal conditions (at the constant temperature), expressing the conversion degree (α) as a function of time. Hence, the Figure 5 presents predictions for the investigated UF adhesive systems at the curing temperatures of 60, 80, 100, and 120 °C. According to this model, the addition of PDDA seems to have different impacts on the curing behaviour of the UF adhesive at different curing temperatures. Thus, in regard to the control UF adhesive, the curing reaction of UF/PDDA systems was slower at lower temperatures (T_{iso} <80 °C), while having similar or shorter curing times at the temperatures above 100 °C.

4. CONCLUSION

The addition of PDDA into the UF adhesive showed positive effects concerning thickness swelling and internal bond strengths of experimental particleboards. Both of these properties were improved with the application of the higher PDDA content of 3 % per dry UF adhesive.

DSC measurements showed that the addition of PDDA into the UF adhesive did not affect significantly peak temperatures and enthalpy of the curing reaction. However, application of the general Kissinger model showed that the 3 % PDDA addition into the UF adhesive slightly decreased its activation energy to 76.4 kJ·mol^{-1} in comparison to 79.3 kJ·mol^{-1} determined for the control UF adhesive.

The dependence of activation energy on the curing degree for each of the UF adhesive systems was determined by application of the KAS and Friedman methods. Both methods depicted the increase in activation energy values at the end of conversion, related to the UF systems with PDDA.

The curing reactions of UF adhesive systems were modeled for isothermal conditions using the Friedman iso-conversional method, *i.e.* showing the conversion degree as a function of time at the constant temperature. It was interesting to notice that the conversion rate for the UF adhesive systems with PDDA was lower for the curing temperatures below 80 °C, while curing of these adhesives was faster at 120 °C in comparison to the control UF adhesive.

The positive effects of the PDDA polymer addition into the UF adhesive have been observed in this work through the improvement of thickness swelling and internal bond of the experimental panel samples. In general, we may suggest that

the application of this method could improve physical and mechanical properties of particleboards manufactured in the real processing conditions and in capacities of modern particleboard factories. The addition of PDDA have also showed a possible increase of the reaction rate of the UF adhesives, at the temperatures above 120 °C, which in turn may lead to an increase of the production rate during the hot press operation in the particleboards manufacturing process.

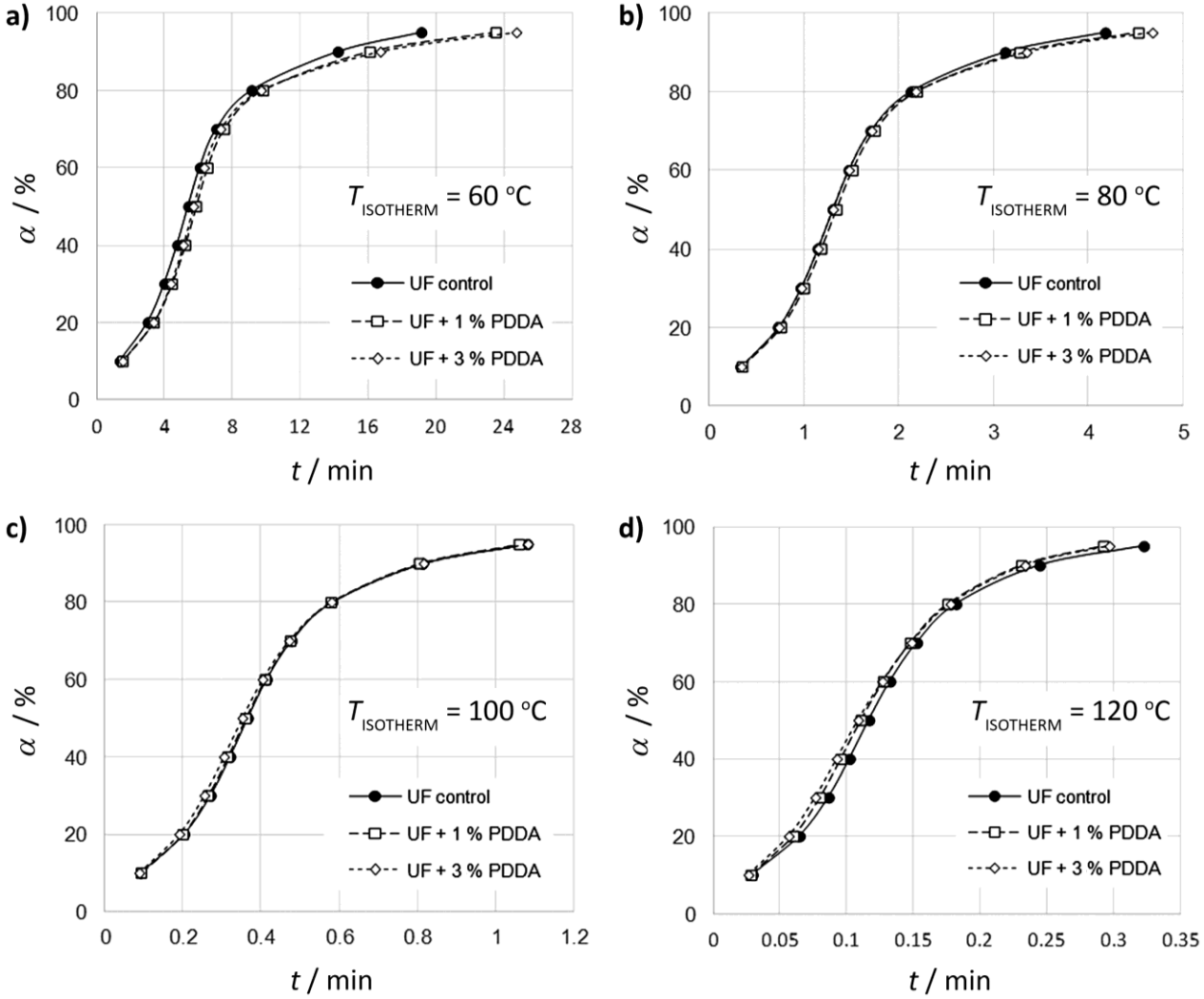

Figure 5. Conversion degree of UF adhesive samples (α) as a function of time by the Friedman model at constant temperatures: a) 60 °C, b) 80 °C; c) 100 °C and d) 120 °C

Acknowledgements: This paper was realized as a part of the project "Establishment of Wood Plantations Intended for Afforestation of Serbia" (TP 31041) financed by the Ministry of Education, Science and Technological Development of the Republic of Serbia.

REFERENCES

[1] Li H, Wang L, Sheng K, Zou L, Ye B. Highly sensitive determination of esculetin on TiO2-NPs-coated poly(diallyldimethylammonium chloride)-functionalized graphene modified electrode. *Talanta*. 2016;161:838-846 https://doi.org/10.1016/j.talanta.2016.09.050

[2] Wang B, Okoth OK, Yan K, Zhang J. A highly selective electrochemical sensor for 4-chlorophenol determination based on molecularly imprinted polymer and PDDA-functionalized graphene. *Sensors Actuators, B Chem*. 2016;236(236):294-303 https://doi.org/10.1016/j.snb.2016.06.017

[3] Okoth OK, Yan K, Liu L, Zhang J. Simultaneous Electrochemical Determination of Paracetamol and Diclofenac Based on Poly(diallyldimethylammonium chloride) Functionalized Graphene. *Electroanalysis*. 2016;28(1):76-82 https://doi.org/10.1002/elan.201500360

[4] Lu J, Liu Y, Liu X, Lu X, Liu X. Construction of a highly sensitive NADH sensing platform based on PDDA-rGO nanocomposite modified electrode. *Ionics (Kiel)*. 2016;22(11):2225-2233 https://doi.org/10.1007/s11581-016-1753-7
[5] Borowiec J, Yan K, Tin C-C, Zhang J. Synthesis of PDDA Functionalized Reduced Graphene Oxide Decorated with Gold Nanoparticles and Its Electrochemical Response toward Levofloxacin. *J Electrochem Soc*. 2015;162(3):H164-H169 https://doi.org/10.1149/2.0811503jes
[6] Li F, Yang Q, Qiu F, Liu Y. Modification of superparamagnetic iron oxide nanoparticles with poly(diallyldimethylammonium chloride) at air atmosphere. *Polym Adv Technol*. 2016;27(11):1530-1534 https://doi.org/10.1002/pat.3834
[7] Cho E, Won J. Novel composite membrane coated with a poly(diallyldimethylammonium chloride)/urushi semi-interpenetrating polymer network for non-aqueous redox flow battery application. *J Power Sources*. 2016;335:12-19 https://doi.org/10.1016/j.jpowsour.2016.10.020
[8] Zhang J, Qiao J, Jiang G, Liu L, Liu Y. Cross-linked poly(vinyl alcohol)/poly (diallyldimethylammonium chloride) as anion-exchange membrane for fuel cell applications. *J Power Sources*. 2013;240:359-367 https://doi.org/10.1016/j.jpowsour.2013.03.162
[9] Pandit S, Khilari S, Bera K, Pradhan D, Das D. Application of PVA-PDDA polymer electrolyte composite anion exchange membrane separator for improved bioelectricity production in a single chambered microbial fuel cell. *Chem Eng J*. 2014;257:138-147 https://doi.org/10.1016/j.cej.2014.06.077
[10] Lin Z, Renneckar S, Hindman DP. Nanocomposite-based lignocellulosic fibers 1. Thermal stability of modified fibers with clay-polyelectrolyte multilayers. *Cellulose*. 2008;15(2):333-346 https://doi.org/10.1007/s10570-007-9188-y
[11] Pillai K V., Renneckar S. Dynamic mechanical analysis of layer-by-layer cellulose nanocomposites. *Ind Crops Prod*. 2016;93:267-275 https://doi.org/10.1016/j.indcrop.2016.02.037
[12] Zhang L, Chen H, Sun J, Shen J. Layer-by-layer deposition of poly(diallyldimethylammonium chloride) and sodium silicate multilayers on silica-sphere-coated substrate-facile method to prepare a superhydrophobic surface. *Chem Mater*. 2007;19(4):948-953 https://doi.org/10.1021/cm062535i
[13] Sadeghi B, Pourahmad A. Synthesis of silver/poly (diallyldimethylammonium chloride) hybride nanocomposite. *Adv Powder Technol*. 2011;22(5):669-673 https://doi.org/10.1016/j.apt.2010.10.001
[14] Huang J, Liu X, Thormann E. Surface Forces between Highly Charged Cationic Polyelectrolytes Adsorbed to Silica: How Control of pH and the Adsorbed Amount Determines the Net Surface Charge. *Langmuir*. 2018;34(25):7264-7271 https://doi.org/10.1021/acs.langmuir.8b00909
[15] Zhang H, Zhao C, Li Z, Li J. The fiber charge measurement depending on the poly-DADMAC accessibility to cellulose fibers. *Cellul 2015 231*. 2015;23(1):163-173 https://doi.org/10.1007/s10570-015-0793-x
[16] McLean D, Agarwal V, Stack K, Horne H, Richardson D. Synthesis of guar gum-graft-poly (acrylamide-co-diallyldimethylammonium chloride) and its application in the pulp and paper industry. *BioResources*. 2011;6(4):4168-4180 https://bioresources.cnr.ncsu.edu/resources/synthesis-of-guar-gum-graft-polyacrylamide-co-diallyldimethylammonium-chloride-and-its-application-in-the-pulp-and-paper-industry/
[17] EN 827: Adhesives - Determination of conventional solids content and constant mass solids. 2005
[18] EN 12092: Adhesives - Determination of viscosity. 2001
[19] EN 1245: Adhesives - Determination of pH - Test method. 1998
[20] EN 322: Wood-based panels - Determination of moisture content. 1993
[21] EN 323: Wood-based panels - Determination of density. 1993
[22] EN 317: Particleboards and fibreboards - Determination of swelling in thickness after. 1993
[23] EN 319: Particleboards and fibreboards - Determination of tensile strength perpendicular to the plane of the board. 1993
[24] Popović M, Popović J, Điporovic-Momčilović M, Vukić N, Budinski-Simendić J, Gavrilović-Grmuša I, Hamid F. The curing behavior of urea-formaldehyde adhesive in the presence of chemically treated narrow-leaved ash. *Zast Mater*. 2019;60(1):64-69 https://doi.org/10.5937/zasmat1901064P
[25] Vyazovkin S. Modification of the integral isoconversional method to account for variation in the activation energy. *J Comput Chem*. 2001;22(2):178-183 https://doi.org/10.1002/1096-987X(20010130)22:2<178::AID-JCC5>3.0.CO;2-%23
[26] Kandelbauer A, Wuzella G, Mahendran A, Taudes I, Widsten P. Model-free kinetic analysis of melamine-formaldehyde resin cure. *Chem Eng J*. 2009;152(2-3):556-565 https://doi.org/10.1016/j.cej.2009.05.027
[27] Sbirrazzuoli N, Vincent L, Mija A, Guigo N. Integral, differential and advanced isoconversional methods. Complex mechanisms and isothermal predicted conversion-time curves. *Chemom Intell Lab Syst*. 2009;96(2):219-226 https://doi.org/10.1016/j.chemolab.2009.02.002
[28] Zhang C, Binienda WK, Zeng L, Ye X, Chen S. Kinetic study of the novolac resin curing process using model fitting and model-free methods. *Thermochim Acta*. 2011;523(1-2):63-69 https://doi.org/10.1016/j.tca.2011.04.033
[29] Starink MJ. The determination of activation energy from linear heating rate experiments: A comparison of the accuracy of isoconversion methods. *Thermochim Acta*. 2003;404(1-2):163-176 https://doi.org/10.1016/S0040-6031(03)00144-8
[30] EN 312: Particleboards - Specifications. 2010
[31] Tischer S, Börnhorst M, Amsler J, Schoch G, Deutschmann O. Thermodynamics and reaction mechanism of urea decomposition. *Phys Chem Chem Phys*. 2019;21(30):16785-16797 https://doi.org/10.1039/C9CP01529A

[32] Gao J, Zhao M, Qin J. Curing Kinetics of o-Cresol-formaldehyde Epoxy Resin/3-Methyl-tetrahydrophthalic Anhydride/Organic-Montmorillonite Nanocomposite by Isoconversional Methods. *Iran Polym J*. 2006;15(5):425-432 https://www.sid.ir/en/journal/ViewPaper.aspx?id=103253

Uticaj dodatka poli(dialildimetilamonijum hlorida) na kinetiku očvršćavanja urea-formaldehidnog adheziva za ploče iverice

Mlađan M. Popović[1], Nevena Vukić[2], Milanka R. Điporović-Momčilović[1], Jaroslava Budinski-Simendić[3], Ivana Gavrilović-Grmuša[1], Jasmina J. Popović[1] i Ivan Ristić[3]

[1]Univerzitet u Beogradu - Šumarski fakultet, Kneza Višeslava 1, 11030 Beograd, Srbija
[2]Univerzitet u Kragujevcu - Fakultet tehničkih nauka u Čačku, Svetog Save 65, 32102 Čačak, Srbija
[3]Univerzitet u Novom Sadu - Tehnološki fakultet Novi Sad, Bulevar cara Lazara 1, 21102 Novi Sad, Srbija

(Naučni rad)

Izvod

U ovom radu ispitan je uticaj dodatka poli(dialildimetilamonijum hlorida) (PDDA) na performanse urea-formaldehidnog (UF) adheziva. U tom cilju pripremljene su tri serije UF adheziva: bez dodatka PDDA i sa dodatkom PDDA od 1 i 3 % suve supstance po masi suve supstance adheziva. Dodatak PDDA smanjio je debljinsko bubrenje uzoraka eksperimentlano dobijenih ploča iverica, dok je zatezna čvrstoća upravno na površinu ploče značajno povećana tek pri dodatku PDDA od 3 %. Metoda diferencijalne skeirajuće kalorimetrije (*engl.* differential scanning calorimetry, DSC) primenjena je u cilju ispitivanja uticaja dodatka PDDA na kinetiku očvršćavanja UF adheziva. DSC merenja sprovedena su u dinamičkom režimu korišćenjem različitih brzina zagrevanja (5, 10 i 20 °C·min^{-1}). Povećanje koncentracije PDDA uticalo je na smanjenje vrednosti energije aktivacije očvršćavanja UF adheziva, izračunate po opštem Kisindžerovom modelu. Zavisnost energije aktivacije u odnosu na stepen konverzije određena je za sva tri ispitivana adhezivna sistema korišćenjem izo-konverzionih modela (*Kissinger-Akahira-Sunose* i *Friedman*), što je omogućilo detaljniji uvid u uticaj PDDA na tok reakcije očvršćavanja UF adheziva.

Ključne reči: polielektrolit; termoreaktivni adheziv; diferencijalna skeirajuća kalorimetrija; izokonverziona metoda; svojstva ploča na bazi drveta

Low energy nanoemulsions as carriers for essential oils in topical formulations for antioxidant skin protection

Ana Gledović[1], Danica Bajuk-Bogdanović[2], Snežana Uskoković-Marković[3], Leposava Pavun[4], Snežana Savić[1] and Aleksandra Janošević Lezaić[4]

[1]*University of Belgrade, Faculty of Pharmacy, Department of Pharmaceutical Technology and Cosmetology, 11000 Belgrade, Serbia*
[2]*University of Belgrade, Faculty of Physical Chemistry, Serbia*
[3]*University of Belgrade, Faculty of Pharmacy, Department of Analytical Chemistry, Serbia*
[4]*University of Belgrade, Faculty of Pharmacy, Department of Physical Chemistry and Instrumental Methods, Serbia*

Abstract

In this study several essential oils (EOs): basil – BA, lemon balm – LB and oregano – OR were incorporated into nanoemulsions (NEs) as prospective carriers for natural and sensitive bioactives. NEs were prepared *via* the phase inversion composition (PIC) method, which is an energy-efficient cold process. Physicochemical stability of NEs was confirmed by particle size distribution analysis, electrical conductivity and pH value measurements, as well as by optical microscopy observations. The type of EO and the surfactant and oil mix concentration were found to be crucial factors governing the NE properties and stability. Raman spectra of the EOs confirmed main active ingredients and provided detection of interactions with the nanocarrier, which is a novel application of this technique. The antioxidant activity towards DPPH radical in methanol was concentration-dependent with a similar trend for individual oils and oil-loaded NEs (OR> LB> BA). However, the ABTS test in an aqueous medium revealed notable change in the order of activity after EO nanonisation at higher EO concentrations. Overall, it was found that OR-NE was the most effective and stable system, since OR acted as a co-stabiliser in the NE formulation, and its remarkably high antioxidant activity was successfully preserved during 6 months of storage.

Keywords: oregano; basil; lemon balm; nanonisation; Raman spectroscopy; stability.

Available on-line at the Journal web address: http://www.ache.org.rs/HI/

ORIGINAL SCIENTIFIC PAPER

UDC: 532.695:665.52:66.094.3.097.8

Hem. Ind. **76 (1)** 29-42 (2022)

1. INTRODUCTION

Aromatic plants have been used since ancient times as a source of essential oils (EOs), which are known as natural remedies in traditional medicine systems – phytotherapy and aromatherapy. They are also widely used for everyday purposes, for example, as fragrant components in skincare preparations and perfumery, and as flavouring agents and natural preservatives in food industry [1−3]. With respect to chemical composition, EOs represent complex mixtures of various volatile and lipophilic molecules that can be classified as terpenoids (monoterpenes, sesquiterpenes, and diterpenes), phenylpropanoids, and other low molecular weight molecules (aliphatic hydrocarbons, acids, alcohols, aldehydes, and esters). In each EO, there are usually two or three principal compounds which can be used for the EO identification and these molecules are usually linked to the oil bioactivity and application (*i.e.*, antimicrobial, anti-inflammatory, antioxidant, and anticarcinogenic activities, *etc.*) [1,4,5].

Despite the renewed popularity of EOs in personal care and pharmaceutical products, their volatile nature and sensitivity to heat, light and air require optimised formulations to preserve the activity and to avoid side effects related to the usage [2−4,6]. Since EOs have to be diluted for the use, different carrier systems such emulsions [7] and nanoemulsions [8,9] are proposed as a convenient solution for oil solubilization into the aqueous-based, oil-in-water

Corresponding authors: Ana Gledović, University of Belgrade, Faculty of Pharmacy, Department of Pharmaceutical Technology and Cosmetology, 11000 Belgrade, Serbia
E-mail: ana.gledovic@pharmacy.bg.ac.rs
Paper received: 9 May 2021; Paper accepted: 15 February 2022; Paper published: 28 February 2022.
https://doi.org/10.2298/HEMIND210509004G

(O/W) products. Nanoemulsions (NEs), particularly those produced by low energy methods, can fulfil the above-mentioned requirements and ensure optimal characteristics for topical application. NEs of the O/W type represent colloidal dispersions of oil in the aqueous phase, in the form of ultra-fine nano-droplets (preferably < 200 nm), stabilised by a surfactant (and/or co-surfactant) monolayer. Due to fine droplet sizes, NEs have a pleasant visual appearance with characteristic bluish shine (they can be milky white, or semi-transparent, if small droplet sizes of < 100 nm are achieved) [10−12]. NEs can provide modified release and stabilisation of delicate ingredients, so that improved physical stability is expected as compared to conventional emulsions, while at the same time NEs have better safety profiles compared to microemulsions, which are typically produced with higher surfactant concentrations [12,13]. Due to the good spreadability of NEs, homogenous and compact film of nano-droplets is formed on the skin surface, enabling better skin hydration and enhanced penetration of active substances as compared to conventional emulsions [12,14]. Moreover, an important property of O/W NEs is that they can be diluted with water without damaging the emulsion structure: for example, they can be used as concentrated products (*i.e.*, NEs with orange or lemon essential oil), which can be incorporated in beverages and other food systems, acting as flavouring agents [15,16]. It is also possible to convert NEs into nanoemulgels either by adding rheology modifiers directly into the NE aqueous phase [17] or by adding the NE into the gel [18]. Therefore, NEs are particularly suitable for potential applications in pharmaceutical or cosmetic products of different consistencies (*i.e.*, sprays, lotions, creams or gel-nanoemulsions) [12,19].

It is known that many EOs contain molecules with considerable antioxidant activity, such as phenolic compounds, flavonoids and terpenoids, acting alone or synergistically [20,21]. Besides antimicrobial action [22], EOs prepared from basil−BA (*Ocimum basilicum*), oregano – OR (*Origanum vulgare*) and lemon balm − LB (*Melissa officinalis*) leaves are reported to scavenge free radicals [9,23−25]. Therefore, these particular EOs and their bioactives could be good candidates for skin-protective formulations. However, there is a lack of literature data on the concentration-dependent and substrate-dependent (type of free radical) behaviour of these EOs. Moreover, comparative studies done with neat EOs and EO-loaded NEs are scarce, although such studies could reveal important information regarding potential usage of these systems in pharmaceutics and cosmetics.

Having all the above mentioned in mind, this research was organized into three main parts.

1. Preparation of stable NEs containing 1 wt.% EOs (BA, OR or LB) with polyethylene glycol free (PEG-free) natural surfactant mixture (containing polyglycerol-4 laurate as the main surfactant) suitable for cold processing *via* the phase inversion concentration (PIC) method [26].
2. Screening of chemical compositions of EOs and EO-loaded NEs *via* Raman spectroscopy, as a suitable and quick method that can identify chemical compositions of plant and essential oils [26,27] and track the interactions between formulation ingredients [10]. These investigations aimed to reveal additional information on the composition/ structure of EOs before and after nanoemulsification, which can be linked to the stability and performance of EO-loaded NEs.
3. Screening study of antioxidant activity of neat EOs and EO-loaded NEs was performed by using different sample concentrations and methods (DPPH and ABTS) to gain insight into free radical scavenging profiles of EOs before and after nanoemulsification, as a proof of concept that NEs can be used as effective carriers of EOs with antioxidant properties.

2. MATERIALS AND METHODS

2. 1. Chemicals and reagents

2. 1. 1. Essential oils

For this study several EOs prepared from leaves of plants from the *Lamiaceae* family were used: *Ocimum basilicum* (basil – BA), *Origanum vulgare* (oregano – OR) and *Melissa officinalis* (lemon balm – LB). EOs were produced by Aromaaz International, New Delhi, India, for domestic brand Eterra/company Terra Co, Novi Sad, Serbia, and they were obtained from a local distributor with the certificates of analysis.

2. 1. 2. Nanoemulsion ingredients

In this study a commercially available mixture of PEG-free surfactant and oil (SO mix) was used, consisting of polyglyceryl-4 laurate and dilauryl citrate, diethylhexyl carbonate, phenoxyethanol (Tego®Wipe DE PF, Evonik Goldschmidt GmbH, Essen, Germany) without parabens. The water phase was ultra-purified water (obtained by a GenPure apparatus, TKA Wasseranfbereitungssysteme GmbH, Neiderelbert, Germany) without any additives.

2. 1. 3. Reagents for antioxidant assays

The following reagents were used: 2,2-diphenyl-1-picrylhydrazyl (DPPH), 2,2'-azino-bis (3-ethylbenzothiazoline-6-sulfonic acid) diammonium salt (ABTS), potassium persulfate, (±)-6-hydroxy-2,5,7,8-tetramethylchromane-2-carboxylic acid (Trolox) and methanol (HPLC grade), all produced by Sigma-Aldrich, Steinheim, Germany. Phosphate buffered saline (PBS buffer, pH 7.4) was prepared fresh before the ABTS assay.

2. 2. Nanoemulsion preparation and characterisation

2. 2. 1. Phase inversion composition (PIC) method

In order to preserve the stability and activity of EOs, EO-loaded NEs were prepared by using the phase inversion composition (PIC) method at room temperature (RT), which is an energy-efficient cold process [11,12,26]. Firstly, one of the selected EOs – BA, OR or LB (1 wt.%) was added to the commercially available SO mix (5 or 10 wt.% in the final NE) and vortex mixed for 3 min at 1300 rpm. Then, ultra-purified water was added gradually to the SO-EO mix (at continuous vortex-mixing at 1300 rpm), until the total water content of 89 or 94 wt.% was reached, and the obtained NEs were shortly homogenized (3 min at the same stirring speed). All samples were prepared in triplicate.

2. 2. 2. Nanoemulsion particle size distribution

Z-average droplet size (*Z*-ave) and polydispersity index (PDI) as crucial parameters describing particle size distribution were obtained by a dynamic light scattering (DLS) device (Zeta Sizer Nano ZS, Malvern Instruments, Malvern, UK) applied to NEs freshly diluted with ultra-purified water (1:100 v/v), as a standard procedure to avoid multiple light scattering [9,16]. Measurements were performed in triplicate, initially 24 to 48 h after preparation, then after 30 days, and finally after 6 months of storage at RT (stability study).

2. 2. 3. pH value and electrical conductivity

Electrical conductivity of undiluted intermedium/transient phases and NEs was measured by using the Sension+EC71 apparatus (HACH, Loveland, CO, USA). The pH value of the undiluted NEs was measured by using a HI9321 microprocessor pH meter (Hanna Instruments Inc., Ann Arbor, Michigan, USA). The measurements were performed in triplicate at 25±2 °C.

2. 2. 4. Optical microscopy

Optical microscopy was employed to investigate the signs of anisotropy in the intermedium phases and the corresponding EO-loaded nanoemulsions. Micrographs of undiluted samples were taken by an Olympus BX53P polarizing microscope, at 100x magnification. The obtained images were analysed by the Olympus cellSens software Entry version 1.14 (Olympus, Tokyo, Japan).

2. 3. Raman spectroscopy

Raman spectra excited with a diode-pumped solid-state laser (excitation wavelength 532 nm) were collected on a DXR Raman microscope (Thermo Scientific, Waltham, MA, USA), equipped with a research optical microscope, motorized X–Y stage and CCD detector. The Raman spectra were recorded for the small volume (5 µl) samples (EOs or EO-loaded NEs) transferred onto a gold support (Gold EZ-Spot Micro Mount sample slide from Thermo Scientific), which was placed on an X-Y motorized sample stage and the laser beam was focused on the sample by using a 10× objective

magnification. The laser power applied to the sample was kept at 8 mW. The spectra were recorded using an exposure time of 10 s and 10 exposures per spectrum.

2. 4. In vitro antioxidant activity

2. 4. 1. The DPPH method

The DPPH assay was performed in methanol according to our previous work [10], with small modifications. Free radical scavenging activity was tested by mixing different sample amounts with 5 ml of 0.004 % DPPH test solution in methanol, and methanol was added up to 10 ml to obtain total sample concentrations of 0.5, 2.5, 5 and 10 µL ml^{-1} for EOs, or 10, 20, 30 and 50 µL ml^{-1} for EO-loaded NEs in the reaction vials. The samples were kept in dark glass volumetric flasks, with slight shaking every 5 min, at RT. After 30 min, the absorbance was measured at 514 nm by a spectrophotometer (Beckman DU 650, Beckman Coulter, California, USA). The obtained results were expressed as INH, % (DPPH inhibition) according to the equation (1):

$$\mathrm{INH}_{\mathrm{DPPH}} = \frac{A_{\mathrm{DPPH}} - A_{\mathrm{SAMPLE}}}{A_{\mathrm{DPPH}}} 100 \quad (1)$$

where A_{DPPH} is the absorbance of the DPPH standard sample (5 ml of DPPH standard solution mixed with 5 ml of methanol) and A_{SAMPLE} is the absorbance of samples after 30 min. Trolox was used as a standard compound to validate the method, and methanol was used as a blank.

2.4.2. The ABTS method

The ABTS assay was performed in PBS buffer as described in our previous work [10], with small modifications. Free radical scavenging was tested by mixing the necessary sample amounts with 9.9 ml of the activated ABTS^{+} radical solution (absorbance of 0.7±0.05 units), and the reaction vial was filled up to 10 ml with PBS buffer (pH of 7.4). Therefore, the final tested sample concentrations in the reaction vials for the EOs were 0.1, 0.5, 2.5, 5 and 10 µL ml^{-1}, while for the EO-loaded NEs, only 10 µL ml^{-1} could be used because there was an increase in turbidity of the reaction mixtures at higher concentrations. Trolox was used as a standard compound to validate the method, and PBS buffer was used as a blank, except for the EO-loaded NEs (blank was NE in PBS buffer). The mixtures were kept for 20 min at RT (with slight shaking repeated every 5 min), and the decrease in absorbance was measured at 734 nm. The obtained results were expressed as INH, % (ABTS^{+} inhibition) according to the equation (2):

$$\mathrm{INH}_{\mathrm{ABTS}} = \frac{A_{\mathrm{ABTS}} - A_{\mathrm{SAMPLE}}}{A_{\mathrm{DPPH}}} 100 \quad (2)$$

where A_{ABTS} is the absorbance of the ABTS^{+} solution (0.7) and A_{SAMPLE} is the absorbance of samples, after 20 min of reaction time.

2. 5. Statistical analysis

Student's t-test was performed to compare the antioxidant activity of pure EOs before and after nanoemulsification. Two-way ANOVA with Tukey post hoc test was performed for three and more normally distributed data groups when the two factors (for example, EO type and SO concentration, or EO type *vs*. EO concentration) were varied at the same time, with the significance level set to $p<0.05$ (OriginPro8.5, Originlab Corporation, Northampton, MA, USA).

3. RESULTS AND DISCUSSION

3. 1. Nanoemulsions as potential carriers for essential oils

In this study, three different essential oils prepared from the leaves of aromatic plants were incorporated into a natural nanoemulsion carrier system suitable for topical application. Besides antimicrobial action [22], EOs prepared from basil - BA, oregano - OR and lemon balm - LB leaves are reported to scavenge free radicals [9,23−25]. Thus, these particular EOs and their bioactives could be good candidates for topical formulations intended for antioxidant skin protection.

Since EOs are typically natural products, to create natural final formulations it is necessary to use natural surfactants as well. Polyglycerol esters of vegetable fatty acids are naturally-derived, biodegradable and biocompatible surfactants suitable for production of nanoemulsions by using low energy methods [26,29]. It was previously reported that the commercially available PEG-free surfactant and oil (SO) mix consisting of polyglyceryl-4 laurate and dilauryl citrate (main surfactant and cosurfactant), diethylhexyl carbonate (carrier oil) and phenoxyethanol (preservative/cosurfactant) can form O/W NEs by simple dilution with water *via* a low energy mechanism termed as the phase inversion concentration (PIC) method [26]. Since the PIC process does not require heating or high-shear/pressure devices to obtain NE, it is particularly suitable for natural and sensitive ingredients (such as those in EOs), aiming to preserve their bioactivity [10,11,19].

In brief, this eco-friendly and cost-efficient preparation procedure starts from the appropriate surfactant-oil (SO) mixtures, and as water is gradually added, several characteristic intermedium phases appear depending on the water content: W/O emulsion or microemulsion (at low water content), liquid crystalline (LC) phase/ microemulsion (ME)/ /O/W/O multiple emulsion (at the phase transition point), before the system turns into the final O/W NE (at higher water contents) [10−12,26,30]. The crucial intermedium phase at the phase transition point is always characterised by low interfacial tension, thus enabling the formation of nanodroplets [12]. Therefore, it was important to investigate the phase behaviour of the SO-EO mixtures during water titration to detect mutual ratios of the key ingredients, which provided formation of homogenous EO-loaded NEs. It was found that all tested EOs exhibited similar phase behaviour, since they were all found to be compatible with the SO mix used in this study. As it can be seen from the representative phase diagram of OR-loaded NE (Fig. 1), the system passes through different types of liquid phases (W/O emulsion and a bicontinuous emulsion phase) prior to its conversion into the O/W NE, at ~75 wt.% of water in the SOW system. This was in line with the electrical conductivity measurements during the water titration, where a sharp increase in electrical conductivity appeared at ≥45 wt.% of water, indicating a transition from W/O emulsion to a bicontinuous transient phase [26,30]. At this point the excess amount of oil, which was not solubilized yet, was still visible *via* the optical microscope, while at ≥ 75 wt.% of water in the system the oil droplets were not visible anymore since they were fully incorporated into the nanoemulsion submicron system (Fig. 2).

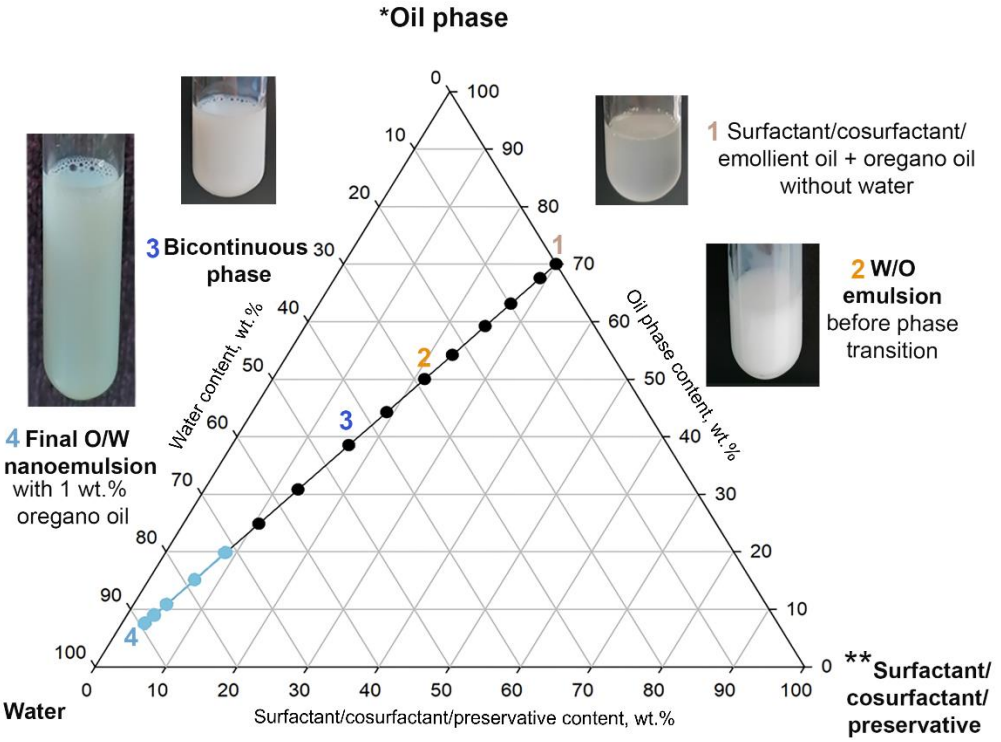

*Figure 1. Phase behaviour of the surfactant/cosurfactant/preservative and oil phase mixture with oregano oil at the optimal ratio 70:30 w/w during the nanoemulsion formation by water titration (according to the phase inversion composition - PIC method). The characteristic intermedium phases are marked with numbers while the nanoemulsion region is marked in blue. *diethylhexyl carbonate: oregano oil = 6.6 : 1 w/w; **polyglyceril-4 laurate: dilauryl citrate: phenoxyethanol = 23.4 : 1 : 13.3 w/w*

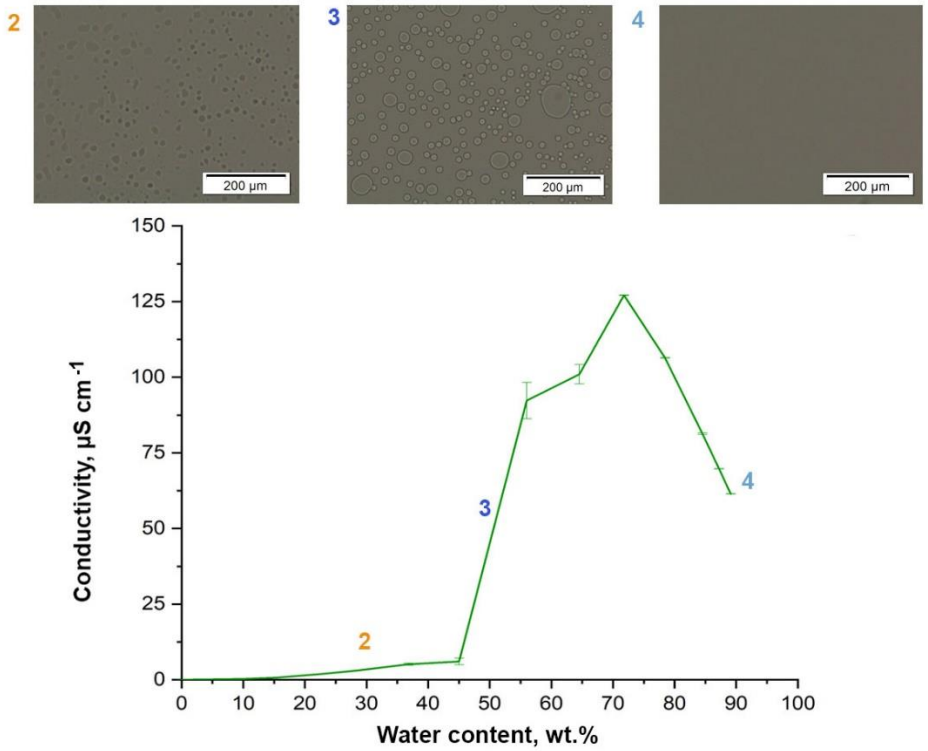

Figure 2. Electrical conductivity curve along the optimal 70:30 w/w surfactant/cosurfactant: oil phase line (the PIC method) and op tical micrographs of the characteristic intermedium phases during the nanoemulsions formation (2,3) and the final nanoemulsion (4) containing 1 wt.% oregano oil

After the NE region was detected, two important factors were investigated simultaneously to optimise the formulation: the type of EO and the SO mix concentration. These parameters were analysed regarding the effects on the *Z*-average droplet size (*Z*-ave) and mean polydispersity index (PDI) of the EO-loaded NEs and the blank NE. It was found that there was a significant difference in *Z*-ave between all EO-loaded NEs and between the EO-loaded NEs and the blank NE (Fig. 3). Influence of the SO mix concentration on the *Z*-ave was also very prominent, with higher SO mix concentration leading to the significant reduction in *Z*-ave in all EO-loaded NEs, contrary to the blank NE. PDI values (Fig. 4) were insignificantly different between the NEs prepared with different EOs or between the NEs prepared with the same EO but at different SO concentrations, since the obtained PDI values were all below 0.15, implying narrow droplet size distribution leading to system stability [23].

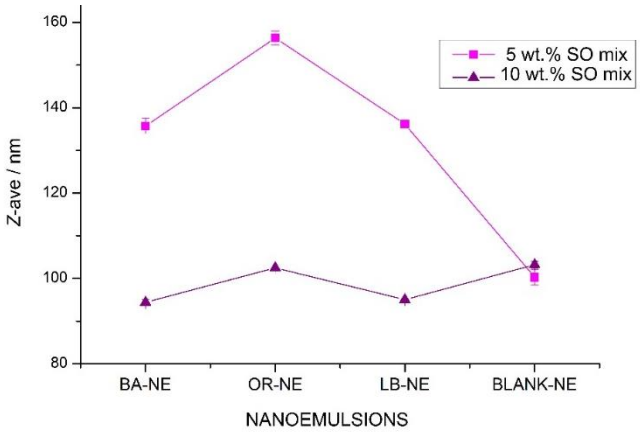

Figure 3. Z-average droplet sizes (Z-ave) in nanoemulsions prepared with different essential oils (BA – basil, OR – oregano, LB – lemon balm) and in the blank nanoemulsion at different concentrations of the surfactant and oil (SO) mix

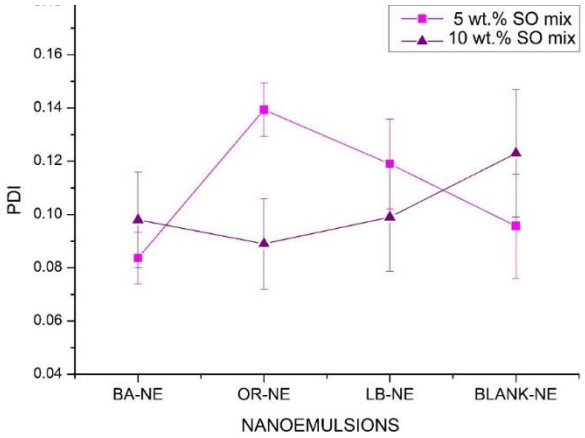

Figure 4. Mean polydispersity index (PDI) of the nanoemulsions prepared with different essential oils (BA – basil, OR – oregano, LB – lemon balm) and the blank nanoemulsion at different concentrations of the surfactant and oil (SO) mix

To conclude, all EO-loaded NEs had uniform droplet size distribution and droplet sizes were in the desired nanorange (*Z*-ave ≤200 nm), confirming the possibility for the formation of NEs with all studied EOs. However, since the EO-loaded NEs prepared with 10 wt.% of the SO mix had significantly lower droplet sizes (*Z*-ave ≤102.5 nm) than the ones prepared with 5 wt.% SO mix (*Z*-ave ≤156.3 nm), for all further investigations the NEs containing 1 wt.% EOs and 10 wt.% of SO mix were chosen.

The physico-chemical properties (*Z*-ave, PDI, pH value and electrical conductivity) of the NEs prepared with 10 wt.% SO mix were measured 24 h and one month after preparation, during storage at RT (Table 1). It was concluded that all EO-loaded NEs were preliminary stable since major signs of instability (*i.e*., creaming or phase separation as a result of a rapid droplet growth) or some other critical changes in the studied physicochemical parameters were not found after one-month storage at RT. According to the literature, the upper limit for the nanoemulsion droplet sizes varies between 100 and 500 nm while better stability is expected in the ones with smaller droplets (preferably ≤ 100 nm) or lower PDI values (preferably < 0.2) [12,13].

Table 1. Mean droplet size (Z-ave), polydispersity index (PDI), pH value and electrical conductivity of essential oil-loaded low energy nanoemulsions, 24 h and one month after preparation, stored at room temperature. The results represent mean ± standard deviation of the measured parameters, with each measurement repeated 3 times

Sample name/ measured parameter	*Z*-ave / nm		PDI		pH		Conductivity, μS cm^{-1}	
	24 h	1 month	24 h	1 month	24 h	1 month	24h	1 month
BA-loaded NE	94.39± 0.64	97.23± 1.73	0.098± 0.018	0.109± 0.025	5.67± 0.01	5.07± 0.02	82.70± 0.26	92.43± 0.12
LB-loaded NE	95.02± 0.20	95.87± 0.64	0.089± 0.017	0.073± 0.21	5.36± 0.07	5.03± 0.06	89.53± 0.06	104.90± 0.26
OR-loaded NE	102.50± 0.79	98.86± 1.25	0.099± 0.021	0.106± 0.025	5.74± 0.09	5.36± 0.01	94.73± 0.65	92.97± 0.06
Blank NE	103.2± 0.81	104.8± 1.02	0.123± 0.02	0.088± 0.018	5.56± 0.03	5.27± 0.05	79.53± 0.70	88.77± 0.31

However, after 6 months of storage at RT, significant differences in the stability were apparent among NEs prepared with different EOs. It was observed that only OR-loaded NEs remained stable during the prolonged storage (*Z*-ave ~97 nm, PDI ~0.033, pH ~5.4 and electrical conductivity ~136.6 μS cm^{-1}), without the signs of droplet aggregation or phase separation (as observed by using optical microscopy). Moreover, this formulation showed superior stability compared to the blank NE, which exhibited a dramatic increase in the droplet size and some moderate changes of the other relevant parameters (*Z*-ave ~187 nm, PDI ~0.056, pH ~5.38 and electrical conductivity ~128.8 μS cm^{-1}). Thus, the EO type and the SO mix concentration were both found to be crucial factors governing the NE properties and stability. The optimal SO mix concentration of 10 wt.% (containing ~2.2 wt.% of surfactant) can be considered favourable having in mind that potential skin irritation is typically associated with high surfactant concentrations in topical formulations [19,30].

4. 2. Raman spectroscopy study of the essential oils before and after nanoemulsification

It is known that each EO can contain up to 100 different molecules, with usually two or three principal compounds comprising up to 80–90 wt.% of the EO. Therefore, it is particularly important to identify more precisely the oil composition, having in mind that it can vary significantly depending on the plant genetics, harvesting time, production process, *etc*. [31,32]. Principal compounds in the EOs we used were reported in the producer specifications as follows: basil oil – methyl chavicol (syn. estragole), oregano oil – carvacrol and thymol, and lemon balm oil – geranial (citral a), neral (citral b) and β-caryophyllene oxide. This was in accordance with the literature data [8,9,23,24,31−33].

Raman spectra of the studied EOs are presented in Figure 5. As expected, the most intense bands in the Raman spectrum of OR observed at: 1623, 1460, 1445, 1380, 1261, 1180, 1067, 869 and 760 cm^{-1} are the ones characteristic for carvacrol, since it is the main component of OR [27,34]. Additionally, the presence of the weak band at 740 cm^{-1} (visible as a shoulder on the band at 760 cm^{-1}), which is characteristic for the ring vibration of thymol [27,34], confirms the presence of thymol in OR. Thus, the Raman spectrum of OR was in line with the producer's specification and the literature.

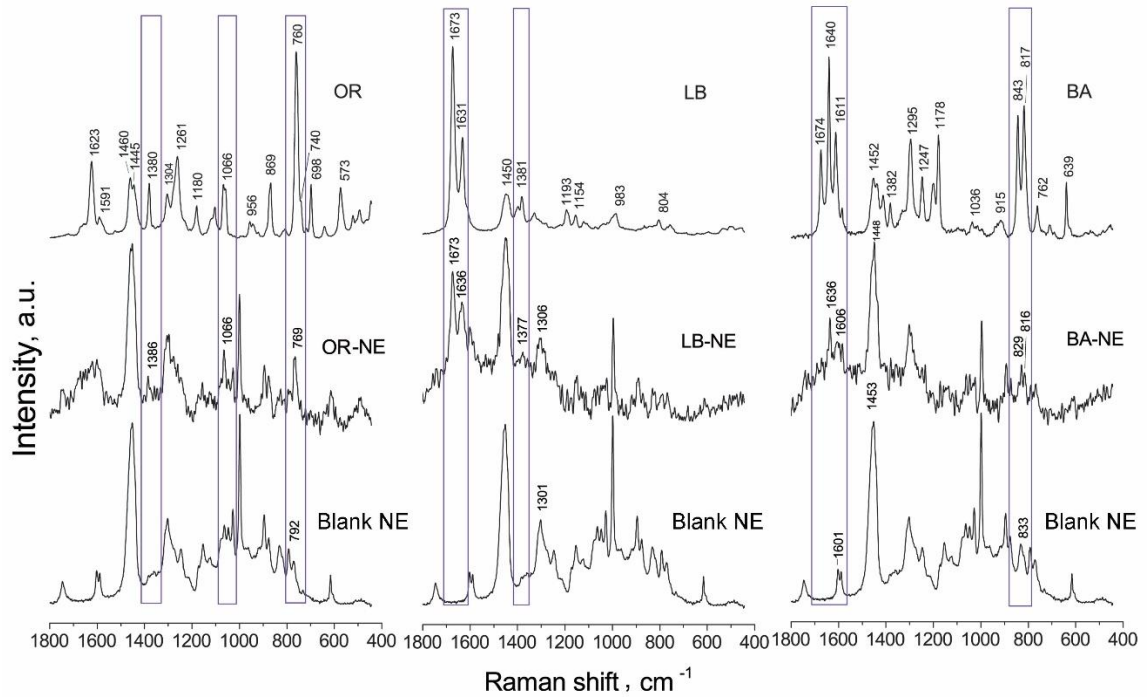

Figure 5. Comparison of Raman spectra of the blank nanoemulsions – Blank NE (bottom row), the EO-loaded nanoemulsions – BA-NE, OR-NE, LB-NE (middle row) and neat essential oils – BA, OR, LB (upper row). Each spectrum represents the average of 3 measurements acquired from a different place in the sample

Raman spectroscopy is suitable to detect different chemotypes of plant oils, such as in the case of BA, with methyl chavicol and linalool being the usual principal components, although eugenol and 1,8-cineole have been also reported [28,31]. According to the declared composition, the principal component of BA used in our study is methyl chavicol. The bands observed in the Raman spectrum of BA (Fig. 5) are in line with the earlier reported Raman spectrum of methyl chavicol at 1640, 1611, 1295, 1178, 843, 817, and 639 cm^{-1} [28]. The additional bands observed at 1674, 1640, 1452, and 1382 cm^{-1} suggest the significant presence of linalool in BA [28] as the second principal component, which was not stated by the producer. Still, this component can significantly influence antioxidant activity of BA, due to the synergism with methyl chavicol [31].

To the best of our knowledge, the Raman spectrum of LB has not been published yet. The bands observed in the Raman spectrum of LB (Fig. 5) can be identified as the characteristic peaks of the main components of this oil – geranial and neral (two geometric isomers of citral) at 1673, 1631, 1445 and 1382 cm^{-1} [28,35]. Since the lemon balm EO also has the same two main components as lemongrass, one can easily notice great similarity between the LB Raman spectrum obtained here and the one reported for lemongrass [35]. However, the LB Raman spectrum exhibited following distinguishable differences: a band at 1397 cm^{-1} assigned to the CH_2, scissoring (deformation) mode due to the presence of *β*-caryophyllene oxide, as well as a complex band at 1450/1441 cm^{-1} which probably includes a contribution from the antisymmetric methyl deformation mode of the CH_3-C group [36]. Since the LB Raman spectrum did not show intensive bands in the range between 600 and 800 cm^{-1}, it was confirmed that components containing aromatic rings were not present, unlike BA and OR oils containing aromatic molecules as their principal compounds.

Recently, novel applications of Raman spectroscopy were reported, for example, to detect structural changes in nanosystems, when oils and curcumin [37] or proteins [38] are incorporated into nanodroplets, as well as to study interactions among nanoemulsion components. Therefore, after the main components of the tested EOs were confirmed by the Raman spectroscopy, the next goal was to track potential interactions of these oils with the proposed NE carrier, by using the same approach as in our previous work investigating the interactions of red raspberry seed oil in polysorbate 80-stabilised NEs [10]. Raman spectra of the EO-loaded nanoemulsions (OR-NE, BA-NE and LB-NE) are shown in Figure 5. Although the EO concentration was low (1 wt.%), bands characteristic for each EO were still visible in the Raman spectra of all EO-loaded NEs. Still, the Raman spectra of the EO-NEs were not informative in the whole

region recognized for the qualitative differentiation of the tested EOs because the blank nanoemulsion had a very pronounced spectrum. However, some differences in the position of Raman bands of EO-loaded NEs as compared to the corresponding spectra of EOs and the blank NE were observed. This implies occurrence of some interactions in the NE after addition of the EOs. It should be noted that the Raman spectrum of OR-NE remained without significant changes after 6 months of storage (Supplementary Fig. 1), which could be attributed to the observed physicochemical stability of this particular system.

3. 3. *In vitro* antioxidant activity of EOs before and after nanoemulsification

Antioxidant activity investigations aimed to gain an insight into free radical scavenging profiles of EOs before and after nanoemulsification, as a proof of concept that nanoemulsions can be used as effective carriers for EOs exhibiting antioxidant properties. It is particularly beneficial to test the concentration dependence of the antioxidant activity and to combine different assays to gain a broader picture of the antioxidant profiles of the tested molecules/systems, given the fact that the activity of EOs depends not only on the composition but also on the concentration and the type of substrate, physical state of the system, temperature, *etc.* [16,18,24]. Therefore, two different methods (DPPH and ABTS) were employed in our study.

DPPH test is a standard assay for antioxidant activity screening, a fast, reliable and sensitive procedure suitable for studies of neat EOs and EO-containing emulsions dissolved in an organic solvent (usually methanol). To address the activity of more hydrophilic compounds in the EOs and the influence of conversion of EOs into O/W NEs, the $ABTS^+$ assay was chosen, since it can be performed in an aqueous medium (*e.g*. in PBS buffer).

Test results of the DPPH assay revealed that there are significant differences in the antioxidant activity between all EOs used at the same concentration, as well as for each EO used at different concentrations (Fig. 6). Interactions among the type of EO and concentration were also significant (two-way ANOVA, Tukey post hoc test). The order of EO antioxidant activity was: OR > LB > BA (Fig. 6). A very high percentage of free radical inhibition (INH_{DPPH} > 80 %) was observed for neat oregano oil (even at the smallest test concentration of 0.5 µl ml^{-1}). In previous studies in literature high antioxidant activities of OR were also reported by using the DPPH test in methanol (*e.g*. [23], INH over 80 % [26]). This is a consequence of the presence of carvacrol and thymol in OR, acting as excellent free radical scavengers due to the free hydroxyl group [20,23,25]. BA oil we used in this study contained mainly methyl chavicol and linalool, and it exhibited intermediate antioxidant activity, which was in line with the results of the DPPH study in ethanol performed with a similar BA chemotype, from Ararat and Napoletano cultivars [31]. In the case of LB, a slightly lower antioxidant activity was observed compared to the work of de Souza *et al.*, who reported an IC50 value of 2 µl ml^{-1} (DPPH in ethanol) for LB with similar main compounds as in our study (citral a and citral b) [17].

As can be seen in Figure 7 and Table 2, according to the DPPH test, the order of EO activity remained the same after nanoemulsification. However, there was a significant decrease in antioxidant activities of BA and LB in the NE carrier, on the contrary to the OR-loaded NE, which successfully preserved the activity (INH_{DPPH} of 87.8 to 88.5 %). This implies some significant interactions between each EO and the nanocarrier, inducing changes in the EO antioxidant activity after nanoemulsification.

However, results of the ABTS test revealed a more complicated concentration-dependent behaviour of antioxidant molecules in the EOs when tested in the aqueous medium (Fig. 8). The statistical analysis once more confirmed that all EOs exhibited significantly different INH of ABTS radical when used at the same concentrations, as well as when different concentrations of the same oil are used, with the interactions of these two factors also being significant (two-way ANOVA, $p < 0.05$). The observed order of antioxidant activity of the EOs at lower concentrations (0.1, 0.5 and 2.5 µl ml^{-1}) was the same as in the case of the DPPH test (OR> LB> BA), but with a higher INH ABTS (up to 98.5 % in the case of OR). However, when 5 µl ml^{-1} of EOs were employed the order of activity changed to LB> OR> BA, and finally, at 10 µl ml^{-1} another change in order occurred: BA> OR> LB, with all three oils exhibiting very high INH_{ABTS} (>87 %). Therefore, when these EOs were employed at higher concentrations, slightly hydrophilic antioxidant molecules in the BA (*e.g*., linalool) and LB (*e.g*., beta-caryophyllene oxide) or some other components not stated in the product specifications, could be dispersed in the aqueous phase. The result of this combined activity among the EO components is reflected in the

effective scavenging of the ABTS free radical. It is not unusual that the biological activity cannot be attributed only to the principal compound in an EO, because of naturally occurring synergistic interactions among oxygen-containing compounds in EOs [23,31].

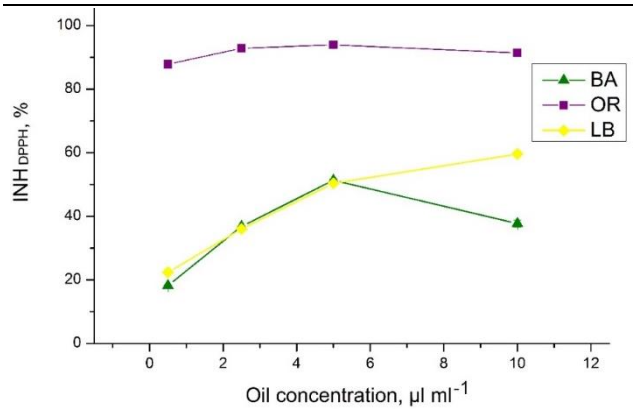

Figure 6. Antioxidant activity of neat basil (BA), lemon balm (LB) and oregano (OR) essential oil at different concentrations, measured by the DDPH assay in methanol. The results are expressed as inhibition of the DPPH free radical (INH_{DPPH})

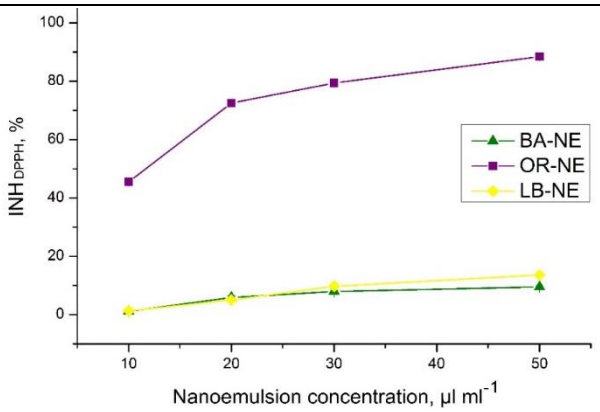

Figure 7. Antioxidant activity of nanoemulsions containing 1 wt.% of basil (BA), lemon balm (LB) or oregano (OR) essential oil at different concentrations, measured by the DDPH assay in methanol. The results are expressed as inhibition of the DPPH free radical (INH_{DPPH})

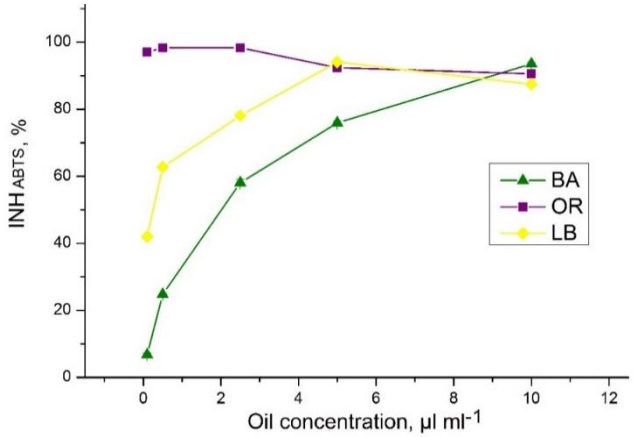

Figure 8. Antioxidant activity of basil (BA), lemon balm (LB) and oregano (OR) essential oil at different concentrations, measured by the ABTS assay in an aqueous medium (PBS buffer). The results are expressed as inhibition of the ABTS free radical (INH_{ABTS})

Table 2. Antioxidant activity of neat oils vs. essential oil-loaded nanoemulsions obtained using two different assays (DPPH in methanol and ABTS in an aqueous medium). The results are presented as INH (free radical inhibition), for the maximum nanoemulsion sample concentrations compared to the corresponding neat oil concentrations (Student's t-test, $p < 0.05$).

	INH, %			
	DPPH		ABTS	
Sample name (concentration)	Neat oil (0.5 µl ml^{-1})	Oil-loaded nanoemulsion (50 µl ml^{-1})	Neat oil (0.1 µl ml^{-1})	Oil-loaded nanoemulsion (10 µl ml^{-1})
Basil	18.22 ± 0.11	9.49 ± 0.53	6.76 ± 0.56	32.01 ± 0.99
Lemon balm	22.38 ± 0.06	13.62 ± 0.27	42.02 ± 0.47	5.97 ± 0.18
Oregano	87.85 ± 0.04	88.46 ± 0.27	97.05 ± 0.04	95.09 ± 0.16

Essential oil-loaded nanoemulsion composition: 1 wt.% essential oil, 10 wt.% SO mixture, 89 wt.% ultra-purified water while Blank nanoemulsion had the same composition, except the EO;
The results represent mean ± standard deviation of the INH of the free radicals, with each measurement repeated three times;
INH values for Blank nanoemulsions did not exceed 2 % for all tested concentrations.

In the studies of the antioxidant activity of EO-loaded NEs, the DPPH test could be performed at several different test concentrations (since both, the carrier and EO were dissolved in methanol), while the concentration range for the ABTS

assay was more limited due to the increase in turbidity when higher concentrations of these non-transparent NEs were employed. Therefore, only 10 µl ml^{-1} of EO-loaded NE was used for comparison with the results obtained for the corresponding concentration of pure EOs (*i.e*. 0.1 µl ml^{-1}) in which case the order of activity changed from OR > LB > BA for neat EOs to OR > BA > LB for EO-loaded NEs. The increase in activity of BA in the NE system (INH_{ABTS} from 6.8 to 32.0 %) can be associated with the increased solubility of the hydrophilic EO component (linalool) due to oil emulsification, *i.e*. increased total contact area with the aquatic surrounding. In fact, several EOs are reported to act as cosurfactants in nanoemulsion systems due to their positioning at the oil-water interface [39−40], which could also explain their changed antioxidant activity compared to the neat oil. The opposite behaviour, *i.e*., decrease in the activity of the LB in NE (INH_{ABTS} from 42 to 6 %) implies a different type of EO-SO mix interaction. In this case, LB constituents were packed in such a way that they became unavailable for the reaction with the ABTS radical (probably due to their positioning deep in the nanodroplet oil core). Since LB was the only oil with the aliphatic main components without free hydroxyl groups, some other structural arrangement in the NE compared to the phenolic, bulkier molecules (in BA and OR) is somewhat expected. Finally, in the case of OR, the antioxidant activity remained remarkably high in the nanoemulsion carrier (INH_{ABTS} 97 *vs*. 95 %) implying its optimal packing within the NE, which preserved its high antioxidant performance.

Having in mind the potential application in cosmetic/pharmaceutical products, storage stability is an important property to analyse during the formulation development. All EO-loaded NEs remained stable (Table 1) and without significant changes in the antioxidant activity after 1 month storage at RT (data not shown). However, with time droplet size growth and creaming started to appear even in the case of the blank NE, and the only remaining stable system after six months of storage at RT was the OR-loaded NE (a milky-white fluid emulsion with droplet sizes ~100 nm and a very narrow PDI value of ~0.1), implying that OR served as a co-stabiliser for the studied NE. Since this formulation also maintained a very high INH of DPPH and ABTS free radicals (>85 %), it was concluded that oregano oil was the most compatible with the investigated polyglycerol-ester based nanoemulsion carrier among tested essential oils. Therefore, based on the preliminary stability study and the results of antioxidant assays combined with the Raman investigations, it can be concluded that OR-loaded NEs can be proposed for antioxidant skin protection.

4. CONCLUSIONS

This work represents a feasibility study of polyglycerol-ester based nanoemulsion carrier for several EOs (basil, lemon balm and oregano) in the view of their application for antioxidant skin protection. Since the chemical composition of each EO is complex, at least two different assays were necessary to screen their antioxidant potential as well as the concentration-dependence study of the antioxidant activity. Most importantly, our study revealed that interactions of EOs with NE carriers can have a positive or negative impact on the NE stability, while at the same time nanonisation can increase or decrease the EO effectiveness as a free radical scavenger. Overall, it was found that OR-NE was the most effective and stable system, since OR acted as a co-stabiliser in the NE formulation, and its remarkably high antioxidant activity was successfully preserved during 6 months of storage. The results of this study confirm recent findings that some EOs (or their isolated compounds) could become multifunctional additives in nanoemulsions in the future, due to their cosurfactant/costabilising effect, in addition to their antioxidant and antimicrobial activities.

Acknowledgements: This research was funded by the Ministry of Education, Science and Technological Development, Republic of Serbia (Grant Agreement with University of Belgrade - Faculty of Pharmacy No: 451-03-9/2021-14/200161 and Faculty of Physical Chemistry No: 451-03-9/2021-14/200146).

REFERENCES

[1] Aburjai, T, Natsheh, FM. Plants used in cosmetics. *Phytother. Res*. 2003; 17: 987–1000. https://dx.doi.org/10.1002/ptr.1363

[2] Kaliamurthi, S, Selvaraj, G, Hou, L, Zhao, L, Gu, K, Wei, D. Synergism of essential oils with nanocarriers: emerging trends in preservation of grains and related food products. *Grain Oil Sci. Technol*. 2019; 2: 21–26. https://dx.doi.org/10.1016/j.gaost.2019.04.003

[3] Pavoni, L, Pavela, R, Cespi, M, Bonacucina, G, Maggi, F, Zeni, V, Canale, A, Lucchi, A, Bruschi, F, Benelli,G. Green micro- and nanoemulsions for managing parasites, vectors and pests, *Nanomaterials*. 2019; 9: 1285. https://dx.doi.org/10.3390/nano9091285

[4] Majeed, H, YBian, Y-Y, Ali, B, Jamil, A, Majeed, U, Khan, FO, Iqbal, KJ, Shoemaker, CF, Fang, Z. Essential oil encapsulations: uses, procedures, and trends, *RSC Adv.* 2015; 5: 58449. https://dx.doi.org/10.1039/c5ra06556a

[5] Palic, IR, Ickovski, JD, Djordjevic, AS, Mitic, VD, Stankov Jovanovic VP, Stojanovic, GS. Antioxidant and antimicrobial activities of the essential oil and solvent extracts of Mentha pulegium L. *FU Phys. Chem. Tech*. 2015; 13: 109–119. https://dx.doi.org/10.2298/FUPCT1502109P

[6] Prakash, B, Kujur, A, Yadav, A, Kumar, A, Singh, PP, Dubey, NK. Nanoencapsulation: An efficient technology to boost the antimicrobial potential of plant essential oils in food system, *Food Control.* 2018; 89: 1–11. https://dx.doi.org/10.1016/j.foodcont.2018.01.018

[7] Yakoubi, S, Bourgou, S, Mahfoudhi, N, Hammami, M, Khammassi, S, Horchani-Naifer, K, Msaada, K, Saidani Tounsi, M. Oil-in-water emulsion formulation of cumin/carvi essential oils combination with enhanced antioxidant and antibacterial potentials, *J. Essent. Oil Res*. 2020; 32: 536–544. https://dx.doi.org/10.1080/10412905.2020.1829510

[8] Bhargava, K, Conti, DS, da Rocha, SRP, Zhang, Y. Application of an oregano oil nanoemulsion to the control of foodborne bacteria on fresh lettuce, *Food Microbiol*. 2015; 47: 69–73. https://dx.doi.org/10.1016/j.fm.2014.11.007

[9] da Silva Gundel, S, Velho, MC, Diefenthaler, MK, Favarin, FR, Copetti, PM, Fogaça, AO, Klein, B, Wagner, R, Gundel, A, Sagrillo, MR, Ourique, AF. Basil oil-nanoemulsions: Development, cytotoxicity and evaluation of antioxidant and antimicrobial potential, *J. Drug Deliv. Sci. and Tech.* 2018; 46: 378-383. https://dx.doi.org/10.1016/j.jddst.2018.05.038

[10] Gledovic, A, Janosevic Lezaic, A, Krstonosic, V, Djokovic, J, Nikolic, I, Bajuk-Bogdanovic, D, Antic Stankovic, J, Randjelovic, D, Savic, SM, Filipovic, M, Tamburic, S, Savic, SD. Low-energy nanoemulsions as carriers for red raspberry seed oil: Formulation approach based on Raman spectroscopy and textural analysis, physicochemical properties, stability and in vitro antioxidant/ biological activity. *PLoS ONE.* 2020; 15(4): e0230993. https://dx.doi.org/10.1371/journal.pone.0230993

[11] Solans, C, Sole I. Nano-emulsions: Formation by low-energy methods. *Curr. Opin. Colloid Interface Sci.* 2012; 17: 246–254. https://dx.doi.org/10.1016/j.cocis.2012.07.003

[12] Gupta A, Eral BH, Hatton TA, Doyle PS. Nanoemulsions: formation, properties and applications. Soft Matter. 2016; 12: 2826−2841. https://doi.org/10.1039/c5sm02958a

[13] Mc Clements, DJ. Nanoemulsions versus microemulsions: terminology, differences, and similarities. Soft Matter, 2012,8, 1719-1729. https://doi.org/10.1039/C2SM06903B

[14] Yukuyama MN, Ghisleni DDM, Pinto TJA, Bou-Chacra NA. Nanoemulsion: process selection and application in cosmetics–a review. *Int. J. Cosmet. Sci*. 2016; 38: 13−24. pmid:26171789

[15] Chang, YY and McClements, DJ. Optimization of orange oil nanoemulsion formation by isothermal low-energy methods: Influence of the oil phase, surfactant, and temperature. *J. Agric. Food Chem.* 2014; 62: 2306−2312. https://dx.doi.org/10.1021/jf500160y

[16] Rao, J and Mc Clements, DJ. Food-grade microemulsions and nanoemulsions: Role of oil phase composition on formation and stability. *Food Hydrocoll*. 2012; 9: 326−334. https://doi.org/10.1016/j.foodhyd.2012.04.008

[17] Khurana, S, Jain, NK, Bedi, PMS. Nanoemulsion based gel for transdermal delivery of meloxicam: Physico-chemical, mechanistic investigation. *Life Sci*. 2013; 92: 383−392. https://doi.org/10.1016/j.lfs.2013.01.005

[18] Sengupta, P and Bappaditya Chatterjee, B. Potential and future scope of nanoemulgel formulation for topical delivery of lipophilic drugs. *Int. J. Pharm*. 2017; 526: 353−365. https://doi.org/10.1016/j.ijpharm.2017.04.068

[19] Nastiti CMRR, Ponto T, Abd E, Grice JE, Benson HAE, Roberts. Topical Nano and Microemulsions for Skin Delivery. *Pharmaceutics*. 2017; 9: 37

[20] Dorman, HJD, Surai, P, Deans, SG. In vitro antioxidant activity of a number of plant essential oils and phytoconstituents. *J. Essent. Oil Rex*. 2000; 12: 241–248. https://dx.doi.org/10.1080/10412905.2000.9699508

[21] Raut, JS, Karuppayil, SM. A status review on the medicinal properties of essential oils. *Ind. Crops Prod.* 2014; 62: 250–264. https://dx.doi.org/10.1016/j.indcrop.2014.05.055

[22] Padalia, H, Moteriya, P, Baravalia, Y, Chanda, SV. Antimicrobial and synergistic effects of some essential oils to fight against microbial pathogens – a review, in book: *The Battle Against Microbial Pathogens: Basic Science, Technological Advances and Educational Programs* (Mendez-Vilas, A, Ed.). Formatex research center, Badajoz, Spain. 2015: 35–45.

[23] Kulisic, T, Radonic, A, Katalinic, V, Milos, M. Use of different methods for testing antioxidative activity of oregano essential oi. *Food Chem.* 2004; 85: 633–640. https://dx.doi.org/10.1016/j.foodchem.2003.07.024

[24] de Sousa, AC, Alviano, DS, Blank, AF, Alves, PB, Alviano, CS, Gattass, CR. Melissa officinalis L. essential oil: antitumoral and antioxidant activities. *J Pharm Pharmacol*. 2004; 56: 677–681. https://dx.doi.org/10.1211/0022357023321

[25] Viuda-Martos, M, Navajas, YR, Zapata, ES, Fernandez-Lopez, J, Perez-Alvarez, JA. Antioxidant activity of essential oils of five spice plants widely used in a Mediterranean diet. *Flavour Fragr. J*. 2010; 25: 13–19. https://dx.doi.org/10.1002/ffj.1951

[26] Heunemann, P, Prevost, S, Grillo, I, Marino, CM, Meyer, J, Gradzielski, M. Formation and structure of slightly anionically charged nanoemulsions obtained by the phase inversion concentration (PIC) method. *Soft Matter*. 2011; 7: 5697–5710. https://dx.doi.org/10.1039/c0sm01556c

[27] Daferera, DJ, Tarantilis, PA, Polissiou, MG. Characterization of essential oils from lamiaceae species by fourier transform Raman spectroscopy. *J. Agric. Food Chem.* 2002; 50: 5503-5507. https://dx.doi.org/10.1021/jf0203489

[28] Jentzch, PV, Ramos, LA, Ciobota, V. Handheld Raman spectroscopy for the distinction of essential oils used in the cosmetics industry. *Cosmetics*. 2015; 2: 162–176. https://dx.doi.org/10.3390/cosmetics2020162

[29] Hanno, I, Centini, M, Anselmi, C, Bibiani, C. Green cosmetic surfactant from rice: Characterization and application. *Cosmetics*. 2015; 2: 322-341. https://dx.doi.org/10.3390/cosmetics2040322

[30] Gledovic, A, Janosevic Lezaic, A, Nikolic, I, Tasic-Kostov, M, Antic-Stankovic, J, Krstonosic, V, Randjelovic, D, Bozic, D, Ilic, D, Tamburic, S, Savic, S. Polyglycerol ester-based low energy nanoemulsions with red raspberry seed oil and fruit extracts: Formulation development toward effective in vitro/in vivo bioperformance. *Nanomaterials*. 2021; 11: 217. https://dx.doi.org/10.3390/nano11010217

[31] Couto, HGS, Blank, AF, de Oliveira e Silva, AM, de Lima Nogueira, PC, de Fatima Arrigoni-Blank, M, de Castro Nizio, DA, de Oliveira Pinto, JA. Essential oils of basil chemotypes: Major compounds, binary mixtures, and antioxidant activity. *Food Chem.* 2019; 293: 446–454. https://dx.doi.org/10.1016/j.foodchem.2019.04.078

[32] Patora, J, Majda, T, Gora, J, Klimek, B. Variability in the content and composition of essential oil from lemon balm (Melissa officinalis L.) cultivated in Poland. *Acta Pol. Pharm.* 2003; 60*:* 395– 400.

[33] Nostro, A, Sudano Roccaro, A, Bisignano, G, Marino, A, Cannatelli, MA, Pizzimenti, FC, Cioni, PL, Procopio, F, Blanco, AR. Effects of oregano, carvacrol and thymol on Staphylococcus aureus and Staphylococcus epidermidis biofilms. *J. Med. Microbiol.* 2007; 56: 519–523. https://dx.doi.org/10.1099/jmm.0.46804-0

[34] Schulz, H, Ozkan, G, Baranska, HK, Ozcan, M. Characterisation of essential oil plants from Turkey by IR and Raman spectroscopy. *Vibrational Spectroscopy*. 2005; 39: 249-256. https://dx.doi.org/10.1002/ffj.3203

[35] Jentzch, PV and Ciobota, V. Raman spectroscopy as an analytical tool for analysis of vegetable and essential oils. *Flavour Fragr. J.* 2014; 29: 287–295. https://dx.doi.org/10.1002/ffj.3203

[36] Socrates, G. Infrared and Raman characteristic group frequencies: Tables and charts, 3rd ed. John Wiley & Sons, Ltd, Chichester, 2001.

[37] Rachmawati H, Budiputra DK, Mauludin R. Curcumin nanoemulsion for transdermal application: formulation and evaluation. *Drug Dev. Ind. Pharm*. 2015; 41: 560–566. https://doi.org/10.3109/03639045

[38] Zhu Y, Li Y, Wu C, Teng F, Qi B, Zhang X et al. Stability Mechanism of Two Soybean Protein-Phosphatidylcholine Nanoemulsion Preparation Methods from a Structural Perspective: A Raman Spectroscopy Analysis. *Sci. rep*. 2019; 9: 6985. https://doi.org/10.1038/s41598-019-43439-5

[39] Rocha-Filho, PA, Camargo, MFP, Ferrari, M, Maruno, M. Influence of lavander essential oil addition on passion fruit oil nanoemulsions: Stability and in vivo study. *J Nanomed. Nanotechnol*. 2014; 5: 198. https://dx.doi.org/10.4172/2157-7439.1000198

[40] Nikolic, I, Gledovic, A, Tamburic, S, Major, T, Savic, S. Nanoemulsions as Carriers for Natural Antioxidants: Formulation Development and Optimisation, *in Emulsion-based Encapsulation of Antioxidants,* Aboudzadeh, MA, Ed., Springer Nature Switzerland. 2021: 149 –195. https://dx.doi.org/10.1007/978-3-030-62052-3_4

Niskoenergetske nanoemulzije kao nosači za etarska ulja u topikalnim formulacijama za antioksidantnu zaštitu kože

Ana Gledović[1],*, Danica Bajuk-Bogdanović[2], Snežana Uskoković-Marković[3], Leposava Pavun[4], Snežana Savić[1] i Aleksandra Janošević Ležaić[4]

[1] Univerzitet u Beogradu, Farmaceutski fakultet, Katedra za farmaceutsku tehnologiju i kozmetologiju, 11000 Beograd, Srbija

[2] Univerzitet u Beogradu, Fakultet za fizičku hemiju, Srbija

[3] Univerzitet u Beogradu, Farmaceutski fakultet, Katedra za analitičku hemiju, Srbija

[4] Univerzitet u Beogradu, Farmaceutski fakultet, Katedra za fizičku hemiju i instrumentalne metode, Srbija

(Naučni rad)

Izvod

U ovoj studiji nekoliko različitih etarskih ulja (EU): bosiljak – BO, matičnjak – MA i origano – OR inkorporirano je u nanoemulzije (NE) kao potencijalne nosače za prirodne i osetljive bioaktivne sastojke. NE su pripremljene pomoću metode inverzije faza (engl. *phase inversion composition – PIC method*) koja predstavlja niskoenergetski i ekonomičan postupak izrade. Fizičkohemijska stabilnost nanoemulzija potvrđena je analizom raspodele veličina kapi, merenjem električne provodljivosti i pH vrednosti, kao i optičkom mikroskopijom. Nađeno je da su vrsta EU i koncentracija smeše surfaktanata i uljane faze dva ključna faktora koja su uticala na karakteristike i stabilnost dobijenih emulzija. Tehnikom Ramanske spektroskopije potvrđeni su glavni aktivni sastojci etarskih ulja i detektovane su moguće interakcije sa nanonosačem, što predstavlja noviju primenu pomenute tehnike. Pokazano je da antioksidantna aktivnost prema DPPH radikalu u metanolu zavisi od koncentracije, sa sličnim trendom za čista etarska ulja i za nanoemulzije sa uljima (OR> MA> BO). Međutim, ABTS test u vodenoj sredini pokazao je izrazite promene u redosledu aktivnosti sa povećanjem koncentracije EU i nakon nanonizacije EU. Generalno, dokazano je da je OR-NE najefikasniji i najstabiliniji sistem, s obzirom da je ulje origana ispoljilo ulogu kostabilizatora u formulaciji, uz istovremeno očuvanje njegove veoma visoke antioksidantne aktivnosti u obliku nanoemulzije, tokom 6 meseci čuvanja.

Ključne reči: origano; bosiljak; matičnjak; nanonizacija; Ramanska spektroskopija; stabilnost

Izazovi i dileme elektrohemijske konverzije i skladištenja energije

Aleksandar Dekanski

Univerzitet u Beogradu, Institut za hemiju, tehnologiju i metalurgiju, Centar za elektrohemiju, Njegoševa 12, Beograd, Srbija

Izvod

Civilizacija se od kraja 20. veka suočava sa mnogim izazovima, od koji su neki od njih toliko ozbiljni da ugrožavaju i sam opstanak čovečanstva. Za neke se može reći da su novi, kao što je globalno zagrevanje, ali i oni koji su već duže prisutni poprimaju razmere koje nikada ranije nisu imali – zagađenje životne sredine, kisele kiše, oštećenje ozonskog omotača, sve veći jaz između razvijenih i nerazvijenih zemalja, terorizam, i kriza izbeglica kao posledica toga, ubrzano iscrpljivanje fosilnih goriva i time nagoveštaj svetske energetske krize... Svet postaje svestan da je rešavanje tih izazova od suštinskog značaja za njegov opstanak i, možda kasno, ali nadajmo se ne prekasno, hvata se u koštac sa njima. Ako bi pokušali da postavimo pitanje šta je najvažniji i najveći izazov, sigurno bi dobili mnogo različitih odgovora, ali jasno je da se ni jedan ne sme zapostaviti i da svaki mora biti savladan u dogledno vreme. Ipak, jedan od njih se izdvaja – energija. Razlog je vrlo jednostavan, bez energije ni jedan od problema sa kojima se suočavamo ne može biti rešen.

Ključne reči: fosilna goriva; akumulatori; baterije; galvanski gorivni spregovi; superkondenzatori; emisija CO2; životna sredina.

Dostupno on-line na web adresi časopisa: http://www.ache.org.rs/HI/

PISMO UREDNIKU

UDK: 621.351:165.412

Hem. Ind. **76 (1)** 43-54 (2022)

1. UVOD

Sasvim je izvesno da će fosilna goriva, koja su trenutno najveći izvor energije, biti iscrpljena tokom života generacija koje se sada rađaju (Slika 1.), i da je neophodno razviti i unaprediti nove izvore energije koji će ih zameniti. Ali sasvim je jasno da ti novi izvori, sem što će nadomestiti fosilna goriva, moraju biti obnovljivi i bezbedni po životnu sredinu i planetu, ali i ekonomski isplativi i dovoljno jeftini [1-4].

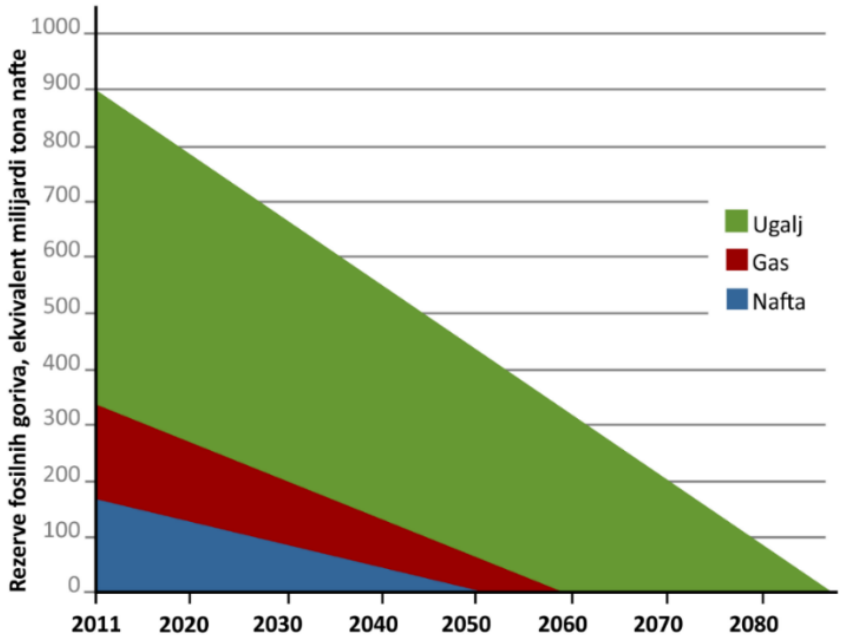

Slika 1. Rezerve fosilnih goriva [5]
Fig. 1. Fossil fuel reserves [5]

Corresponding authors: Aleksandar Dekanski, Univerzitet u Beogradu, IHTM - Centar za elektrohemiju, Njegoševa 12, Beograd, Srbija
E-mail: dekansk@ihtm.bg.ac.rs
Paper received: 01 Februaty 2022; Paper accepted: 10 February 2022; Paper published: 10 February 2022.
https://doi.org/10.2298/HEMIND220201002D

Već dugi niz godina istraživači širom sveta razvijaju mnoge takve sisteme koji mogu zadovoljiti postavljene uslove, a mnogi od njih se već nalaze i u širokoj primeni. Pomenimo samo baterije i galvanske gorivne spregove (gorivne ćelije) električnih automobila, baterije za napajanje mobilnih uređaja, vetrenjače, solarne panele, korišćenje biomase i geotermalne energije… Međutim, nije energija iz svih ovakvih izvora na raspolaganju uvek kada je i potrebna, pa je pored izvora neophodno razvijati i sisteme za skladištenje energije.

2. PODELA SISTEMA ZA SKLADIŠTENJE ENERGIJE

Generalno, skladištenje energije je veoma teško i najčešće zahteva njeno pretvaranje u druge oblike energije koje je lakše skladištiti [6]. To je razlog što se poslednjih decenija intenzivno razvijaju novi materijali i intenzivno radi na razumevanju načina funkcionanja kako postojećih tako i novorazvijenih materijala i procesa [7]. Podelu sistema za skladištenje energije moguće je izvršiti na osnovu različitih kriterijuma, ali najopštija je njihova klasifikacija na osnovu vrste energije koja se skladišti (Tabela 1).

Tebela 1. Klasifikacija sistema za skladištenje energije
Table 1. Classification of energy storage systems

Hemijski	Elektrohemijski	Električni	Mehanički	Termički
• Biogoriva • Sintetički prirodni gas • Vodonik • Termohemijsko skladištenje	• Primarni izvori • Sekundarni izvori ○ akumulatori ○ superkondenzatori • Hibridni izvori ○ Gorivni galvanski spregovi ○ Protočni redoks akumulatori ○ Metal-vazduh elementi	• Kondenzatori • Superprovodni magneti	• Inercioni akumulatori (engl. *Fly wheel energy storage*) • Reverzibilene hidroelektrane • Rezervoari komprimovanog vazduha	• Senzibilna toplota • Latentna toplota • Sorpcioni sistemi (adsorpcija ili apsorpcija)

Od svih nabrojanih sistema, poslednjih decenija razvoj elektrohemijskih sistema je tema sve većeg broja istraživanja, a njihov razvoj i unapređenje osobina su veoma intenzivni [1,8,9]. Razlozi za to su mnogobrojni: najjednostavniji su, najzastupljeniji, a često i jedini mogući izvor napajanja mobilnih uređaja svih vrsta; mogu napajati uređaje i aparate sa najrazličitijim zahtevima snage i energije, od pejsmejkera do automobila i kamiona; najveći deo njih su obnovljivi izvori energije, i praktično ne narušavaju životnu sredinu… Elektrohemijski sistemi za skladištenje su često istovremeno i sistemi za konverziju energije, pa se njihovi kvaliteti i primenljivost najčešće i analiziraju kao osobine sistema za konverziju i skladištenje energije. Ipak, pre detaljnijeg prikaza karakteristika ovih sistema i razmatranja izazova i dilema koji stoje pred njima, kratak opis ostalih sistema za skladištenje energije.

Hemijski sistemi za skladištenje energije zasnovani su na pretvaranju drugih vidova energije u hemijsku – sintezom hemijskih goriva, supstanci sa velikom specifičnom energijom. Vodonik je čisto, energetski kvalitetno (toplotna moć ~142 MJ kg^{-1}) i za životnu sredinu bezbedno gorivo koje se može dobiti na mnogo načina (elektroliza, termoliza, konverzija fosilnih goriva, gasifikacija biomase itd.) [10]. Može se praktično neograničeno dugo čuvati u posudama pod pritiskom. Sintetički prirodni gas se dobija razgradnjom organsih materija, uz gasifikaciju praćenu kondicioniranjem gasa, do supstance slične prirodnom gasu [11]. Ovakvim postupcima se vrši gasifikacija uglja, pogotovo onog koji je niske kalorične vrednosti i čije sagorevanje je pogubno po životnu sredinu. Gorivo se može dobiti i iz biomase (bilo koja organska supstanca koja potiče od biljaka ili životinja – poljoprovreda, šumarstvo, deponije komunalnog smeća i sl.), njenom konverzijom u biogoriva različitim postopcima [12]. Najčešće se biomasa konvertuje u biodizel i alkohol, koji se koriste kao zamena ili dopuna klasičnim fosilnim gotivima. Biomasu je moguće i gasifikovati, odnosno pretvoriti u sintetički prirodni gas [13]. Termohemjsko skladištenje energije se zasniva na reverzibilnoj reakciji, u kojoj jedan materijal apsorbuje toplotnu energiju da bi se hemijski pretvorio u dve komponente. Obrnutom reakcijom, ove komponente se ponovo kombinuju oslobađajući energiju [14].

Električni sistemi energiju skldište ili direktnim skladištenjem električne energije na površinama metalizovanih plastičnih folija ili metalnih elektroda - kondenzatori; ili u magnetnom polju nastalom protokom direktne struje u superprovodnom kalemu koji se drži ispod svoje superprovodljive kritične temperature – superprovodni magnetni

sistemi (engl. *superconducting magnetic energy storage systems* - SMES) [15]. Pošto je gustina energije kondenzatora veoma mala, oni su u stanju da isporuče ili prihvate velike struje, ali samo u vrlo kratkiom vremenu. SMES sistemi isporučuju uskladištenu energiju razelektrisavanjem kalema.

Mehanički sistemi za skladištenje energije zasnivaju se na sledećim principima: primenom gasa pod pritiskom, nategnute opruge i kinetičke i/ili potencijalne energije. Dok su ireverzibilne hidroelektrane, i kompresija gasa dobro i već dugo poznati sistemi, savremeni inercioni sistemi su zasnovani na masivnim rotirajućim cilindrima oslonjenim na stator pomoću magnetno levitiranih ležajeva. Zamajac mehanički skladišti energiju kao kinetičku energiju mase rotora koji se okreće veoma velikim brzinama [16]. Koriste se skoro isključivo u električnim lokomotivama kako bi se garantovalo kretanje duž neelektrifikovanih delova pruge, ali i za skladištenje povratne energije električnih lokomotiva prilikom kočenja. Najkorisnija prednost mehaničkog skladištenja energije je da oni mogu lako da isporuče energiju kad je to potrebno za mehaničke radove [1].

Termički sistemi skladište toplotu ili hladnoću u različitim medijumima, pod različitim uslovima temperature, mesta ili snage [17]. Primenljivi su u industrijske i stambene svrhe (grejanje ili hlađenje prostora, procesno grejanje i hlađenje, proizvodnja tople vode ili proizvodnja električne energije). Skladištenje toplote se može klasifikovati u tri različite kategorije: senzibilna toplota [18], latentna toplota, apsorpcioni i adsorpcioni sistemi [17].

3. ELEKTROHEMIJSKI SISTEMI ZA KONVERZIJU I SKLADIŠTENJE ENERGIJE

Kako i samo njihovo ime govori, elektrohemijski sistemi bi se podjednako tačno mogli svrstati i u hemijske ili električne sisteme za (konverzju) i skladištenje energije, ili podeliti između ove dve kategorije. Međutim, njihove specifičnosti, osobine, fleksibilnost i rasprostranjenost primene sasvim opravdavaju to što su svrstani u posebnu kategoriju. Osnovna podela elektrohemijskih sistema je na primarne, sekundarne i hibridne izvore energije (električne struje). Iako skoro svi ovi sitemi suštinski skladište energiju, uobičajeni je termin izvor, jer njihova primena skoro uvek podrazumeva napajenje nekog električnog uređaja, bilo direktnom isporukom uskladištene električne enengije, bilo isporukom električne energije nastale direktnom konverzijom (interno ili eksterno) uskladištene hemijske energije.

Pod primarnim sistemima podrazumevaju se izvori koji hemijsku energiju ireverzibilno pretvaraju u električnu i nakon upotrebe bi ih trebalo reciklirati. U svakodnevnom životu najčešće se nazivaju nepunjive baterije[1], a najpoznatiji predstavnici ove grupe izvora su cink-mangan, litijum-mangan i cink-srebro elementi.

3. 1. Akumulatori

Akumulatori sa superkondanzatorima čine sekundarne izvore električne energije. Oni imaju mogućnost da, manje ili više reverzibilno, pretvaraju hemijsku energiju u električnu – proces pražnjenja (pri upotrebi akumulatora) i obrnuto, električnu u hemijsku - proces punjenja. Danas se koriste četiri osnovna tipa akumulatora: olovni, akumulatori na bazi nikla, litijum jonski i litijum polimerni.

Olovni akumulatori su najranije razvijeni sekundarni izvori [19], ali su zbog svoje jednostavne konstrukcije, niske cene i velike snage i dalje u veoma širokoj upotrebi. Iako je princip rada nepromenjen još od otkrića, nova tehnička rešenja omogućila su da je njihovo korišćenje ekonomičnije, jednostavnije i sigurnije [20].

Korišćenje **nikal akumulatora** (nikal-kadmijum, nikal-gvožđe i nikal-metal-hidrid) je u stalnom opadanju i oni praktično nestaju iz upotrebe. Nikal-kadmijum akumulatori su skoro potpuno nestali, pre svega zbog toksičnosti kadmijuma, a i ostali akumulatori na bazi nikla se sve manje koriste zbog visoke cene i malog specifičnog kapaciteta i snage u odnosu na baterije na bazi litijuma.

Litijumski akumulatori su, od kada su razvijeni, a zahvaljujući stalnim unapređenjima, kako u konstrukciji tako i u karakteristikama, postali najdominantniji oblik mobilnog izvora električne energije. Princip rada ovih akumulatora zasniva se na interkalaciji - deinterkalaciji jona litijuma u elektrodnim materijalima. Kod *litijum - jon akumulatora*, zbog reagovanja litijuma sa vazduhom i vodom (čak i u tragovima) ne mogu se koristiti vodeni rastvori kao elektroliti, pa su se koristili tečni aprotonski rastvarači, uz dodatak elektroprovodnih soli, na primer onih na bazi $LiClO_4$ ili $LiPF_6$. Sa druge

[1]Termin baterija za ove izvore je suštinski pogrešan, jer baterija podrazumeva sklop od više elemenata povezanih u jedan izvor struje. Tako je ono što se zove baterija od 1,5 V ustvari jedan element (ćelija), ali primerni izvor od 9 V zaista jeste baterija, jer se sastoji od 6 na red vezanih ćelija od 1,5 V.

strane, anodni materijal (najčešće grafitni), kada je interkaliran sa litijumom, u reakcijama sa elektrolitom formira pasivni sloj koji vremenom smanjuje kapacitet akumilatora. Sledeća generacija, tzv. *litijum - polimer akumulatori*, poseduje polimerni elektrolit (najčešće u obliku gela na bazi polietilen-oksida, uz dodatak $LiPF_6$), koji je istovremeno i separator. Tako se značajno smanjuje formiranje pasivnog sloja na grafitnoj anodi, ali to i poskupljuje ovakve sisteme [21].

3. 2. Superkondenzatori

Ovi izvori električne energije nadoknađuju dve bitne mane akumulatora: relativno malu snagu (maksimalno do 200 W kg^{-1}) i dugo vreme punjenja (najmanje nekoliko časova). Međutim, za razliku od akumulatora, superkondanzatori, čija se specifična snaga kreće od jednog do nekoliko desetina kW kg^{-1}, i mogu isporučiti svu energiju za vrlo kratko vreme (reda veličine sekunde), imaju relativno malu specifičnu energiju (5-20 Wh kg^{-1}), te je njihova upotreba ograničena samo kada je neophodna velika snaga u kratkom vremenu (npr. nivelisanje snage električnih uređaja i električnih automobila).

Osnovni princip rada klasičnih superkondenzatora je isti kao i kod klasičnih kondenzatora, s tim da materijali elektroda imaju veoma razvijenu površinu, te tako mogu da akumuliraju mnogo veće količine naelektrisanja [22]. Kako je u pitanju samo elektrostatičko privlačenje, brzine punjenja i pražnjenja su veoma velika, uz mogućnost isporučivanja velike jačine struje. Kako nema razmene elektona kao kod klasičnih elektrohemijskih reakcija, elektrode nisu izložene nikakvim promenama, pa broj ciklusa punjenja i pražnjenja, bez uticaja na osobine akumulatora, može biti veći i od sto hiljada (kod akumulatora on je manji od 1000 ciklusa) [22,23].

Razvoj različitih materijala, pogotovo od sredine 20. veka i pronalaska elektrohemijkih dvojnoslojnih superkondenzatora čiju osnovu čine ugljenični materijali, doveo je do toga da danas postoje čitav niz supekondenzatora raličitih osobina [24]. Posebno treba izdvojiti pseudokapacitivne superkondenzatore, koji koriste neke okside metala ili provodne polimere koji pored akumulacije naelektrisanja na površini, deo energije akumuliraju i isporučuju procesima Faradejske prirode, razmenjuju elektrone kroz niz diskretnih stanja,elektrohemijskom reakcijom. Ovi akumulatori imaju veći sadržaj energije, oko 15 do 20 Wh kg^{-1}, ali manji sadržaj snage, reda kW kg^{-1} i znatno manji broj mogućih ciklusa punjenje-pražnjenje, do nekoliko hiljada [22].

Kako bi se prevazišle mane i iskoristile predosti akumulatora i superkondenzatora, poslednjih godina razvijaju se hibridni superkondenzatori, koji mogu biti simetrični ili asimetrični kompozitni hibridi ili akumulatorski hibridi, koji kombinuju jednu superkapacitivnu elektrodu i jednu akumulatorsku elektrodu [22].

3. 3. Hibridni sistemi

Za razliku od do sada opisanih elektrohemijskih sistema, hibridni elektrohemijski sistemi podrazumevaju da je bar jedna od aktivnih komponenti akumulirana van kućišta izvora. U hibridne sisteme ubrajaju se protočni redoks akumulatori [25], gorivni galvanski spregovi [26] i metal-vazduh akumulatori [27].

Funkcionisanje protočnih redoks akumulatora zasnovano je na elektrohemijskim ćelijama kroz koje cirkuliše elektrolit koji dospeva iz nezavisnog rezervoara. Pri punjenju aktivna supstanca iz rastvora se na negativnoj elektrodi redukuje, a na pozitivnoj oksiduje, a pri pražnjenju se odigravaju suprotni procesi. Snaga i energija ovih sistema su nezavisni jedno od drugog, jer zavise od broja i veličine ćelija, odnosno kapaciteta spoljašnjih rezervoara. Kako su ovi sistemi velikih dimenzija, a mogu koristiti bilo koji konvertor energije, najčešće se koriste za akumulaciju električne energije iz fotonaponskih pretvarača (sunčanih panela), na teško pristupačnim mestima daleko od druge vrste izvora električne energije.

Galvanski gorivni spregovi konvertuju potencijalnu hemijsku energiju goriva, najčešće vodonika (ali i metanola,etana, etanola, biogasa...) u električnu energiju uz veliko iskorištenje. Ukupna elektrohemijska reakcija sagorevanja goriva u prisustvu kiseonika, zbog prostorne razdvojenosti, rezultuje usmerenim protokom naelektrisanja kroz spoljašnje električno kolo (potrošača), dok se u samoj ćeliji balans uspostavlja kretanjem jona kroz elektrolit. Poslednjih godina, istraživanja su usmerena na razvoj spregova zasnovanih na anodnoj oksidaciji zagađujućih otpadnih organskih materija primenom poluprovodnika u foto-elektrohemijskim gorivnim spregovima i biogorivnim ćelijama uz primenu bakterija i enzima [26-28], ali i spregova koji mogu koristiti više vrsta goriva [29]. Matematičkim modelovanjem pokušava se doći do optimalnijih konstrukcija i geometrijskih oblika, koji bi poboljšali karakteristike gorivnih spregova [30].

Metal-vazduh elektrohemijski izvori su danas uglavnom hibridni primarni elementi zasnovani na anodnoj reakciji rastvaranja elektronegativnih metala - cinka, aluminijuma, magnezijuma, kalijuma ili litijuma [27]. No praktičnu primenu imaju samo oni na bazi cinka, dok se najviše pažnje u istraživanjima usmerava na one na bazi litijuma. Izvori na bazi aluminijuma i magnezijuma imaju ograničenu primenljivost, tamo gde je moguće uranjanje elektroda u rastvor neposredno pre korišćenja, a sve zbog korozione nestabilnosti ovih metala. Pronalaskom keramičkih membrana na bazi litijuma i natrijuma – LiSICON [31] i NaSICON [32] (SICON od engl. ***S**uper**I**onic**CON**ductor*) otvaraju se nove mogućnosti u razvoju metal - vazduh hibridnih sistema

3. 4. Izazovi i dileme

Iako elektrohemijski sistemi za konverziju i skladištenje energije na prvi pogled imaju izvrsne osobine, kako sa stanovišta održivosti, obnovljivosti i ne ugrožavanja životne sredine, tako i funkcionalnosti i mogućnosti primene u najrazličitijim oblastima, posebno u mobilnim uređajima, pred njima su mnogobrojni izazovi i sve značajnije dileme.

Izazovi su ponajpre vezani za dalje unapređenje i razvoj, posebno onih sistema koji trenutno, i pored očiglednih prednosti, još uvek nemaju široku upotrebu, bilo zbog svoje cene, ili ograničenosti kapaciteta i specifične snage i/ili specifične energije, da bi se mogli šire koristiti. Na primer električna vozila su i dalje preskupa, domet im je ograničen na par stotina kilometara, a ponovno punjenje baterija zahteva minimum nekoliko sati pauze na putu; efikasnost gorivnih galvanskih spregova je i dalje nedovoljna, rezervoari goriva su ograničenih kapaciteta, a tehnologija je i dalje veoma skupa za široku upotrebu… To je razlog što su istraživanja vezana za ove sisteme sve intenzivnija i mnogobrojnija [21-23,28-28,31-42]. Ona su najčešće multidisciplinarna, bilo da su fundamentalna (koja će razviti nove materijale za unapređenje postojećih i poznatih sistema, ili razviti nove sisteme zasnovane na već stečenim znanjima), ili da su primenjena (koja treba da pojednostave uređaje, ali i povećaju njihovu efikasnost i smanje njihovu cenu).

Odlična ilustracija svih tih izazova je monografija koja detaljno razmatra elektrohemijske sisteme za konverziju i skladištenje energije sa stanovišta buduće održivosti [43]. Između ostalih ona razmatra aktuelne izazove fotoelektrohemijske redukcije CO_2 i oksidacije CO, hibridne polimerne nanokompozte kao potencijalne materijale sa ovakve sisteme, dizajn i nova tehnološka rešenja fleksibilnih mikrosuperkondenzatora, katalizatore za reakciju oksidacije vodonika u procesima skladištenja i konverzije energije, modelovanje materijala i elektrolita litijum-jonskih baterija, nove materijale i procese za oksidaciju metanola i mravlje kiseline u gorivnim spregovima itd. Poslednjih godina posebna pažnja se posvećuje i zameni litijum-jonskih baterija izvorima zasnovanim na drugim metalima, pre svega aluminijumu i magnezijumu [32,34].

Razlozi za to su vrlo jasni – količina raspoloživog litijuma na planeti zemlji je premala da bi zadovoljila sve buduće potrebe za ovakvim izvorima energija, a njegova eksploatacija je skupa, pogotovo ako se uzme u obzir neophodnost da ne ostavlja posledice na životnu sredinu. Upravo proteklih meseci smo svedoci protesta i napora u našoj zemlji da se spreči eksploatacija litijuma u dolini Jadra. Sa stanovišta potencijalne ugroženosti životne sredine i moguće devastacije prirode takvi napori su potpuno razumljivi i opravdani, ali autor ovih redova ostaje u nedoumici da li su pravilno usmereni, i da li je cilj koji žele da postignu najispravniji. Svaki zahtev da se stavi moratorijum na eksploataciju bilo koje sirovine, pa tako i litijuma, koja je neophodna za razvoj tehnologija i/ili proizvodnju bilo kog sistema ili uređaja koji omogućava, ili će omogućiti, razvoj i lakši život, sam po sebi je besmislen. Svaki takav zahtev, ako je već neophodan u nekom trenutku, mora biti ograničen uslovima da takva eksploatacija ne ugrožava životnu sredinu i uništava prirodu, primenom svih tehnologija i resursa kojima sadašnji trenutak raspolaže, ili da se takva eksploatacija odloži do trenutka kada budu razvijene takve tehnologije koji će obezbediti čiste i za životnu sredinu neškodljive postupke, pod ekonomsko prihvatljivim uslovima. Zato apsolutni moratorijum na eksploataciju litijuma, ali i svake druge sirovine, ne sme i ne može biti predmet nijednog zahteva.

Ovo je samo jedna od dilema pred kojima sa nalaze elektrohemijski sistemi za konverziju i skladištenje energije. Kako je već rečeno, ovi sistemi deluju kao idealni sa stanovišta održivosti i očuvanja životne sredine: baterija ili superkondenzator koji se napuni i pokreće mobilni telefon, automobil ili kakav drugi uređaj ne izbacuje gasove u atmosferu i može se ponovo napuniti, a lako se reciklira; većina galvanskih gorivnih spregova sagorevanjem goriva (vodonika) emituje samo vodenu paru, akumulatori metal vazduh koriste samo obnovljive materijale i ne zagađuju

vazduh… Međutim, većina energije koju oni skladište ili konvertuju i dalje se najvećim delom proizvodi sagorevanjem fosilnih ili nuklearnih goriva. I pored velikih napora i očiglednog napretka u razvijanju i korščenju obnovljivih izvora, sve veće potrebe za energijom uslovile su da je smanjenje korišćenja fosilnih goriva mnogo manje nego što je to željeno i potrebno, kako sa stanovišta smanjenja emisije gasova staklene bašte, tako i nalaženja rešenja za zamenu goriva koje ima ograničene resurse. Zbog toga je za budućnost elektohemijskih sistema podjednako važno da njihov razvoj nije usmeren samo na unapređenje njihovih karakteristika i njihove ekonomičnosti, već i da budu prilagođeni lakom i efikasnom korišćenju obnovljivih izvora primerne energije. Na slici 2 prikazana je šema idealne proizvodnje, konverzije i skladištenja energije pomoću elektrohemijskih sistema.

Koliko su obnovljivi izvori primarne energije ekonomičniji i po životnu sredinu prihvatljiviji od konvencionalnih očito je iz podataka prikazanih u Tabeli 2 [45-47]. Oni proizvode energiju i po značajno manjoj ceni i uz minimalno emitovanje ugljendioksida

Tabela 2. Cena energije i emisija CO_2 u zavisnosti od načina proizvodnje

	Ugalj	Prirodni gas	Nuklearna energija	Energija sunca	Vetroparkovi	Hidrocentrale
Cena, \$ kWh^{-1}	0.16	0.11	0.14-0.19	0.02-0.06	0.04-0.10[a]	0.05
Emisija* CO_2, g kWh^{-1}	1,034[b]	443	117	33	7-9	4

*uzeta je u obzir emisija svih štetnih gasova, izražena kroz ekvivalent emisije CO?
[a]0.04-0.05 \$ na vetrovitim, 0.06-0.08 \$ na manje vetrovitim lokacijama, oko 0.10 \$za vetroparkove u moru, zbog cene izgradnje.
[b]za lignit, 864 g g kWh^{-1}za mrki ugalj i antracit

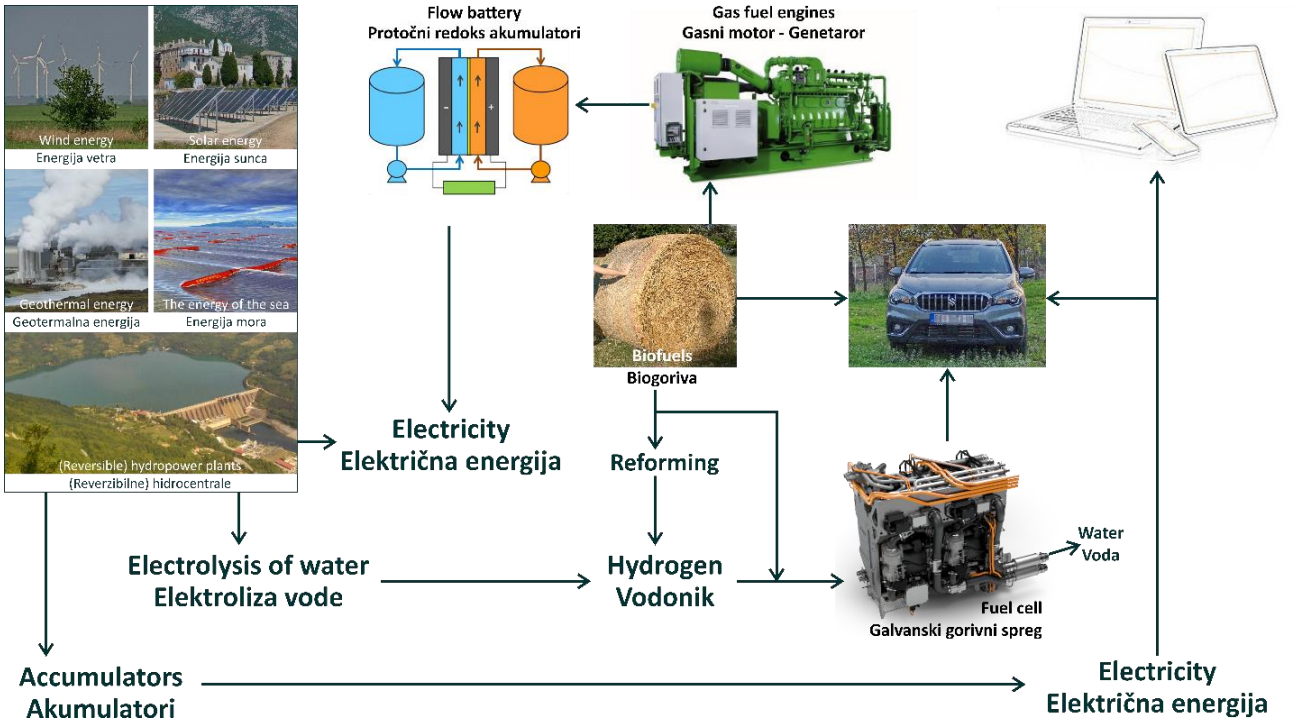

Slika 2. Održivo i za životnu sredinu optimalno korišćenje elektrohemijskih sistema za konverziju i skladištenje energije
Figure 2. Sustainable and environmentally optimal use of electrochemical systems for energy conversion and storage

Treba imati u vidu i relativno visoke troškove i veliku potrošnju energije za izgradnju postrojenja za dobijanje obnovljivih oblika energije. Smatra se, na primer, da svaki vetrogenerator treba da radi 3-11 meseci (zavisno od lokacije i veličine) kako bi proizveo onoliko energije koliko je potrebno za njegovu izgradnju [48]. Poseban problem predstavlja odlaganje i moguće recikliranje ovih postrojenja nakon kraja njihovog životnog veka. Solarni paneli se većim delom mogu uspešno reciklirati, posebno stakleni deo (koji čini oko 75 % svakog panela), ali postoje i delovi panela kao što su metali, čije recikliranje je i teško i skupo, jer je njihova količina u panelima mala. Predviđa se da će do 2030. godine samo u Americi biti potrebno više od 450 miliona dolara za recikliranje i odlaganje solarnih panela, što je suma dovoljna da se

proizvede oko 40 miliona novih panela [47]. Kada su vetrogeneratori u pitanju, njihov dugačak životni vek, i do 40 godina, čini da je trenutno taj problem minimalan, jer je broj onih koje je potrebo ukloniti mali, ali kako im se od početka ovog milenijuma broj geometrijski povećava, problem njihovog recikliranja postaje sve aktuelniji. Do 2050. godine oko 50,000 vetrogeneratora će morati biti ugašeno i zamenjeno novim, što će svakako zahtevati dodatna ulaganja i nalaženje novih rešenja za njihovo odlaganje i/ili recikliranje [48].

Konačno, ali ne najmanje važno, treba imati u vidu direktan uticaj postrojenja za dobijanje obnovljivih vidova energije na živi svet. Vetroparkovi su često opasnost za ptice, posebno ako se nađu na rutama njihovih migracija. Zato su neki od njih uveli stalni nadzor okoline kamerama, pa se u slučaju približavanja velikih jata ptica rad obustavlja. Uređaji koji koriste energiju mora (talasa, vodenih struja ili plime i oseke) mogu stvoriti veštačke ekološke sisteme koji mogu narušiti prirodne lance ishrane, njihova svetlost može privući, biti i uzrok povreda pa i smrti ptica, riba i drugih stanovnika mora, a elektromagnetni talasi mogu poremetiti orijentaciju i ishranu mnogih morskih vrsta [49]. Zbog ogromnih površina koje zauzimaju solarne elektrane, one mogu drastično izmeniti zemljište i staništa za mnoge životinjske i biljne vrste, ali i poremetiti režime prirodnih voda, posebno ako su u pitanju solarne termoelektrane koje zahtevaju ogromne količine vode za hlađenje [50]. Sa stanovišta održivosti i uticaja na životnu sredinu geotermalne elektrane su najoptimalnije, ali njihova izgradnja je ograničena na relativno mali broj lokacija na kojima postoje preduslovi za njihovu izgradnju.

4. ZAKLJUČAK

Savremeni elektrohemijski sistemi za konverziju i skladištenje energije omogućili su razvoj i masovno korišćenje prenosivih uređaja, sve veću upotrebu električnih vozila i omogućili da se energijom lako i ekonomično mogu snabdevati potrošači udaljeni od konvencionalnih izvora ili mreža za prenos energije. Omogućili su i razvoj čitavog niza uređaja koji bez njih skoro da ne bi bili mogući, kao što su na primer pametni telefoni, dronovi, električna invalidska kolica ili sistemi za nadzor i na najudaljenijim lokacijama i mnogi drugi. Uz to, oni su skoro neškodljivi za životnu sredinu. Iako su na prvi pogled skoro idealni sa stanovišta održivosti, čitav niz izazova i dilema stoji pred njihovim daljim razvojem. Pored toga što treba da postanu ekonomičniji, da se unaprede njihovi kapaciteti i specifična snaga i/ili specifična energije, neophodno je unaprediti njihove mogućnosti da jednostavno i efikasno koriste obnovljive izvore primarne energije, ali i omogućiti da ti izvori budu prilagođeni i kompatibilni sa zahtevima elektrohemijskih sistema za konverziju i skladištenje energije. Neophodno je takođe unapređivati postojeće i razvijati nove materijale i postupke bezbedne po životnu sredinu, kako u proizvodnji, tako i u eksploataciji, ali i odlaganju i recikliranju nakon isteka njihovog životnog veka. Isto tako, potrebno je kritički razmotriti da li neki od sistema, kao na primer galvanski gorivi spregovi, i kada (ili u doglednoj budućnosti) mogu dostići takve performanse da njihova upotreba bude ekonomična i široko rasprostranjena. Možda je uputnije znanje i vreme prvenstveno usmeriti na one sisteme za koji je sigurno da su u bliskoj budućnosti održivi u svakom smislu?

Zahvalnica: Ovaj rad je podržalo Ministarstvo prosvete, nauke i tehnološkog razvoja, Republike Srbije, Ugovor broj 451-03-68/2022-14/200026.

REFERENCES

[1] Guney MS, Tepe Y. Classification and assessment of energy storage systems. *Renew Sustain Energy Rev* 2017;75:1187–97. https://doi.org/10.1016/J.RSER.2016.11.102

[2] Energyland - New and Renewable Energy, https://www.emsd.gov.hk/energyland/en/energy/renewable/index.html (pristupljeno 8. decembra 2021.)

[3] Energy Sources: Types and Examples,https://group.met.com/energy-insight/energy-sources/21 (pristupljeno 22. decembra 2021.)

[4] Share of electricity in total final energy consumption, historical and SDS – Charts – Data & Statistics - IEA, https://www.iea.org/data-and-statistics/charts/share-of-electricity-in-total-final-energy-consumption-historical-and-sds (pristupljeno 8. decembra 2021.)

[5] Mohsen M, Bagher AM, Reza BM, Abadi Vahid MM, Mahdi T. Comparing the generation of electricity from renewable and non-renewable energy sources in Iran and the world: Now and future. *World J Eng* 2015;12(6):627–38. https://doi.org/10.1260/1708-5284.12.6.627

[6] Kiehne HA, Battery Technology Handbook. Marcel Dekker, New York, USA 2003, ISBN 978-0824756420

[7] Northeast Center for Chemical Energy Storage - The NorthEast Center for Chemical Energy Storage, Binghamton University https://www.binghamton.edu/centers/necces/ (pristupljeno 9. decembra 2021.)
[8] Ibrahim H, Ilinca A, Perron J. Energy storage systems-Characteristics and comparisons. *Renew Sustain Energy Rev* 2008;12(5):1221–50. https://doi.org/10.1016/J.RSER.2007.01.023
[9] Koohi-Fayegh S, Rosen MA. A review of energy storage types, applications and recent developments. *J Energy Storage* 2020;27. https://doi.org/10.1016/J.EST.2019.101047
[10] Niaz S, Manzoor T, Pandith AH. Hydrogen storage: Materials, methods and perspectives. *Renew Sustain Energy Rev* 2015;50:457–69. https://doi.org/10.1016/J.RSER.2015.05.011
[11] Kopyscinski J, Schildhauer TJ, Biollaz SMA. Production of synthetic natural gas (SNG) from coal and dry biomass – A technology review from 1950 to 2009. *Fuel* 2010;89(8):1763–83. https://doi.org/10.1016/J.FUEL.2010.01.027
[12] Saxena RC, Adhikari DK, Goyal HB. Biomass-based energy fuel through biochemical routes: A review. *Renew Sustain Energy Rev* 2009;13(1):167–78. https://doi.org/10.1016/J.RSER.2007.07.011
[13] Synthetic Natural Gas (SNG): Technology, Environmental Implications, and Economics | The Nicholas Institute for Environmental Policy Solutions, https://nicholasinstitute.duke.edu/climate/carbon-capture-and-storage/natgas (pristupljeno 13. decembra 2021.)
[14] Abedin AH. A Critical Review of Thermochemical Energy Storage Systems. *Open Renew Energy J* 2011;4(1):42–6. https://doi.org/10.2174/1876387101004010042
[15] Zakeri B, Syri S. Electrical energy storage systems: A comparative life cycle cost analysis. *Renew Sustain Energy Rev* 2015;42:569–96. https://doi.org/10.1016/J.RSER.2014.10.011
[16] Mechanical Electricity Storage Technology | Energy Storage Association, https://energystorage.org/why-energy-storage/technologies/mechanical-energy-storage/ (pristupljeno 3. januara 2022.)
[17] Cabeza LF, Martorell I, Miró L, *et al.* Introduction to thermal energy storage systems. *Adv Therm Energy Storage Syst* 2021:1–33. https://doi.org/10.1016/B978-0-12-819885-8.00001-2
[18] Nithyanandam K, Stekli J, Pitchumani R. High-temperature latent heat storage for concentrating solar thermal (CST) systems. *Adv Conc Sol Therm Res Technol* 2017:213–46. https://doi.org/10.1016/B978-0-08-100516-3.00010-1
[19] HISTORY OF LEAD - Batteries International n.d. https://www.batteriesinternational.com/2016/09/21/history-of-lead/ (pristupljeno 3. januara 2022.)
[20] Pfleger N, Bauer T, Martin C, Eck M, Wörner A. Thermal energy storage – overview and specific insight into nitrate salts for sensible and latent heat storage. *Beilstein J Nanotechnol 6154* 2015;6(1):1487–97. https://doi.org/10.3762/BJNANO.6.154
[21] Nitta N, Wu F, Lee JT, Yushin G. Li-ion battery materials: present and future. *Mater Today* 2015;18(5):252–64. https://doi.org/10.1016/J.MATTOD.2014.10.040
[22] Декански АБ, Панић ВВ. Електрохемијски суперкондензатори: Принцип рада, компоненте и активни материјали. *Hem Ind* 2018;72(4):229–51. https://doi.org/10.2298/10.2298/HEMIND180515016D
[23] Poonam, Sharma K, Arora A, Tripathi SK. Review of supercapacitors: Materials and devices. *J Energy Storage* 2019;21:801–25. https://doi.org/10.1016/J.EST.2019.01.010
[24] Rajaputra SS, Pennada N, Yerramilli A, Kummara NM. Graphene based sulfonated polyvinyl alcohol hydrogel nanocomposite for flexible supercapacitors. *J Electrochem Sci Eng* 2021;11(3):197–207. https://doi.org/10.5599/JESE.1031
[25] Sánchez-Díez E, Ventosa E, Guarnieri M, *et al.* Redox flow batteries: Status and perspective towards sustainable stationary energy storage. *J Power Sources* 2021;481:228804. https://doi.org/10.1016/J.JPOWSOUR.2020.228804
[26] Sazali N, Salleh WNW, Jamaludin AS, Razali MNM. New Perspectives on Fuel Cell Technology: A Brief Review. *Membranes (Basel)* 2020;10(5). https://doi.org/10.3390/MEMBRANES10050099
[27] Olabi AG, Sayed ET, Wilberforce T, *et al.* Metal-Air Batteries—A Review. *Energies 2021, Vol 14, Page 7373* 2021;14(21):7373. https://doi.org/10.3390/EN14217373
[28] Choudhury P, Bhunia B, Bandyopadhyaya TK. Screening technique on the selection of potent microorganisms for operation in microbial fuel cell for generation of power. *J Electrochem Sci Eng* 2021;11(2):129–42. https://doi.org/10.5599/JESE.924
[29] Sivakumar JU, Rao LT, Rewatkar P, *et al.* Single microfluidic fuel cell with three fuels – formic acid, glucose and microbes: A comparative performance investigation: *J Electrochem Sci Eng* 2021;11(4):305–16. https://doi.org/10.5599/JESE.1092
[30] Jha V, Surasani VK, Krishnamurthy B. Three-dimensional mathematical model to study effects of geometrical parameters on performance of solid oxide fuel cell: *J Electrochem Sci Eng* 2021;11(4):291–304. https://doi.org/10.5599/JESE.1097
[31] Okumura T, Taminato S, Miyazaki Y, *et al.* LISICON-Based Amorphous Oxide for Bulk-Type All-Solid-State Lithium-Ion Battery. *ACS Appl Energy Mater* 2020;3(4):3220–9. https://doi.org/10.1021/acsaem.9b01949
[32] Singh B, Wang Z, Park S, *et al.* A chemical map of NaSICON electrode materials for sodium-ion batteries. *J Mater Chem A* 2021;9(1):281–92. https://doi.org/10.1039/D0TA10688G
[33] Luo X, Wang J, Dooner M, Clarke J. Overview of current development in electrical energy storage technologies and the application potential in power system operation. *Appl Energy* 2015;137:511–36. https://doi.org/10.3866/PKU.WHXB20190500
[34] Cao B, Li X. Recent progress on carbon-based anode materials for na-ion batteries. *Wuli Huaxue Xuebao/ Acta Phys - Chim Sin* 2020;36(5). https://doi.org/10.3866/PKU.WHXB201905003

[35] Patil SS, Bhat TS, Teli AM, *et al.* Hybrid Solid State Supercapacitors (HSSC's) for High Energy & Power Density: An Overview. *Eng Sci* 2020;12:38–51. https://doi.org/10.30919/ES8D1140

[36] Goodenough JB, Park KS. The Li-ion rechargeable battery: A perspective. *J Am Chem Soc* 2013;135(4):1167–76. https://doi.org/10.1021/JA3091438

[37] Vaalma C, Buchholz D, Weil M, Passerini S. A cost and resource analysis of sodium-ion batteries. *Nat Rev Mater* 2018;3. https://doi.org/10.1038/NATREVMATS.2018.13

[38] Malka D, Attias R, Shpigel N, Malchik F, Levi MD, Aurbach D. Horizons for Modern Electrochemistry Related to Energy Storage and Conversion, a Review. *Isr J Chem* 2021;61(1–2):11–25. https://doi.org/10.1002/ijch.202100002

[39] Moškon J, Talian SD, Dominko R, Gaberšček M. Advances in understanding Li battery mechanisms using impedance spectroscopy. *J Electrochem Sci Eng* 2020;10(2):79–93. https://doi.org/10.5599/JESE.734

[40] Dobrota AS, Pašti IA. Chemisorption as the essential step in electrochemical energy conversion. *J Electrochem Sci Eng* 2020;10(2):141–59. https://doi.org/10.5599/JESE.742

[41] Slavova M, Mihaylova-Dimitrova E, Mladenova E, Abrashev B, Burdin B, Vladikova D. Zeolite based gas-diffusion electrodes for secondary metal air batteries. *J Electrochem Sci Eng* 2020;10(2):229–34. https://doi.org/10.5599/JESE.763

[42] Thackeray MM, Wolverton C, Isaacs ED. Electrical energy storage for transportation - Approaching the limits of, and going beyond, lithium-ion batteries. *Energy Environ Sci* 2012;5(7):7854–63. https://doi.org/10.1039/C2EE21892E

[43] Samantara AK, Ratha S, editors. Electrochemical Energy Conversion and Storage Systems for Future Sustainability. New York: Apple Academic Press; 2020. https://doi.org/10.1201/9781003009320

[44] Verma J, Kumar D. Metal-ion batteries for electric vehicles: current state of the technology, issues and future perspectives. *Nanoscale Adv* 2021;3(12):3384–94. https://doi.org/10.1039/D1NA00214G

[45] Hydropower remains the lowest-cost source of electricity globally, https://www.hydroreview.com/business-finance/hydropower-remains-the-lowest-cost-source-of-electricity-globally/#gref (pristupljeno 27. januara 2022.)

[46] Where does wind power make sense? All topics from climate change to conservation, https://www.dw.com/en/wind-power-costs-renewable-energy/a-60046761 (pristupljeno 27. januara 2022.)

[47] Solar Panel Recycling, US EPA, https://www.epa.gov/hw/solar-panel-recycling (pristupljeno 8. decembra 2021.)

[48] How sustainable is wind power? All topics from climate change to conservation, https://www.dw.com/en/how-sustainable-is-wind-power/a-60268971 (pristupljeno 12. januara 2022.)

[49] Wave-Energy Devices Might Affect the Natural Environment, Oregon Sea Grant, Oregon State University, https://seagrant.oregonstate.edu/sgpubs/wave-energy-devices-might-affect-natural-environment (pristupljeno 2. januara 2022.)

[50] Environmental Impacts of Solar Power | Union of Concerned Scientists n.d. https://www.ucsusa.org/resources/environmental-impacts-solar-power (pristupljeno 27. januara 2022.)

Challenges and doubts of electrochemical energy conversion and storage

Aleksandar Dekanski

University of Belgrade, Institute of Chemistry, Technology and Metallurgy, Department of Electrochemistry, Njegoševa 12, Belgrade, Serbia

Abstract

Although electrochemical systems for energy conversion and storage at first glance have excellent properties, both in terms of sustainability, renewable and environment safety, as well as functionality and application in various fields, especially in mobile devices, advance and application of these systems face many challenges and increasingly significant dilemmas.

Keywords: fossil fuels; batteries; fuel cells; supercapacitors; CO_2 emission; environment

LETTER TO EDITOR

UDC: 621.351:165.412

Hem. Ind. **76 (1)** 43-54 (2022)

The challenges are primarily related to the further improvement and development, especially of those systems that currently, despite the obvious advantages, are still not widely used, either due to their cost or limited capacity and specific power and/or specific energy. For example, electric vehicles are still too expensive, their range is limited to a few hundred kilometers, and recharging of batteries requires a minimum break of several hours on the road; the efficiency of fuel cells is still insufficient, fuel tanks have limited capacities, and the technology is still very expensive for wider use… This is the reason why the research related to these systems is becoming more intensive and wide-ranging. Research activities are usually multidisciplinary, whether they are fundamental (focused on development of new materials to improve existing and known systems, or on development of new systems based on already acquired knowledge), or applied (aimed to simplify devices, but also to increase the efficiency and reduce the price).

An excellent illustration of all these challenges is the book *Electrochemical Energy Conversion and Storage Systems for Future Sustainability* edited by Samantara and Ratha, which examines these systems in detail, from the point of view of future sustainability. Among other things, the book discusses current challenges in photoelectrochemical reduction of CO_2 and CO oxidation, hybrid polymer nanocomposites as potential materials for such a systems, designs, and new technological solutions for flexible microsupercapacitors, catalysts for hydrogen oxidation reaction in storage and energy conversion processes -ionic batteries, new materials and processes for the oxidation of methanol and formic acid in fuel cells, *etc.*

In recent years, special attention has been paid to the replacement of lithium-ion batteries with sources based on other metals, primarily aluminium and magnesium. The reasons for such a trend are very clear - the amount of lithium available on the planet is too limited to meet all future needs for such energy sources, and its exploitation is expensive, especially considering the need to avoid adverse consequences in the environment. In recent months, we have witnessed protests and efforts in Serbia to prevent exploitation of lithium in the Jadar valley. From the standpoint of potential environmental threat and possible devastation of nature, such efforts are completely understandable and justified, but the author of these lines remains in doubt whether they are properly directed and whether the goal they want to achieve is the most correct. Any request to put a moratorium on exploitation of any raw material, including lithium, which is necessary for the development of technologies and / or production of any system or device that enables, or will enable, development and easier life, is in itself meaningless. Any such request, if necessary, must be limited to the conditions that such exploitation does not endanger the environment and destroy nature, using all technologies and resources currently available, or that such exploitation is postponed until technologies which will ensure clean and environmentally friendly production are developed, under economically acceptable conditions. Therefore, the absolute moratorium on the exploitation of lithium, but also of any other raw material, must not and cannot be the subject of any request.

This is just one of the dilemmas facing electrochemical energy conversion and storage systems. As already mentioned, these systems seem ideal from the point of view of sustainability and environmental protection: a battery

or supercapacitor that charges and drives a mobile phone, car or any other device does not emit gases into the atmosphere and can be recharged and easily recycled; most fuel cells emit only water vapor by burning fuel (hydrogen), metal air batteries use only renewable materials and do not pollute the air… However, most of the energy they store or convert is still mostly produced by burning fossil or nuclear fuels. Despite great efforts and obvious progress in the development and use of renewable sources, increasing energy needs have led to a reduction in the use of fossil fuels much less than desired and necessary, both in terms of reducing greenhouse gas emissions and finding solutions to replacing fuels that have limited resources. Therefore, it is equally important for the future of electrochemical systems that their development is not only aimed at improving their characteristics and their economy, but also that they are adapted to the easy and efficient use of renewable sources of primary energy. Figure 1 shows the scheme of ideal energy production, conversion and storage using electrochemical systems.

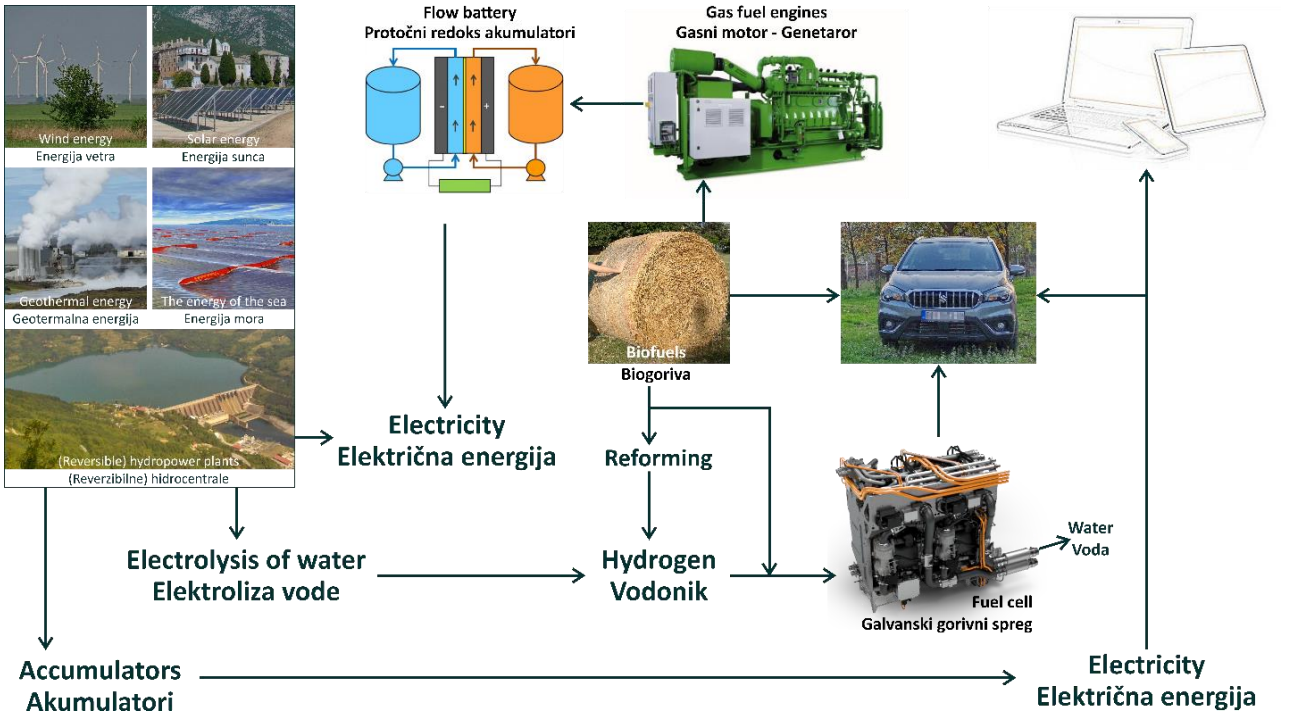

Figure 1. Sustainable and environmentally optimal use of electrochemical systems for energy conversion and storage

Relatively high costs and high energy consumption for the construction of renewable energy plants should be also considered. It is supposed, for example, that each wind turbine has to operate for 3-11 months (depending on location and size) to produce as much energy as needed to build one. Special attention should be paid to the disposal and possible recycling of these plants after the end of their service life. Most solar panels can be successfully recycled, especially the glass part (which makes up about 75% of each panel), but there are also parts such as metals, which are difficult and expensive to recycle because of the small quantity in the panels. It is estimated that more than 450 million USD will be needed to recycle and dispose of solar panels by 2030 in the United States alone, which is sufficient to produce about 40 million new panels. When it comes to wind turbines, their long lifetime, up to 40 years, seems to be a minor problem at the moment, due to currently low number of those that need to be removed, but as the number of wind turbines increased geometrically since the beginning of this millennium, their recycling problem is becoming increasingly actual. By 2050, about 50,000 wind turbines will have to be shut down and replaced with new ones, which will certainly require additional investments and finding new solutions for their disposal and/or recycling.

Last but not least, direct impact of renewable energy plants on the living world should be kept in mind. Windfarms are often a danger to birds, especially if they are built on migration routes. That is why some of these windfarms have introduced constant video surveillance of the environment, in order to stop working when large flocks of birds are approaching. Devices that use sea energy (waves, water currents or tides) can create artificial ecological systems that

can disrupt natural food chains, their light can attract, cause injury and even death to birds, fish and other marine life, and electromagnetic waves can disrupt orientation and diet of many marine species. Due to the huge areas that solar power plants occupy, land and habitats of many animal and plant species can be drastically changed, but also natural water regimes may be disrupted especially by solar thermal power plants that require huge amounts of cooling water. From the point of view of sustainability and environmental impact, geothermal power plants are the most optimal, but their construction is limited to a relatively small number of locations.

Finally, it may be necessary to critically consider whether some of the systems, *e.g.* fuel cells, can ever (or in the foreseeable future) achieve such performance that will provide economical and widespread use. Perhaps it is more advisable to focus knowledge and time primarily on those systems that are certainly going to be sustainable in every sense in the near future?

Kompanija koloid – pametne inovacije

Trajna ultrazvučna integracija jona srebra za biomedicinsku primenu

Maja Kovačević

Koloid d.o.o., Sektor za inovacije i razvoj, Beograd, Srbija

Izvod

Istraživanja i rezultati primene koloidnog srebra u cilju zadovoljenja zdravstvenih (medicinskih) potreba, ukazuju kako na mogućnosti, tako i na opravdanost primene i perspektive razvoja tehnologije jo¬na srebra u pogledu unapređenja zdravlja i kvaliteta življenja.

Ključne reči: Inovacije; razvoj; koloidno srebro

VESTI

Hem. Ind. **76 (1)** 55-60 (2022)

Dostupno on-line na web adresi časopisa: http://www.ache.org.rs/HI/

U svakom inovacionom procesu prva faza je uvek proces kreiranja ideja, a upravo se ovom premisom vodila i visoko-tehnološka nacionalna kompanija Koloid, sa sedištem u Beogradu i Moskvi, kao i poslovnicama u širem regionu, koja je još pre 15 godina imala viziju da je tehnologija dobijanja koloidnog srebra i njegova integracija u biomaterijale budućnost. Na taj način, idući korak ispred vremena, Koloid je uspeo da svojim inovacijama inicira promene u sferi biomedicine.

1. SPECIFIČNOSTI KOMPANIJE KOLOID

U vreme ubrzanog napretka tehnologija, kompanija Koloid je fokusirana na implementaciju najsavremenijih tehnoloških rešenja, koja nisu samo dizajnirana da obezbede specifičnu namenu, već i da pruže drugačije korisničko

Autor za korespodenciju: Koloid d.o.o., Sektor za inovacije i razvoj, Prva pruga 7, 11000 Beograd, Srbija
E-mail: inovacijeirazvoj@koloid.rs

iskustvo. U sopstvenoj laboratoriji i proizvodnom pogonu, ova kompanija u svoja medicinska sredstva široke namene, ultrazvučnom jonizacijom trajno integriše jone srebra čistoće 99,99 Ag+ u nevidljivi molekularni film (1-2 mikrometra debljine), čime se vrši postupak filtriranja i eliminacije patogenih mikroorganizama, a samim tim i neutralizacija njihovog prisustva. Ovo su potvrdili i rezultati testiranja obavljeni od strane eksperata u Institutu za nuklearna istraživanja Vinča i Fakulteta medicinskih nauka (Institut za javno zdravlje Kragujevac), sa kojima Koloid sarađuje, a rezultati eksplicitno dokazuju da izloženost emitovanja koloidnog srebra korišćenjem medicinskih materijala u koje su joni srebra trajno ultrazvučno integrisani, ubija do 99,9 % bakterija.

2. MOĆ JONA SREBRA, Ag^+

Nakon višegodišnjeg istraživanja na polju tehnologije jona srebra, savremenim tehnološkim postupkom i po principima najviših svetskih standarda, Koloid testira i proizvodi širok dijapazon medicinskih materijala vrhunskog kvaliteta, čija se aktivna komponenta (joni srebra) vrlo često dopunjava i drugom aktivnom komponentom (zeolit klinoptilolit), a njihovom trajnom integracijom u tkanine za medicinske svrhe, pruža dugoročnu zaštitu od patogena. Efikasnost korišćenja ovakvih materijala za biomedicinsku primenu se tokom vremena njihovog korišćenja ne smanjuje, jer ovi antimikrobni agensi imaju jako dejstvo, a manju podložnost rezistentnosti, te se njihova bezbedna primena svrstava u red najdugoročnijeg korišćenja, bez nus pojava.

U svojim naučnim ekspertizama, sinergijom znanja i iskustva naučnika i stručnjaka sa *Instituta za nuklearna istraživanja Vinča* i Fakulteta medicinskih nauka u Kragujevcu, Koloid je prepoznao da je koloidno srebro, trajno integrisano u medicinske materijale širokog spektra, najprirodniji branilac svakog organizma. Koloidno srebro se proizvodi nehemijskim, elektrodisperznim postupkom pomoću ultračistog srebra u ultračistoj redestilovanoj vodi. Po svom hemijskom sastavu, to je čista redestilovana voda koja sadrži submikroskopske klastere srebra (fizičko-hemijski fenomen).

Prema sprovedenim studijama koloidno srebro deluje na naše telo na tri različita načina:

Katalitičkom oksidacijom: Kiseonik reaguje sa srebrom, dajući srebro-oksid. Taj proces daje energiju potrebnu da ćelija deluje, stvarajući adenozin trifosfat (ATP), izvor energije koji ćelija može direktno da koristi.

Reakcijom sa ćelijskom membranom bakterija. Joni srebra se vezuju za ćelijsku membranu bakterija i tako blokiraju njihovo ćelijsko disanje. Mehanizam delovanja srebra zapravo je inhibicija respiratornog enzima ćelije patogenog mikroorganizma. Srebro deluje kao katalizator, blokirajući određene enzime koje bakterije, virusi i gljivice koriste u svom metabolizmu, usled čega ovi izazivači bolesti ostaju bez kiseonika i hrane i raspadaju se. Ovaj proces odvija se tako brzo i efikasno, da nijedan mikroorganizam ne stiže da mutira, odnosno stekne otpornost, dok istovremeno, ćelije tkiva ostaju netaknute.

Prodiranjem u DNK bakterija. Pokazalo se da koloidno srebro prodire i veže se za DNK bakterija, sprečava odvijanje DNK bakterija i stoga trajno blokira njihov proces replikacije. Specifičnost jona srebra ogleda se u činjenici da ono „ne bira" koju bolest ili virus napada, a njegova efikasnost u eliminaciji patogena je dokazana na više od 650 oboljenja organizma.

Sa druge strane, aktivna komponenta zeolit klinoptilolit, ima strukturu rešetkastog kaveza sa snažnim negativnim nabojem, koji privlači i apsorbuje jone pozitivnog naboja (slobodne radikale i ostale štetne tvari). Zbog same strukture materijala i snažnog jonizujućeg dejstva srebrnih jona i zeolita, svi medicinski materijali u koje su ove komponente trajno integrisane imaju produženi efekat delovanja za razliku od drugih medicinskih materijala na tržištu. Klinički je dokazano da Zeolit klinoptilolit (kao i joni srebra), ima snažno antibakterijsko dejstvo, jer vezuje bakterije poput *Pseudomonas aeruginosa*, *Staphylococcus aureus, Escherichie coli*, *Candide*, *Shigella Boydi, Streptococcus pneumoniei* drugih. Zeolit klinoptilolit podleže procesu jedinstvene tribomehaničke mikronizacije i aktivacije, a dodatkom jona srebra njihova se antimikrobna svojstva multipliciraju.

3. KOLOID – VIŠE OD INOVACIJA

Ako se sagleda način na koji u današnje vreme jedna visoko-tehnološka, inovativna kompanija predstavlja svoje poslovanje, može se uočiti koncept koji se zasniva isključivo na korisničkom iskustvu, jer kompanija Koloid prepoznaje

da usluga ili proizvod sami po sebi više nisu dovoljni. Koloid pruža drugačiji doprinos u primeni najsavremenijih tehnoloških rešenja u korist svojih korisnika, sa tendencijom da postane nezaobilazni akter i partner u razvoju novih thenologija i njihovoj sofisticiranoj primeni.

Vizija ove kompanije je vrlo vidljiva i odnosi se na povećanje naučnog i tehnološkog kapaciteta kompanije, efikasnim prenošenjem znanja i ekspertize partnera. Uspešno udruživanje i prateće akcije stvaraju novu generaciju eksperata sposobnih da dizajniraju, koordiniraju i sprovode eksperimentalna istraživanja sa jasnom vizijom mape puta, posebno usmerene na razvoj i implementaciju inovacija u sferi tehnologije jona srebra.

Prateći najnovije trendove u nauci i visokoj tehnologiji, Koloid koristi najmodernija thenološka dostignuća, a u cilju najvišeg standarda usluga, čime će, kao i do sada, kreirati biomedicinske materijale široke namene i na taj način pružati neophodnu i kompletnu zaštitu.

Koloid company – smart innovations

Permanent ultrasound integration of silver ions for biomedical application

Maja Kovačević

Koloid d.o.o., Sector for Innovation and Development, Belgrade, Serbia

Abstract

The research cited and findings in respect of the application of colloidal silver aimed at meeting health (medical) needs point not only to the possibilities but also to the justification for using and the prospects for developing silver ion technology with a view to improving health and quality of life.

Keywords: innovation; development; colloidal silver

NEWS

In every innovation process stage, one is brainstorming, which is what has been a guide for the high-tech national company *Koloid*, operating from Belgrade and Moscow, and via regional branches, with a vision born 15 years ago that the technology for producing colloidal silver and integrating it into biomaterials was the future. By doing so, and being ahead of its time, *Koloid* has succeeded in initiating change in biomedicine through its innovations.

1. WHAT SETS KOLOID APART FROM OTHERS

In times of rapid technological advances, *Koloid* has been focused on implementing the latest technological solutions, designed not only as purpose-specific, but also to provide a distinct user experience altogether. In its own laboratory and production facility, the company permanently integrates in its wide range of medical supplies silver ions of a 99,99 Ag+ purity using ultrasound ionisation forming an invisible molecular coat (1-2 micrometres thick) to filter and eliminate pathogens, resulting in their neutralisation. This was also validated by the findings of the tests conducted by experts at the Institute for Nuclear Research Vinca and the Medical School (Public Health Institute Kragujevac), with whom *Koloid* collaborates, where the findings explicitly prove that exposure to emitted colloidal silver or the use of medical materials with permanently integrated silver ions using ultrasound ionisation kills up to 99.9 % of bacteria.

2. POWER OF SILVER IONS, Ag^+

Following years of research into silver ion technology, using a state-of-the-art process and in line with the principles of the highest global standards, *Koloid* tests and produces a wide range of top-quality medical materials, where the active component (silver ions) is very often complemented by another active component (zeolite clinoptilolite). The permanent integration of these two components into medical-grade fabrics provides lasting protection against pathogens. The efficiency of using such materials for biomedical application does not diminish over time because these antimicrobial agents are highly effective with a lower susceptibility of becoming resistant, so their safe application ranks them among most durable agents, free from side effects.

In its scientific expertise, by harnessing the synergy of know-how of scientists and experts at the Institute for Nuclear Research Vinca and the Medical School Kragujevac, *Koloid* recognised that colloidal silver, permanently integrated into a wide range of medical materials, is the most natural safeguard of the human body. Colloidal silver is produced using a non-chemical electrodispersion method on pristinely pure silver in pristinely pure redistilled water. In terms of its chemical composition, it is pure redistilled water containing submicroscopic silver clusters (a physical-chemical phenomenon).

Studies show that colloidal silver works on our body in three different ways:

Catalytic oxidation: Oxygen reacts with silver, producing silver oxide. That process provides the energy needed for the cell to function, creating adenosine triphosphate (ATP), a source of energy that the cell may directly use.

Reaction with the bacterial cell membrane. Silver ions bind to the cell membrane of bacteria, blocking their cellular respiration. Silver works to inhibit a pathogen cell's respiratory enzyme. Silver acts as a catalyst blocking certain enzymes, which bacteria, viruses and fungi use in their metabolism. In the process, these infectious agents are starved of oxygen and nutrients and then decay. It happens so fast and so effectively that no microorganism can mutate or become resistant. At the same time, our tissue cells remain intact.

Penetration into bacterial DNA. It has been demonstrated that colloidal silver penetrates and binds to the bacterial DNA, prevents bacterial DNA unwinding, and therefore permanently blocks the bacterial replication process. What sets silver ions apart is the fact that they "do not choose" which disease or virus to attack, and their effectiveness in eliminating pathogens has been proven on more than 650 conditions.

On the other hand, zeolite, as an active component, has a cage structure with a strong negative charge, attracting and absorbing positively charged ions (free radicals and other harmful substances). Owing to the structure of the materials and the strong ionising effect of silver ions and zeolite, all medical materials into which these components are permanently integrated have a prolonged effect unlike other medical materials on the market. It is clinically proven that zeolite clinoptilolite (as well as silver ions), has a potent antibacterial effect, as it binds bacteria such as *Pseudomonas aeruginosa*, *Staphylococcus aureus, Escherichia coli*, *Candida*, *Shigella boydi, Streptococcus pneumoniae* and others. Zeolite clinoptilolite undergoes unique tribomechanical micronisation and activation, and the addition of silver ions boosts the antimicrobial properties.

3. KOLOID – MORE THAN A VISION

If we look at how a high-tech innovative company presents its business nowadays, there is a noticeable, purely user-experience look to it, as *Koloid* recognises that a service or product *per se* is no longer sufficient. *Koloid* lends a different contribution to the application of the latest technological solutions to benefit its customers, endeavouring to become a go-to participant and partner in developing the latest technological solutions and their sophisticated application.

The company's vision is crystal clear and centres on bolstering the scientific and technological capacity of the company, through the efficient transfer of partners' know-how. Successful collaboration and related activities create a

new generation of experts capable of designing, coordinating, and conducting experimental research with a clear vision of the road ahead, focused on developing and implementing innovations in silver ion technology.

By keeping abreast of trends in science and high-tech, *Koloid* employs state-of-the-art technological advancements to ensure the highest service standards, providing its customers, as it has done so far, with a wide range of medical materials and by doing so affording the full protection needed.

DOKTORSKE DISERTACIJE HEMIJSKO–TEHNOLOŠKE STRUKE ODBRANJENE NA UNIVERZITETIMA U SRBIJI U 2021. GODINI

TEHNOLOŠKO-METALURŠKI FAKULTET, UNIVERZITET U BEOGRADU

	Ime i prezime	Naslov	Mentor/i
1.	**Popović Ana**	Sinteza, karakterizacija i primena modifikovanih mikrosfera na bazi lignina za uklanjanje jona teških metala, oksianjona i diklofenaka iz vode	Aleksandar Marinković Jelena Rusmirović
2.	**Abubkr Mohamed Hemer**	Elastoplastično ponašanje zavarenog spoja čelika visoke čvrstoće pri delovanju statičkog i dinamičkog opterećenja	Ljubica Milović
3.	**Abdusalam Ahmed Elmadani**	Sinteza i karakterizacija hibridnih dentalnih polimernih kompozita poboljšanih mehaničkih svojstavaSinteza i karakterizacija hibridnih dentalnih polimernih kompozita poboljšanih mehaničkih svojstava	Vesna Radojević
4.	**Košević Milica**	Sinteza i karakterizacija strukturno uređenih interaktivnih elektrokatalitičkih kompozita zasnovanih na oksidima metala i platini	Snežana Gojković Vladimir Panić
5.	**Abdalla Ali Salim**	Proizvodnja hidrolitičkih enzima fermentacijom na poljo-privrednom otpadu pomoću različitih vrsta iz roda *Bacillus*	Zorica Knežević-Jugović
6.	**Nenad Jevremović**	Uticaj pesticida na strukturu polimera pri ubrzanom starenju poli(etilen tereftalata)	Ivanka Popović Melina Kalagasidis Krušić
7.	**Stupar Stevan**	Uklanjanje antrahinonskih boja iz vodenih rastvora adsorpcijom, elektrohemijskom oksidacijom i višim oksidacionim procesima	Dušan Mijin, Branimir Grgur
8.	**Mladenović Ivana**	Sinteza i karakterizacija slojevitih kompozitnih struktura za primenu u mikro elektro mehaničkim sistemima	Vesna Radojević Jelena Lamovec
9.	**Ilić Pajić Jovana**	Eksperimentalno određivanje volumetrijskih karakteristika biogoriva na visokom pritisku i njihovo modelovanje korišćenjem SAFT i PC-SAFT modela	Mirjana Kijevčanin
10.	**Mitrović Tatjana**	Hemometrijske metode za predviđanje parametara kvaliteta rečnih voda i razgradnje zagađujućih materija	Mirjana Ristić Saša Lazović
11.	**Radovanović Neda**	Biostimulatori biljnog rasta poreklom iz morske sredine za primenu u agroindustriji	Suzana Dimitrijević-Branković
12.	**Barjaktarević Dragana**	Površinska nanostrukturna modifikacija i karakterizacija materijala na bazi titana za primenu u medicini	Marko Rakin Veljko Đokić
13.	**Perendija Jovana**	Uklanjanje toksičnih jona iz vodenih rastvora primenom adsorbenata na bazi modifikovane celuloze	Antonije Onjia
14.	**Марковић Марија**	Kobaltom impregnisane pilarene gline kao katalizatori oksidativne degradacije zagađujućih materija vode	Aleksandra Perić-Grujić Sanja Marinović
15.	**Ivanović Marija**	Uticaj termodinamičkih parametara na sintezu poroznih silikatnih materijala i njihova funkcionalna primenena	Ivona Radović Snežana Nenadović
16.	**Ivanović Tijana**	Termodinamička karakterizacija elektrolitnih sistema sa fosfatnim jonima	Jelena Miladinović
17.	**Ranković Bojan**	Tretman otpadnih muljeva iz postrojenja za pripremu vode za piće primenom jonizujućeg zračenja	Vladimir Pavićević Ivica Vujčić
18.	**Sekulić Zoran**	Predviđanje separacionih karakteristika kompleksirajuće–mikrofiltracionog procesa primenom veštačkih neuronskih mreža	Katarina Trivunac
19.	**Nešović Katarina**	Hidrogelovi polivinil-alkohola i hitozana sa elektrohemijski sintetisanim nanočesticama srebra za medicinske primene	Vesna Mišković-Stanković

	Ime i prezime	Naslov	Mentor/i
20.	**Vasović Valentina**	Raspodela vlage i degradacija izolacionog sistema energetskih transformatora sa mineralnim i biljnim uljima	Aleksandar Orlović
21.	**Milošević Milena**	Vinil i imino derivati piridina: sinteza, fizičko-hemijska karakterizacija, biološka aktivnost i teorijske studije elektronske strukture	Nevena Prlainović Ilija Cvijetić
22.	**Timotijević Ljubinko**	Radijaciona kompatibilnost tankoslojnih otpornika u integrisanoj tehnologiji	Aco Janićijević, Nenad Kartalović
23.	**Tadić Julijana**	Sinteza , struktura i svojstva novih potencijalno biološki aktivnih azo derivata 2(1*H*)-pirimidinona	Dušan Mijin
24.	**Radomirović Milena**	Zagađenje površinskog sedimenta Bokokotorskog zaliva teškim metalima i radionuklidima i procena rizika usled njihove biodostupnosti	Antonije Onjia

TEHNOLOŠKI FAKULTET, UNIVERZITET U NOVOM SADU

	Ime i prezime	Naslov	Mentor/i
1.	**Novica Sovtić**	Uticaj ekološki prihvatljivih ekstender ulja na svojstva gume	Dragan Govedarica
2.	**Igor Antić**	Procena kvaliteta vode i sedimenta rečnog sliva AP Vojvodine i rizika po zdravlje u odnosu na prisustvo regulisanih i novootkrivenih mikropolutanata	Biljana Škrbić
3.	**Vuk Rajović**	Eko-energetska analiza i simulacija kogenerativnih postrojenja na naftnim poljima	Oskar Bera Dragan Govedarica
4.	**Vanja Šeregelj**	Inkapsulirani karotenoidi iz sporednog proizvoda prerade šargarepe u funkcionalnoj hrani	Gordana Ćetković
5.	**Sandra Bulut**	Istraživanje dobijanja, karakterizacija i optimizacija svojstava aktivnog, biorazgradivog, ambalažnog materijala na bazi pogače uljane tikve golice	Vera Lazić
6.	**Dragana Plavšić**	Održivost pekarskog proizvoda sa povišenim sadržajem vlage sa dodatkom lekovitog i začinskog bilja	Sunčica Kocić-Tanackov Đorđe Psodorov
7.	**Anastasija Selaković**	Efekat šok zamrzavanja testa na tehnološke osobine lisnatog peciva obogaćenog vlaknima šećerne repe i semenom čije (Salvia hispanica)	Dragana Šoronja Simović Olivera Šimurina
8.	**Nemanja Bojanić**	Primena reverzibilnosti matrica usitnjavanja i metode odzivne površine za kontrolu efekata usitnjavanja u tehnološkom postupku mlevenja pšenice	Aleksandar Fišteš Dušan Rakić
9.	**Tanja Lužaić**	Mogućnost i ograničenja proizvodnje hladno presovanog ulja i pogače od semena odabranih hibrida suncokreta najnovijeg sortimenta	Ranko Romanić
10.	**Ljiljana Spasojević**	Priprema nanočestica zeina i njihova primena kao funkcionalnih koloida	Jaroslav Katona
11.	**Olja Šovljanski**	Mikrobiološka precipitacija karbonata - od odabira induktora do ispitivanja bioprocesnih parametara	Siniša Markov
12.	**Vanja Vlajkov**	Razvoj tehnologije proizvodnje agenasa biološke kontrole toksigenih izolata roda Aspergillus	Jovana Grahovac
13.	**Ida Zahović**	Optimizacija proizvodnje ksantana na sirovom glicerolu primenom lokalnog izolata Xanthomonas sp.	Zorana Trivunović
14.	**Jelena Čakarević**	In vitro digestija i njen uticaj na aktivnost, stabilnost i dostupnost biološki aktivnih jedinjenja	Ljiljana Popović

TEHNOLOŠKI FAKULTET U LESKOVCU, UNIVERZITET U NIŠU

	Ime i prezime	Naslov	Mentor/i
1.	**Sandra J. Stamenković Stojanović**	Optimizacija postupka dobijanja mikrobne biomase i formulacije mikrobiološkog preparata sa potencijalnim biopesticidnim i fitostimulatornim dejstvom	Miodrag Lazić
2.	**Dušica R. Đokić-Stojanović**	Uticaj kosolvenata na etanolizu suncokretovog ulja katalizovanoj kalcijum oksidom	Zoran Todorović

TEHNIČKI FAKULTET U BORU, UNIVERZITET U BEOGRADU

	Ime i prezime	Naslov	Mentor/i
1.	**Marina S. Pešić**	Fizičko -hemijska karakterizacija i simulacioni model za pojavu mutnoće voda u cilju optimizacije procesa prerade voda	Snežana Milić
2.	**Jelena J. Milosavljević**	Uticaj toksičnih elemenata na aktivnost enzima u rizosferi *plantago lanceolata* i *taraxacum officinale* i potencijalna upotreba biljaka u biomonitoringu i fitoremedijaciji	Snežana Šerbula
3.	**Dragana V. Medić**	Valorizacija kobalta iz katodnog materijala istrošenih litijum-jonskih baterija	Snežana Milić